

THE LABELING OF DTPA-COUPLED ANTIBODIES WITH TECHNETIUM-99M

D.J. Hnatowich, R.L. Childs and D. Lanteigne  
Department of Nuclear Medicine, University of Massachusetts Medical School,  
Worcester, Massachusetts 01605.

Although methods have been developed for labeling proteins with  $^{99m}\text{Tc}$  (technetium), both the mechanism of labeling and the site of attachment are unknown. More importantly, since these methods rely upon the protein to stabilize technetium in a reduced oxidation state and prevent both reoxidation to pertechnetate and the formation of radiocolloids, proteins labeled by these methods are often contaminated with loosely bound or unbound chemical forms of technetium. In addition to increasing the rate of blood clearance and uptake in several organs, these radio-contaminants may permit exchange of technetium among plasma proteins.

Labeling proteins in which strong chelating groups have been covalently attached has the potential of eliminating these difficulties by providing specific sites on the protein which form stable chelates with reduced technetium. We are investigating the use of DTPA-coupled proteins for this purpose in which technetium labeling is accomplished with stannous ion and mildly acidic conditions.

Initially, we investigated the degree to which proteins can compete with DTPA for reduced technetium by labeling free DTPA (100  $\mu\text{g}/\text{ml}$ ) with technetium in the presence of one of eight proteins (20  $\text{mg}/\text{ml}$ ) using stannous ion (DTPA:tin molar ratio about 2) at pH 6. Although the degree of competition varied, each protein was able to compete with DTPA for technetium. Nevertheless, for many proteins the extent of this competition should permit labeling the DTPA groups preferentially. For example, in the case of lysosyme, a protein which does not compete strongly with DTPA, we obtained identical biodistributions at 1 hour post injection in normal mice for  $^{111}\text{In}$  (indium) and technetium labeled to the protein coupled with an average of 0.6 DTPA groups per molecule (i.e. 106  $\mu\text{g}/\text{ml}$  of DTPA at 9.6  $\text{mg}/\text{ml}$  of protein) using stannous ion at pH 6 for technetium labeling. When the same experiment was performed with IgG antibody containing an average of 5.4 groups per molecule (and therefore 106  $\mu\text{g}/\text{ml}$  of DTPA at 6.4  $\text{mg}/\text{ml}$  of protein) we again obtained identical biodistributions at 2 hours post injection except that kidney and blood were elevated with technetium. When these biodistributions are compared to that obtained for uncoupled IgG labeled with technetium by the identical procedure, most tissues are significantly different. These results show that the DTPA groups on at least two proteins may be preferentially labeled with technetium using stannous reduction and mild conditions, although more non-specific binding to protein occurred in the case of IgG presumably because this protein competes more effectively with DTPA for technetium (1).

Subsequent studies were performed exclusively with IgG to optimize conditions for labeling the DTPA-coupled protein with technetium. The effect of DTPA:tin molar ratio on the labeling of free DTPA, the stability of the resulting label in saline and the degree of non-specific binding of protein in the presence of DTPA was determined. In addition, the effect of free DTPA concentration on the extent of labeling and the stability of labeled DTPA and uncoupled IgG was determined.

Using a 1:1.5 DTPA:tin molar ratio at pH 4, IgG containing an average of 1.9 groups per molecule was labeled with technetium and its stability determined with respect to uncoupled IgG labeled under identical conditions. The labeled proteins were incubated at pH 4 with a 100-fold molar excess of DTPA. HPLC analysis of the IgG solutions before incubation showed very little pertechnetate in both cases and 94–95% of the activity bound to IgG whereas after 3 hours in the DTPA solution, the percentage of activity bound to IgG decreased by about 10% in the case of coupled IgG and about 40% in the case of uncoupled IgG. The increased loss of activity in both cases appeared as labeled free DTPA and pertechnetate.

A similar stability study was also performed in 90% serum at 37°C. Whereas in both cases 95-97% of the activity was on IgG initially, after 3 hours of incubation coupled IgG lost 4% of its activity while uncoupled IgG lost 45%. Lost activity appeared as pertechnetate and, in the case of uncoupled IgG, primarily as labeled proteins of lower molecular weight.

Biodistribution studies in normal mice were conducted at 1 hour and 20 hours post injection with DTPA-coupled IgG labeled with technetium by the above method and with indium. In addition, uncoupled IgG labeled in the same manner with technetium was also studied. Since antibody catabolism with label redistribution is unlikely to occur by 1 hour post injection, the results of this study were expected to confirm that technetium was primarily attached to the DTPA groups by showing identical biodistributions for indium and technetium. Indeed, the agreement was good, with most tissues, such as liver, showing identical accumulation. In contrast, tissue accumulation for uncoupled IgG labeled with technetium were generally different from indium with most tissues, such as liver, showing elevated activity levels.

The 20 hour study was conducted to determine if the biodistribution of the two labels would now be quite different. Since serum incubation studies have shown both labels to be generally stable in serum, differences in biodistribution would indicate that redistribution of the labels occurred, possibly as a result of antibody catabolism. The results do show differences in all tissues considered. In particular, indium liver levels were unchanged from 1 hour while technetium liver levels decreased.

We conclude that the presence of the DTPA groups facilitates the labeling of IgG with technetium such that the product shows increased stability during in vitro incubations and in vivo. The in vivo results at 20 hours may show the effect of technetium clearance from liver, in contrast to indium, following catabolism of the protein. We were unable to reduce to negligible levels non-specific binding of technetium to IgG.

- (1) Lanteigne D. and Hnatowich D.J., "The Labeling of DTPA-coupled Proteins with  $^{99m}\text{Tc}$ ", *Int. J. Appl. Rad. Isotopes* (in press).

TABLE 1

Percentages of  $^{99m}\text{Tc}$  activity appearing as labeled protein in the HPLC analysis of DTPA-coupled and uncoupled IgG labeled at pH 4 and following incubation in 100-fold molar excess of DTPA and in 90% serum at 37°C.

	<u>Coupled</u>	<u>Uncoupled</u>
DTPA solution initially	95	94
DTPA solution 3 hours	83	58
Saline initially	97	95
Serum 1 hour	95	63
Serum 3 hours	93	50
Serum 24 hours	67	24

TABLE 2

Biodistribution in normal mice at one hour and 20 hours post injection with indium and technetium-labeled DTPA-coupled IgG antibody and technetium-labeled uncoupled IgG. Expressed as percent injected dose per gram wet weight as the mean and one standard deviation (N=5-7)

	<u>One hour post injection</u>		
	<u><math>^{111}\text{In-DTPA-IgG}</math></u>	<u><math>^{99m}\text{Tc-DTPA-IgG}</math></u>	<u><math>^{99m}\text{Tc-IgG}</math></u>
Blood	40.8 ± 3.0	36.0 ± 6.3	24.7 ± 11.7
Heart	6.1 ± 0.6	5.1 ± 0.8	3.2 ± 0.5
Lungs	12.6 ± 5.0	8.0 ± 0.9	7.1 ± 3.2
Liver	12.8 ± 1.5	13.3 ± 0.9	22.8 ± 1.8
Spleen	8.2 ± 1.3	6.8 ± 0.6	10.7 ± 1.1
Kidney	11.0 ± 0.8	14.6 ± 1.0	19.8 ± 2.5
Stomach*	2.5 ± 0.6	13.6 ± 1.6	13.2 ± 1.5

	<u>20 hours post injection</u>		
	<u><math>^{111}\text{In-DTPA-IgG}</math></u>	<u><math>^{99m}\text{Tc-DTPA-IgG}</math></u>	<u><math>^{99m}\text{Tc-IgG}</math></u>
Blood	22.1 ± 1.0	10.9 ± 1.5	4.3 ± 0.8
Heart	4.2 ± 0.3	2.0 ± 0.3	1.5 ± 0.6
Lungs	7.1 ± 1.2	3.1 ± 0.3	2.1 ± 1.3
Liver	12.3 ± 1.1	5.5 ± 0.9	10.4 ± 1.7
Spleen	7.1 ± 1.0	2.8 ± 0.3	6.4 ± 0.9
Kidney	17.0 ± 1.4	5.9 ± 0.5	6.1 ± 0.8
Stomach*	2.3 ± 0.3	1.4 ± 0.5	0.9 ± 0.2

\*percent injected dose per total organ and contents.

OPTIMIZATION OF  $^{99m}\text{Tc}$  DTPA FORMATION IN COMPETITION WITH DIRECT LABELING OF  $\text{F}(\text{ab}')_2$

C.H. Paik, L.N.B. Phan, J.J. Hong, S.Heald, M.S. Sahami, R.C. Reba and W.C. Eckelman<sup>1</sup>. Radiopharmaceutical Chemistry Section, The George Washington University Medical Center, Washington, D.C., 20037

Stable labeling of the  $\text{F}(\text{ab}')_2$  fragment of antibody with  $^{99m}\text{Tc}$  can be achieved via the conjugation of DTPA to  $\text{F}(\text{ab}')_2$  fragment using an acylation reaction(2) and subsequent complexation of the DTPA moiety of the  $\text{F}(\text{ab}')_2$  - DTPA conjugate with  $^{99m}\text{Tc}$  using the  $\text{SnCl}_2$  reduction method. The complexation reaction of DTPA with reduced  $^{99m}\text{Tc}$ , however, has three side reactions; re-oxidation of the reduced  $^{99m}\text{Tc}$  to form  $^{99m}\text{TcO}_4^-$ , hydrolysis of the reduced  $^{99m}\text{Tc}$  to form  $^{99m}\text{Tc}$  colloid, and complexation of the reduced  $^{99m}\text{Tc}$  directly with  $\text{F}(\text{ab}')_2$  to form a less stable complex. The outcome of these competing reactions could be influenced by the molar ratio of DTPA to  $\text{F}(\text{ab}')_2$ , the amount of stannous ions, the pH of the medium, the buffer system, the atmosphere, and the incubation time of stannous ion with DTPA and  $\text{F}(\text{ab}')_2$ . For this study, we used 0.1M acetate buffer to maintain pH at 4.5. The reaction solutions were purged with  $\text{N}_2$  and the reaction vials were evacuated in order to minimize the formation of  $^{99m}\text{TcO}_4^-$ . We then varied two parameters, DTPA/ $\text{F}(\text{ab}')_2$  and DTPA/ $\text{Sn}^{2+}$  ratios in order to optimize the complexation of  $^{99m}\text{Tc}$  with DTPA in the presence of  $\text{F}(\text{ab}')_2$ . As control experiments, free DTPA and  $\text{F}(\text{ab}')_2$  at a DTPA/ $\text{F}(\text{ab}')_2$  molar ratio of 4 were incubated with stannous chloride at a DTPA/ $\text{Sn}^{2+}$  molar ratio of 0.33, 1.0, 2.0 and 4.0 for 30 min. at pH 4.5. These solutions were then incubated with 200uCi of  $^{99m}\text{TcO}_4^-$  for 15 min. The final concentration of  $\text{F}(\text{ab}')_2$  was  $3.1 \times 10^{-5}\text{M}$  (155ug/50ul). The complexation reactions at the above DTPA/ $\text{Sn}^{2+}$  ratios gave rise to about equal percentage of both DTPA- $^{99m}\text{Tc}$  and  $\text{F}(\text{ab}')_2$ - $^{99m}\text{Tc}$ . However, the formation of DTPA- $^{99m}\text{Tc}$  was proportional to the DTPA/ $\text{F}(\text{ab}')_2$  ratio up to the ratio of 8 and leveled off at 84% DTPA- $^{99m}\text{Tc}$ . This indicates that a fraction of total  $\text{F}(\text{ab}')_2$  -  $^{99m}\text{Tc}$  has a higher formation constant than that of DTPA -  $^{99m}\text{Tc}$ . This side reaction to form directly labeled -  $^{99m}\text{Tc}$ - $\text{F}(\text{ab}')_2$  produced a 16% radiochemical impurity; the side reaction for  $^{99m}\text{TcO}_4^-$  and  $^{99m}\text{Tc}$  colloid were negligible under these conditions.

We then investigated the relative reactivity between  $\text{F}(\text{ab}')_2$ - conjugated DTPA and free DTPA toward  $^{99m}\text{Tc}$  by reacting reduced  $^{99m}\text{Tc}$  with a solution containing 1 DTPA molecule conjugated per  $\text{F}(\text{ab}')_2$  and various molar ratios of free DTPA. Competition studies at molar ratios of 7, 11, 15, 19, 29, 39 produced radiochemical yields of  $\text{F}(\text{ab}')_2$  - DTPA -  $^{99m}\text{Tc}$  of 30, 31.3, 32.8, 14.2, 9.0 and 3.8%. Using the molar ratios of free DTPA to  $\text{F}(\text{ab}')_2$  - DTPA the average relative rate of formation of  $\text{F}(\text{ab}')_2$  DTPA -  $^{99m}\text{Tc}$  was 4.9. This allows the addition of an excess of free DTPA in order to decrease the yield of directly bound  $\text{F}(\text{ab}')_2$  -  $^{99m}\text{Tc}$ .

Under optimal conditions using 1 conjugated DTPA for  $\text{F}(\text{ab}')_2$  in the presence of a 7 times molar excess of DTPA we can obtain 30% radiochemically pure  $\text{F}(\text{ab}')_2$  - DTPA- $^{99m}\text{Tc}$ .

- (1) Present Address: Department of Nuclear Medicine, Clinical Center, National Institutes of Health, Bethesda, MD 20205
- (2) Paik, C.H., Ebbert, M.A., Murphy, P.R., et al: J. Nucl Med 24, 1158, 1983.

$^{99m}\text{Tc}$  complexation of DTPA in competition with  $\text{F(ab}')_2$  ( $3.1 \times 10^{-5}\text{M}$ ) in 0.1M acetate at pH 4.5.

$\frac{\text{DTPA}}{\text{F(ab}')_2}$	$\frac{\text{DTPA}}{\text{Sn}^{2+}}$	$\frac{\text{SnCl}_2 \cdot 2\text{H}_2\text{O}}{\text{ug/ml}}$	DTPA - $^{99m}\text{Tc}$ (%)	$\text{F(ab}')_2$ - $^{99m}\text{Tc}$ (%)	$^{99m}\text{Tc}$ colloids(%)
1	0.33	21.0	19.2(14.2-24.7)	80.8(75.3-85.8)	-
2	0.33	42.0	28.9(26.2-32.1)	71.1(67.9-72.8)	-
4	0.17	168.0	23.6(23.3-23.9)	54.1(51.7-56.4)	22.3(19.7 25.0)
4	0.33	84.0	52.9(51.9-53.9)	47.1(46.1-48.1)	-
4	1.0	28.0	49.1(43.1-55.1)	50.9(44.9-56.9)	-
4	2.0	14.0	59.4(53.3-65.5)	40.6(34.5-46.7)	-
4	4.0	7.0	51.7(47.8-53.2)	48.3(46.0-52.2)	-
8	2.0	28.0	82.2(75.0-93.0)	17.8( 7.0-25.0)	-
12	1.5	56.0	81.0(72.0-90.0)	19.0(10.0-28.0)	-
16	2.0	56	84.5(80.0-89.0)	15.5(11.0-20.0)	-
20	2.5	56.0	84.5(83.8-85.2)	15.5(14.8-16.2)	-
28	3.5	56.0	87.6(87.4-88.1)	12.4(11.9-12.6)	-

The data are averages of duplicate to quadruplet experiments and their ranges in parenthesis.

Competition between  $\text{F(ab}')_2$  - DTPA and DTPA for  $^{99m}\text{Tc}$

$\frac{\text{Conjugated DTPA}}{\text{F(ab}')_2}$	$\frac{\text{Free DTPA}}{\text{F(ab}')_2}$	$\text{F(ab}')_2$ - DTPA - $^{99m}\text{Tc}$ (%) <sup>a</sup>	DTPA - $^{99m}\text{Tc}$ (%)	Relative Rate <sup>b</sup>
1	7	30.0 (27.5, 32.5)	54.0 (51.5, 56.5)	3.9
1	11	31.3	52.7	6.5
1	15	32.8 (32.6, 33.1)	51.2 (50.9, 51.4)	9.6
1	19	14.2 (12.3, 16.2)	69.8 (67.8, 71.7)	3.9
1	29	9.0 (8.1, 9.9)	75.0 (74.1, 75.9)	3.5
1	39	3.8 (3.6, 4.0)	81.8 (80.0, 83.7)	1.8
			Average	4.9

a. The data are obtained after subtracting 16% from total  $^{99m}\text{Tc}$  incorporated into  $\text{F(ab}')_2$  fragments.

b.  $\frac{\% \text{F(ab}') - \text{DTPA} - ^{99m}\text{Tc}}{\% \text{DTPA} - ^{99m}\text{Tc}} \times \frac{\text{DTPA}}{\text{conjugated DTPA}}$

$R_f$  values of radiochemicals in several solvent systems.

Radiochemicals	Chromatography	Solvent System	$R_f$
$TcO_4^-$	Whatman paper	Saline	0.7
$TcO_4^-$	Whatman paper	1.5:1 Acetonitrile:H <sub>2</sub> O	0.9
$TcO_4^-$	Silica gel	Acetone	1.0
Reduced-Hydrolysed Tc	Whatman paper	Saline	0
Reduced-Hydrolysed Tc	Whatman paper	1.5:1 Acetonitrile:H <sub>2</sub> O	0
Reduced-Hydrolysed Tc	Silica gel	Acetone	0
DTPA-Tc	Whatman paper	Saline	0.9
DTPA-Tc	Whatman paper	1.5:1 Acetonitrile:H <sub>2</sub> O	0.4
DTPA-Tc	Silica gel	Acetone	0
F(ab') <sub>2</sub> -DTPA-Tc	Whatman paper	Saline	0.9
F(ab') <sub>2</sub> -DTPA-Tc	Whatman paper	1.5:1 Acetonitrile:H <sub>2</sub> O	0
F(ab') <sub>2</sub> -DTPA-Tc	Silica gel	Acetone	0

GALLIUM-68 CHEMISTRY FOR LABELING PLATELETS, PROTEINS AND LIPOPROTEINS

Y. Yano, T. F. Budinger, C.A. Mathis, M. Singh, D. H. Moore, J. Hunter, R. M. Jones and S. N. Ebbe

Donner Laboratory, Lawrence Berkeley Laboratory, University of California, Berkeley, California 94720 USA

Generator produced  $^{68}\text{Ga}$  is a useful positron emitter for PET studies with a high resolution (2–4 mm) PET system for the study of thrombosis and atherosclerosis in cardiovascular disease.

Following the early work of Welch and Thakur with  $^{68}\text{Ga}$  and  $^{111}\text{In}$  (1, 2), we have studied the effects of trace metal contaminants in 1-N HCl eluates of  $^{68}\text{Ga}$  from a  $\text{SnO}_2$   $^{68}\text{Ga}$  generator (3). Both anion exchange resins,  $\text{AgI} \times 8$  (4) and semiautomated solvent extraction were (5) used to reduce trace metals in  $^{68}\text{Ga}$  eluates. Various ligands (L) such as oxine (Ox)(1), tropolone (Tro)(6), and mercaptopyridine oxide (MPO)(7) were used to assess the effect of their different binding constants for  $^{68}\text{Ga}$  on the labeling yields of platelets separated from rabbit, dog, and human plasma.

Chromatographic analysis of  $^{68}\text{Ga}$ -L formation was by ITLC and HPLC to determine the effects of trace metals, L concentration, pH, and buffers.  $^{68}\text{Ga}$ -Ox and  $^{68}\text{Ga}$ -Tro were analyzed by ITLC (SG) and  $\text{CH}_3\text{OH}:\text{CHCl}_3$  (5:95).  $^{68}\text{Ga}$ -MPO was analyzed by HPLC with  $\text{C}_{18}$  column and  $\text{CH}_3\text{OH}:\text{H}_2\text{O}$  (25:75) and 5–10 mM citrate. These chromatograms are shown in Figure 1. The  $^{68}\text{Ga}$ -L with optimum concentration of L were incubated with platelets and the labeling yields of  $^{68}\text{Ga}$ -platelets were determined in ACD:normal saline (1:7) normal saline, and plasma, Table I, below.

Ga-68 Pure	Vol	Ligand		Platelets*		After				
		Type	Conc. ( $\mu\text{g}$ )	Type	Conc.	Media	Initial Label (%)	Saline Wash (%)	Buffer-pH	
EE+	0.5/6.0	oxine	200	rab	$1.0 \times 10^{10}$	ACD:Sal	26	19	AC	6.8
EE	0.5/6.0	oxine	400	rab	$1.9 \times 10^{10}$	ACD:Sal	84	50	AC	6.8
EE	0.5/6.0	oxine	400	rab	$3.9 \times 10^9$	ACD:Sal	59	32	AC	6.8
EE	0.5/6.0	oxine	400	rab	$1.9 \times 10^9$	ACD:Sal	42	23	AC	7.0
EE	0.5/6.0	oxine	200	hum	$9.3 \times 10^9$	ACD:Sal	42	31	AC	7.0
EE	0.5/6.0	oxine	200	hum	$9.3 \times 10^9$	PPP	19	6	AC	7.0
AG1XB	0.5	oxine	100	dog	--	ACD:Sal	10	--	OH <sup>-</sup>	6.5
EE	0.5/6.0	Tro	40	dog	--	ACD:Sal	5	--	OH <sup>-</sup>	7.4
EE	0.5/6.0	Tro	20	dog	--	ACD:Sal	12	--	OH <sup>-</sup>	7.4
EE	0.5/6.0	Tro	60	dog	--	ACD:Sal	10	3	OH <sup>-</sup>	7.4
EE	0.5/6.0	MPO	200	hum	$2.3 \times 10^{10}$	Saline	63	56	OH <sup>-</sup>	7.0
EE	0.5/6.0	MPO	200	hum	$2.3 \times 10^{10}$	PPP	43	38	OH <sup>-</sup>	7.0

\*Incubation 25–37°C, 15 min.

+EE - Ether extraction

$^{68}\text{Ga}$ -MPO appears to give the best labeling yields of rabbit platelets for PET studies.  $^{68}\text{Ga}$ -Ox gives variable but adequate labeling of platelets while  $^{68}\text{Ga}$ -Tro is not suitable for platelet labeling.

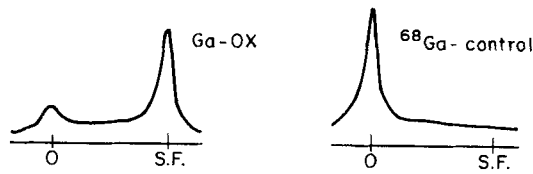
$^{68}\text{Ga}$  was labeled to proteins and low density lipoproteins by the method of Hnatowich (8) using as the bifunctional chelate the cyclic anhydride of DTPA.

Gel column chromatography and HPLC (9, 10) were used to separate the  $^{68}\text{Ga}$ -lipoprotein fraction in yields of 80–85% with a radiochemical purity of 95–98%.

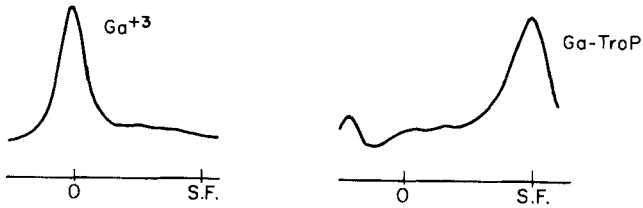
Figure 1.

GALLIUM-68 CHEMISTRY FOR LABELING PLATELETS, PROTEINS, AND LIPOPROTEINS Y. Yano

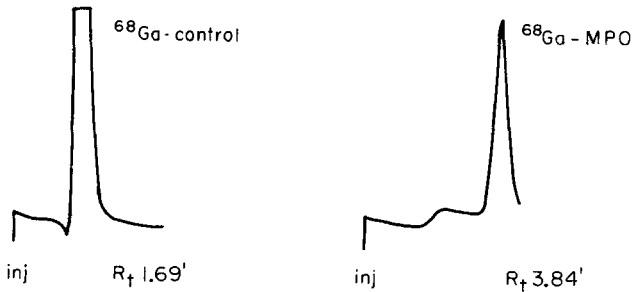
<sup>68</sup>Ga-oxine, 100μg, pH 7  
ITLC (SG)  
CH<sub>3</sub>OH: CH<sub>3</sub>Cl (5:95)



<sup>68</sup>Ga-Tropolone 100μg pH 6.6  
ITLC (SG) : CHCl<sub>3</sub>:CH<sub>3</sub>OH (99:1)



<sup>68</sup>Ga-mercaptopyridine-oxide (MPO)  
HPLC: C<sub>18</sub> Column  
CH<sub>3</sub>OH:H<sub>2</sub>O (25:75), 10mM Citrate





1,1,1-TRIS(5-METHOXYSALICYLIMINOMETHYL)ETHANE: A CHELATING AGENT FOR THE PREPARATION OF LIPOPHILIC GALLIUM AND INDIUM RADIOPHARMACEUTICALS

M.A. Green, C.J. Mathias and M.J. Welch

The Edward Mallinckrodt Institute of Radiology, Washington University School of Medicine, Saint Louis, Missouri 63110, U.S.A.

There is current interest in the preparation of new complexes of generator-produced gallium-68 as possible agents for the quantitation of regional cerebral and myocardial blood flow by positron emission tomography (PET). The desired gallium radiopharmaceutical must be lipophilic and possess sufficient kinetic stability to resist binding of the metal ion by the plasma protein transferrin for the duration of the study. For this purpose we have begun the investigation of a variety of salicylimines which are capable of bonding to the gallium (III) and indium (III) ions as polydentate chelating ligands.

Reaction of 1,1,1-tris(aminomethyl)ethane (1) with 5-methoxysalicylaldehyde affords the title compound (Figure 1). This ligand has the potential to occupy six coordination sites about a metal atom by bonding through the three imino nitrogen lone pairs and three deprotonated phenolic oxygen lone pairs (2). This ligand reacts with  $\text{Ga}(\text{acac})_3$  (where  $\text{acacH} = \text{acetylacetonone}$ ) in ethanol to form a yellow crystalline compound which gives satisfactory analysis (Galbraith Laboratories) for a 1:1 gallium:trisalicylimine complex,  $\text{C}_{29}\text{H}_{30}\text{N}_3\text{O}_6\text{Ga}$  (Calculated: C, 59.41; H, 5.16; N, 7.17; Ga, 11.89%.

Found: C, 59.67; H, 5.30; N, 7.00; Ga, 12.08%.

The gallium-68 complex of this ligand has been prepared using the eluent from the  $\text{SnO}_2/1\text{N HCl}$  generator (3). Evaporation of the generator eluent to dryness followed by addition of an ethanolic ligand solution leads to formation of a gallium-68 complex with an octanol/water partition coefficient of 27 and which migrates with  $R_f = 0.87$  on Whatman 1 paper eluted (4) with  $\text{H}_2\text{O}$  (700 ml):  $\text{EtOH}$  (200 ml):  $\text{NH}_4\text{OH}$  (0.35 ml).

The biodistribution of this gallium-68 complex following intravenous injection in rats has been determined with the results shown in Table 1. The behavior of this compound differs markedly from that of a weak chelate complex (citrate), which undergoes rapid exchange with transferrin (5). The compound does not cross the blood-brain barrier. However, it does show myocardial uptake and washout comparable to that of carbon-11 labeled butanol (6,7), which has been shown to be suitable for measurement of myocardial blood flow (8). These results suggest that the gallium-68 complex of 1,1,1-tris(5-methoxy-salicyliminomethyl)ethane may be suitable for use as a freely diffusible blood flow tracer for PET studies of the heart.

- (1) Fleischer E.B., Gembala A.E., Levey A., and Tasker P.A., *J. Org. Chem.*, **36**, 3042, (1971).
- (2) Dwyer F.P., Gill N.S., Gyrfas E.C., and Lions F., *J. Am. Chem. Soc.*, **79**, 1269, (1957).
- (3) Loc'h C., Maziere B., and Comar D., *J. Nucl. Med.*, **21**, 171, (1980).
- (4) Hnatowich D.J., *J. Nucl. Med.*, **16**, 764, (1975).
- (5) Moerlein S.M., Welch M.J., Raymond K.N., and Weitzl F.L., *J. Nucl. Med.*, **22**, 710, (1981).
- (6) Raichle M.E., Martin W.R.W., Herscovitch P., Kilbourn M.R., and Welch M.J., *J. Nucl. Med.*, **24**, P63, (1983).
- (7) Welch M.J., Human dosimetry data for carbon-11 labeled butanol, unpublished.
- (8) Hack S.N., Eichling J.O., Bergmann S.R., Welch M.J., and Sobel B.E., *J. Clin. Invest.*, **66**, 918, (1980).

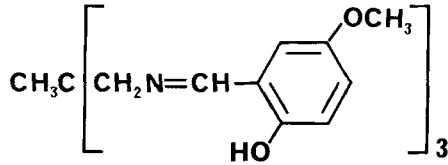


FIGURE 1. The structure of 1,1,1-tris(5-methoxysalicyliminomethyl)ethane.

TABLE 1. The biodistribution of the gallium-68 complex of 1,1,1-tris(5-methoxysalicyliminomethyl)ethane in rats.

	% ID per gram		
	1 minute	5 minute	60 minute
Blood	0.50 ± 0.09	0.27 ± 0.04	0.10 ± 0.01
Heart	0.76 ± 0.08	0.54 ± 0.09	0.16 ± 0.02
Lungs	1.40 ± 0.78	0.75 ± 0.25	0.18 ± 0.02
Liver	1.61 ± 0.19	1.46 ± 0.16	0.57 ± 0.06
Spleen	0.64 ± 0.20	0.39 ± 0.05	0.13 ± 0.01
Kidney	2.48 ± 0.07	1.43 ± 0.33	0.40 ± 0.07
Brain	0.030 ± 0.013	0.012 ± 0.003	0.006 ± 0.001

This work was supported by the United States Department of Energy (DOE) contract DE-AC02-77EV04318.

## DISTRIBUTION OF IN-111 IN GRANULOCYTE AND OTHER CELLULAR ELEMENTS OF BLOOD (CEB) IN HUMAN IN-111-LABELED MIXED WHITE CELL (MWC) AND PLATELET PREPARATIONS.

M. K. Dewanjee, S. Chowdhury, M.L. Brown and H.W. Wahner  
Mayo Clinic and Foundation, Rochester, MN 55905.

A large number of platelets (PLT), red blood cells (RBC) are present along with granulocyte (GC) in In-111 MWC preparation. Distribution of In-111 in CEB was determined by Ficoll-Hypaque gradient (FHG) centrifugation of In-111-MWC and PLT preparation as a quality control procedure. MWC were separated by sedimentation with hydroxyethyl starch; PLT by differential centrifugation. MWC and PLT were labeled with In-111-oxine in saline, ACD-saline or with In-111-tropolone in 0.5 ml of ACD-plasma. 0.3–0.5 ml of labeled cell suspended in plasma was layered on 3 ml FHG of two densities (1.119 and 1.077 gm/ml) and spun in a clear polystyrene tube at 1800 G for 30 min. Four layers (plasma, PLT, GC, and RBC) were separated, and In-111 radioactivity in each fraction was determined with a gamma counter. Simultaneously cell types in MWC and PLT preparations were determined by Coulter counter and differential counting. Percentages of In-111 distribution and cell populations (parentheses) in the preparations are tabulated:

	Plasma(%)	PLT(%)	GC(%)	RBC(%)
In-111-tropolone	9±4	29±15	31±16	31±13
MWC:ACD-plasma(n=9)		(74±2)	(5±3)	(22±23)
In-111-oxine	8±4	22±10	46±19	24±14
MWC:Saline(n=68)		(76±19)	(5±4)	(18±19)

Most of In-111 in In-MWC is associated with the PLT and RBC, GC/lymphocyte ratio is 6/4. GC has higher extraction efficiency than RBC and PLT. PLT preparation is pure and (96±3)% of In-111 is bound to PLT, (4±3)% to RBC and (0.2±0.1)% to GC: PLT preparation contains PLT (97±3)%, RBC (4±3)% and GC (0.2±0.1)%.

- (1) McAfee J.G. and Thakur M. L., *J. Nucl. Med.*, **17**, 480–688 (1976).
- (2) Weiblin B.J., Forstrom L., and McCullough J., *J. Lab. Clin. Med.*, **94**, 246 (1979).
- (3) Davis H.H., Heaton W.A., Siegel B.A., et al, *Lancet*, **1**, 1185 (1978).
- (4) Dewanjee M.K., Rao S.A., and Didisheim P., *J. Nucl. Med.*, **22**, 981–987 (1981).
- (5) Dewanjee M.K., Rao S.A., Chowdhury S., et al, "Indium 111-Labeled Platelets and Leukocytes", 1982, pp.97–125.
- (6) Dewanjee M.K., *Mayo Clinic Proc.*, (1984) In press.

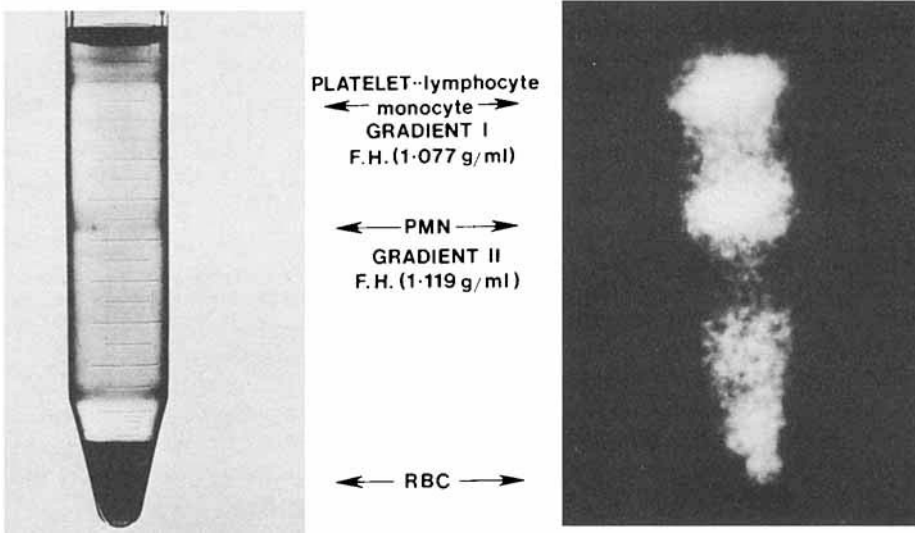


Fig. 1. Ficoll-Hypaque separation of In-111 mixed white cells. Note In-111 activity associated with platelet, RBC along with PMN leukocyte.

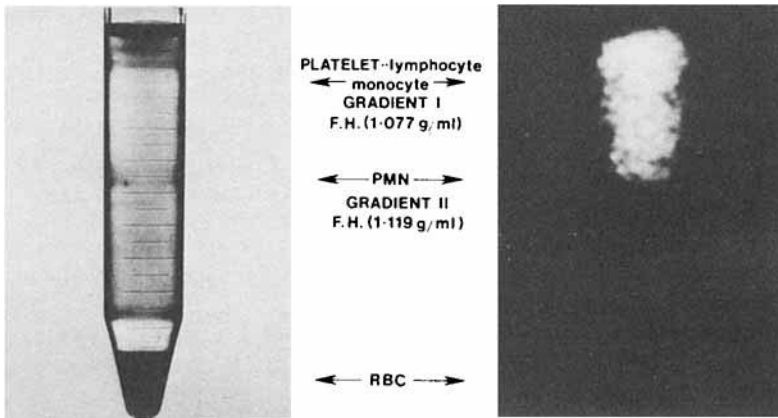


Fig. 2. Ficoll-Hypaque separation of In-111 platelets (human). Note probability of PMN leukocyte contamination by platelet aggregates.

NEW GALLIUM RADIOPHARMACEUTICALS.  
COMPLEXES OF PHENOLIC AMINOCARBOXYLATES

---

F.C. Hunt, Isotope Division, Australian Atomic Energy Commission, Lucas Heights Research Laboratories, PMB Sutherland, NSW 2232, Australia.

The phenolic aminocarboxylic acids, ethylenediamine di [o-hydroxyphenylacetic acid], (EDDHA) I and N, N'-bis [2-hydroxybenzyl] ethylenediamine N, N'-diacetic acid, (HBED) II are chelating agents having high formation constants for ferric and gallic ions ( $\log K > 30$ ). (1) These chelators have been proposed for the decorporation of iron from thalassemia patients. (2) Similarly, they are able to remove pre-injected gallium-67 from the blood of animals bearing tumors, thereby increasing tumor-to-blood ratios. (3)

Because of their high formation constants with gallium, these ligands were complexed with gallium-67 as potential radiopharmaceuticals, as they should resist exchange of gallium with plasma transferrin.

The chelating agents were synthesised by literature methods with substituents in the phenolic ring to direct excretion of gallium complexes via the hepatobiliary or renal routes. (4), (5)

Gallium-67 complexes of the EDDHA and HBED ligands were made by ligand exchange from gallium-67 citrate. Analysis by high performance liquid chromatography confirmed that ligand exchange had occurred, with the formation of gallium-67 phenolic aminocarboxylates having characteristic retention times on reverse-phase columns.

Biodistribution studies in mice revealed patterns of hepatobiliary and renal excretion consistent with complexes having partially lipophilic and hydrophilic properties respectively. The results of the biodistribution studies are shown in table 1 with gallium-67 citrate as control. Gallium-67-Br-EDDHA was excreted via the hepatobiliary route with 85% of the injected dose present in the bile and G.I.T one hour post injection.

The  $^{67}\text{Ga}$ -Br-HBED complex was also excreted via the hepatobiliary route with a greater retention in the liver. In contrast,  $^{67}\text{Ga}$ -COOH-EDDHA was excreted via the renal route with 79% present in the urine one hour post injection.

Scintigraphic images of rabbits injected with  $^{67}\text{Ga}$ -Br-EDDHA demonstrated initial liver images followed by visualisation of the gall bladder and G.I.T.

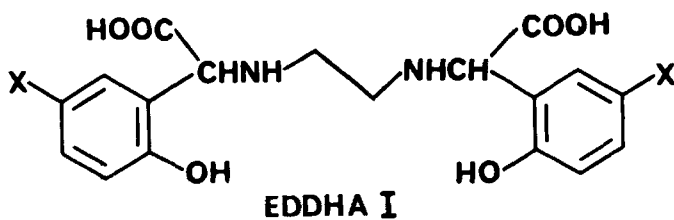
These results indicate that new radiopharmaceuticals of  $^{67}\text{Ga}$  may be formed from the phenolic aminocarboxylates EDDHA and HBED. They may be useful where agents of longer half-life are required or when complexed with  $^{68}\text{Ga}$  for positron emission tomography.

- (1) Harris W.R. and Martell A.E. *Inorg. Chem.* 15, 713 (1976).
- (2) Pitt G.G. and Martell A.E., *The Design of Chelating Agents for the Treatment of Iron Overload*. ACS Symposium No. 140, Elsevier, North Holland. 1980 p. 280.
- (3) Hunt F.C. and Maddalena D.J., *J. Lab. Cpd. Radiopharm.* 19, 1408 (1982).
- (4) Dexter M. and Cranston R.J., U.S. Patent 2, 824, 128 (1958).
- (5) Geigy (A-G)., Brit. Patent 843,003 (1960).

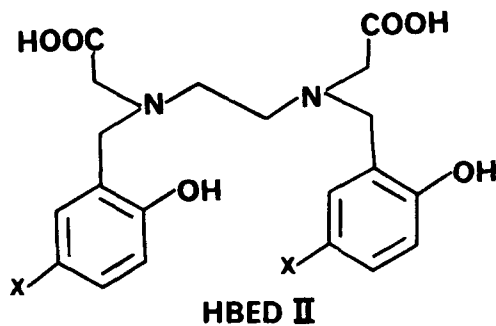
Table 1. Biodistribution of  $^{67}\text{Ga}$ -Chelates  
of Phenolic aminocarboxylates\*

$^{67}\text{Ga}$ -Chelate	Blood	Liver	Kidneys	G.I.T.+Bile	Urine
Citrate	27.0±4.2	5.8±0.8	3.0±0.1	9.9±0.4	7.0±2.2
Br-EDDHA	1.2±0.6	3.9±0.6	0.7±0.3	85.4±7.6	2.9±1.7
Br-HBED	0.4±0.2	17.6±2.5	0.4±0.2	70.7±5.4	7.3±1.8
COOH-EDDHA	0.6±0.1	0.5±0.1	2.0±1.0	0.5±0.1	79.2±4.7

\* Percentage of injected dose 1 hour post injection. Means ± Sd of 3 animals.



$X = \text{H}, \text{COOH}, \text{SO}_3^-, \text{Cl}, \text{Br}$



PRODUCTION AND BIODISTRIBUTION OF SOME ZINC-63 COMPOUNDS

D.J. Schlyer, M.A. Qureshi, D.F. Wolczak and C.R. Martin  
Research Centre, King Faisal Specialist Hospital, Riyadh 11211, Saudi Arabia

Zinc-63 is a positron-emitting isotope with a 38.5 minute half-life which holds great promise for metabolism studies and for the labelling of metal chelating agents. A relatively simple method has been devised for the preparation and purification of this isotope. The preparation is a modification of a procedure used by Bigler et al (1). Biodistribution has been done for the chloride in rats and a dog. Data will also be presented on the biodistribution of hematoporphyrin derivatives.

The target material is cupric oxide powder pressed into a copper target holder at a pressure of 6000 psi. The powder is covered with a 60 mil aluminum foil to degrade the energy from 25 to 17 MeV. The lower energy minimizes the impurities from the  $^{63}\text{Cu}(p,2n)^{62}\text{Zn}$  nuclear reaction.

After irradiation, the target holder is transported from the beam line to the hot cell by means of a pneumatically operated iso-rabbit system. The cup is dissembled from the target, the cover foil removed and the cupric oxide powder dissolved in 2.5 M HCl. After dissolution, a few drops of 30%  $\text{H}_2\text{O}_2$  are added to ensure oxidation to cupric ion. The excess peroxide is decomposed with heat and the solution allowed to cool.

The apparatus used for the separation is shown in Figure 1. A Swinnex-25 mm 0.45  $\mu\text{m}$  filter unit is loaded with 0.5 gram of Bio-Rad AG1-X8 anion exchange resin. The solution is syphoned into the upper syringe from outside the hot cell. The solution is forced through the resin and millipore and rinsed several times with 10 ml volumes of 2.5 M HCl. The zinc is then eluted off the column with 0.05 M NaOH. The solution is neutralized and filtered through a 0.22  $\mu\text{m}$  millipore filter before injection. The total time for processing is twenty-five minutes. The copper concentration in the final solution is less than 5  $\mu\text{g}/\text{ml}$  and the yield of Zn-63 is approximately 150 mCi.

The time course of the biodistribution is shown in Figure 2. These data can be compared to biodistribution studies of Zn-65 chloride solutions, although there is no data at the very short times of this study (2,3). PET scans of Zn-63 chloride in the dog have been done and will be presented along with the PET scans using the zinc-63 hematoporphyrin derivatives.

1. Bigler, R.E., Dahl, J.R., Rotman, L.S., and Zanzonico, P.B., Abstracts Fourth International Symposium on Radiopharmaceutical Chemistry, Julich p.159 (1982).
2. Bergman, B., Acta. Radiologica Therapy Physics Biology 9:577 (1970).
3. Byar, D.D., Anderson, J.E. and Mostofi, F.K., Investigative Urology 7:57 (1969).

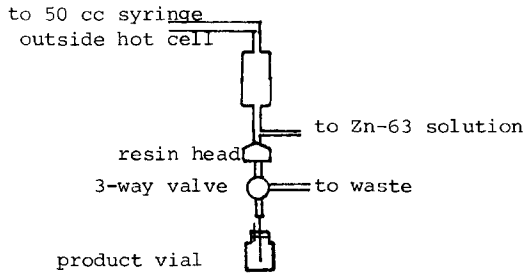


Figure 1: Schematic diagram of Zn-63 purification system

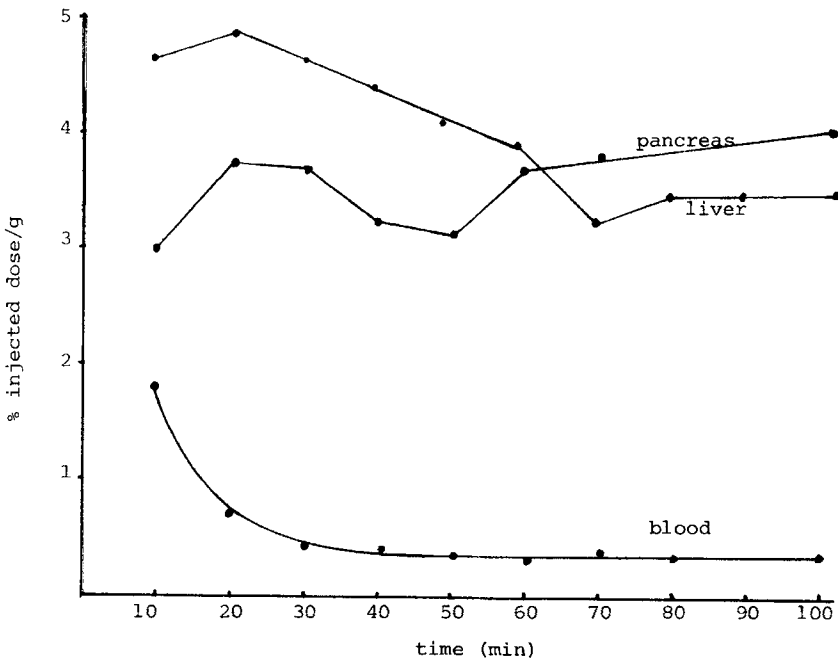


Figure 2: Plot of % injected dose/g versus time  
each point represents average of 4 rats



## Zn-EDDA IN THE PANCREAS: EFFECT OF HORMONAL STIMULATION

Y.Fujibayashi, I.Yomoda, A.Yokoyama, T.Torizuka  
Radioisotopes Laboratory, Kyoto Univ. Hospital, Kawahara-cho  
Shogoin, Sakyo-ku Kyoto 606, Japan

Procurement of morphological and anatomical studies of the pancreas have been made possible with the availability of positron emitting C-11 or N-13 labeled amino acids, actively used in the protein synthesis (1). Being aware of the very interesting physiologic anatomy of pancreatic gland, and its long association with zinc(Zn), an essential metal in the function of this organ, exploitation of Zn pharmacokinetic as a tool for diagnostic studies was conceived. In our early findings (2), high pancreas distribution of radioactive Zn, if administered as Zn-EDDA (Ethylenediamine-N,N'-diacetic acid) was achieved (Fig.1). Since a positron emitting radionuclide of Zn, a Zn-62 (half life = 9 h) has become commercially available, applicability of the newly developed Zn-EDDA in functional studies of the pancreas was visualized.

Pancreas fulfills both, exocrine and endocrine functions, secreting externally (pancreatic juice) under the control of the hormone secretin (Sec) and cholecystokinin-pancreozymin (CCK-PZ), and internally into the blood or lymph (insulin) under the control of blood glucose (3). In the present study, the effect of those hormones on pancreas uptake of Zn (biodistribution in mice), and on the pancreatic secretion of Zn (pancreatic duct cannulation performed in rats by modified Love's method (4) ) were estimated. Thus, upon the intravenous administration of Zn-65 (half life = 270 days), response changes to the stimulation of gastro-intestinal(GI) hormone like Sec,CCK-PZ and its synthetic analog, caerulein as well as glucose were performed. In mice studies, pancreas specific decrease of Zn activity was observed under GI hormone stimulation (Table 1), distinctive from glucose (Table 2). In rat cannulation studies, high Zn-65 secretion was found under CCK-PZ stimulation (pancreatic protein secreting hormone), 3 hrs post Zn-65 injection (Fig.2). These results indicated the great participation of exocrine system in the mobilization of Zn; namely the enhancement of exocrine protein secretion in response to CCK-PZ favoured the functional study of positron computed tomography in dog using Zn-62-EDDA (1 mCi/kg, 10 kg). In order to validate the exocrine Zn secretion state, column chromatography (Sephacryl S-200) analysis of human pancreatic juice was performed. Among the various eluted fractions, most of the native Zn was detected in protein containing fractions. Participation of Zn, administered as Zn-EDDA, in the metabolic pathway of protein synthesis (digestive enzymes), and reliability of exocrine function stimulation as a tool for functional imaging is discussed.

- (1) K.Kubota, et al. Eur. J. Nucl. Med. vol.8, 528 (1983)
- (2) Y.Fujibayashi, et al. J. Nucl. Med. vol.19, P123 (1983)
- (3) A.S.Prasad, "Trace Elements in Human Health and Disease" vol.1 P198, Academic Press (1976)
- (4) J.W.Love, J. Exp. Physiol. vol.42, 279 (1957)

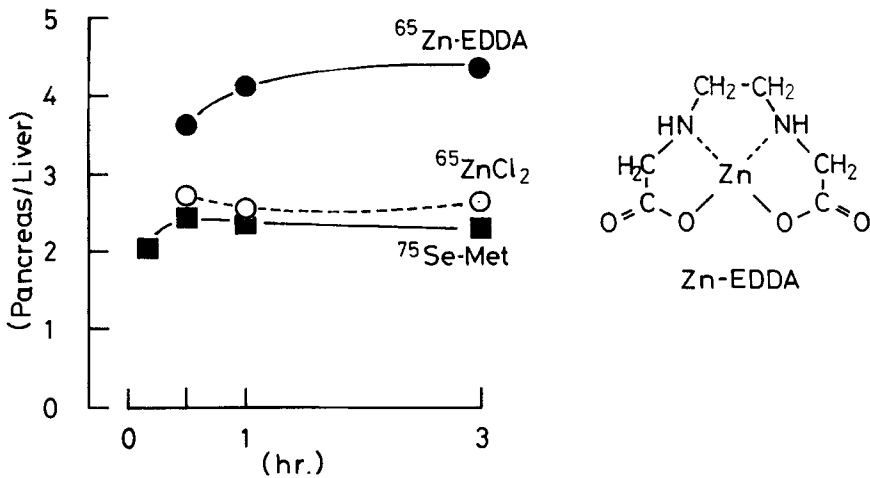


Fig. 1 Mice biodistribution studies: Pancreas to Liver concentration ratio (ddY male mice, average of 5 animals)

Table I. Effect of Gastro-Intestinal Hormone Post-stimulation<sup>a)</sup>  
(Biodistribution of Zinc-65 in mice.)<sup>b)</sup>

Time(hr) <sup>c)</sup>	Secretin		CCK-PZ		Control	
	1	3	1	3	1	3
Blood	1.17 (0.46)	1.02 (0.12)	1.12 (0.33)	0.97 (0.28)	1.30 (0.27)	1.19 (0.45)
Pancreas	9.30 (3.26)	12.85 (5.52)	10.16 (1.51)	10.20 (3.81)	24.67 (4.91)	28.78 (1.45)
Liver	13.33 (3.61)	10.98 (1.93)	12.63 (2.43)	11.83 (1.35)	13.96 (4.02)	13.10 (2.60)
Kidney	15.71 (4.49)	11.94 (1.59)	17.00 (4.11)	13.13 (1.81)	14.36 (1.43)	11.88 (1.08)
Intestine	3.30 (0.95)	4.37 (1.18)	3.86 (0.58)	4.30 (1.67)	6.39 (1.89)	7.56 (0.45)
Pancreas/ Liver	0.69 (0.19)	1.14 (0.33)	0.82 (0.18)	0.85 (0.27)	1.81 (0.29)	2.25 (0.37)

a) Stimulation performed 30 min. before sacrifice.

b) % dose/g organ (1 s.d.) : average of 5 animals.

c) Sacrifice time after Zinc-65 injection.

Table 2. Effect of Glucose Post-stimulation  
(Biodistribution of Zinc-65 in mice)

Time(hr) <sup>c)</sup>	1	3
Blood	1.52 (0.34)	1.06 (0.14)
Pancreas	18.25 (5.25)	28.83 (3.20)
Liver	12.42 (2.60)	14.39 (3.13)
Kidney	16.52 (3.92)	14.39 (2.06)
Intestine	5.80 (1.30)	8.94 (1.15)
Pancreas/ Liver	1.46 (0.28)	2.05 (0.52)

a) Stimulation performed 30 min. before sacrifice.  
 b) %dose/g organ (1 s.d.) : average of 5 animals.  
 c) Sacrifice time after Zinc-65 injection.

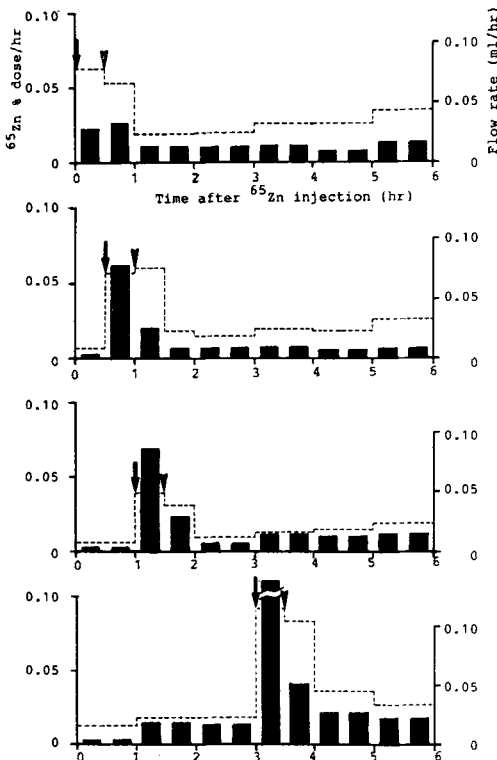


Fig. 2 Stimulation effect on pancreatic secretion(ml/hr:dotted line), and conc. of Zn-65(% dose/hr:black bar) in pancreatic juice. ↓CCK-PZ + ↓Secretin stimulation(arrows)

CARBOXYLIC ACID DERIVATIVES OF OXOTECHNETIUM (+5) BISAMIDO BISTHIOLATES

J. Lister-James, D.E. Brenner, A.G. Jones, A. Davison and A.R. Fritzberg  
Department of Radiology, Harvard Medical School, Boston, Massachusetts 02115

At the last conference in 1982, we reported on the first compounds in two new series of bisamido bithiolates ( $N_2S_2$ ), namely N,N'-bis(2-mercaptoethyl)oxamide and N-(2-mercaptoethyl)mercaptoacetyl-glycinamide and the corresponding oxotechnetium (+5) complexes (1). These compounds are isomers of the first  $N_2S_2$  system investigated,  $[TcO(ema)]^{-1}$  (or Tc-DADS) (2,3). A full account of the synthesis and characterization of these new materials will be published shortly (4). The  $^{99m}Tc$  complexes of these prototype ligands show good, but not optimal, renal clearance as compared to iodohippurate, much as the complex  $TcO(ema)^{-1}$  (3,5). In a continuing search for a more effective replacement for OIH, we have now prepared several carboxylic acid derivatives of the two new series. These include (R)-mercaptoacetyl-glycyl-cysteine; (R)-mercaptoacetyl-glycyl-cysteinyl-glycine; (R)-N-(2-mercaptoethyl)-N'-(1-carboxy-2-mercaptoethyl)oxamide; and (R),(R)-N,N'-bis(1-carboxy-2-mercaptoethyl)oxamide. All four ligands have been fully characterized both as their methyl esters and as their S-benzoyl protected methyl esters.

Using dithionite reduction of  $TcO_4^-$  (3) in ethanolic base we have prepared the  $^{99m}Tc$ -oxotechnetium (+5) complexes of these ligands in  $> 95\%$  yield and  $> 95\%$  purity. The first three ligands each give a pair of diastereomeric complexes (no enantiomers) which are separated as two peaks by reverse-phase ion-pair HPLC. N,N'-bis(1-carboxy-2-mercaptoethyl)oxamide, on the other hand, gives a single meso complex (one peak by HPLC). Preliminary studies in animals show rapid renal clearance for all the complexes except the meso oxamide, which is excreted relatively slowly. Most notably, the diastereomeric complexes of mercaptoacetyl-glycylcysteine both show virtually identical excretion rates which are seen to be comparable to OIH in mice and in dogs. Additionally, there appears to be minimal hepatobiliary clearance in contrast with, for example,  $[^{99m}TcO(ema)]^{-1}$  (3,5). This material would therefore appear to be suitable for testing as a replacement for iodohippurate, particularly since it does not suffer from the need for HPLC separation of the diastereomers as is the case with the  $CO_2$ -DADS complexes (6,7).

- (1) Jones A.J., Davison A., Brodack J.W., and Brenner D., Lister-James J., Costello C.E., Lock C.J.L., Franklin K.J., LaTegola-Graff M.R., Orvig C., and Sohn, M., Proc. 4th Intern. Symp. on Radiopharm. Chem., Julich FRG, 1982, p.333.
- (2) Davison A., Sohn M., Orvig C., Jones A.G., and LaTegola M.R., J. Nucl. Med. 20, 641 (1979).
- (3) Jones A.G., Davison A., LaTegola M.R., Brodack J.W., Orvig C., Sohn M., Toothaker A.K., Lock C.J.L., Franklin K.J., Costello C.E., Carr S.A., Biemann K., and Kaplan M.L., J. Nucl. Med. 23, 801 (1982).
- (4) Brenner D., Davison A., Lister-James J., and Jones A.G., Inorg. Chem. (in press).
- (5) Klingensmith W.C., III, Gerhold J.P., Fritzberg A.R., Singer C., Spitzer V.M., and Kuri C.C., J. Nucl. Med. 22, p.38 (1981).
- (6) Fritzberg A.R., Kuri C.C., Klingensmith W.C., III, Stevens J., and Whitney W.P., J. Nucl. Med. 23, 592 (1982).
- (7) Klingensmith W.C., III, Fritzberg A.R., Spitzer V.M., Johnson D.L., Kuri C.C., Williamson M.R., Washer G., and Weil R., III, J. Nucl. Med. 25, 42 (1984).

(2-Benzoylthioacetyl)-glycyl-(S-benzoyl)-cysteine methyl esterAnalysis for  $C_{22}H_{22}N_2O_6S_2$ :

	C	H	N	S
calculated	55.68	4.67	5.90	13.51
found	55.64	4.71	5.86	13.54

mp: 138–140° C

 $\alpha_D$ : +31° (c=0.43,  $CHCl_3$ )

$^1H$  NMR (250 MHz,  $CDCl_3$ )  $\delta$  3.55 (m, 2H,  $CHCH_2S$ ), 3.72 (s, 3H,  $CH_3$ ), 3.78 (s, 2H,  $COCH_2S$ ), 4.01 (m, 2H,  $COCH_2N$ ), 4.86 (m, 1H, CH), 7.26 (m, 2H, NH), 7.42 (m, 4H, m-aryl), 7.57 (m, p-aryl), 7.93 (m, 4H, o-aryl).

(2-Benzoylthioacetyl)-glycyl-(S-benzoyl)cysteinyl-glycine methyl esterAnalysis for  $C_{24}H_{25}N_3O_7S_2$ :

	C	H	N	S
calculated	54.22	4.74	7.90	12.06
found	53.99	4.76	7.87	12.00

mp: 181–183° C

 $\alpha_D$ : -15.6° (c=0.48, dioxan)

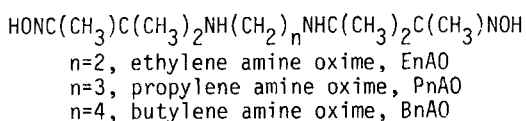
$^1H$  NMR (250 MHz,  $CDCl_3$ )  $\delta$  3.55 (m, 2H,  $CHCH_2S$ ), 3.71 (s, 3H,  $CH_3$ ), 3.78 (s, 2H,  $COCH_2S$ ), 3.9–4.1 (m,  $NCH_2CO$  and  $NCH_2CO$ ), 4.75 (m, 1H, CH), 7.04 (m, 1H, NH), 7.18 (m, 1H, NH), 7.22 (m, 1H, NH), 7.46 (m, 4H, m-aryl), 7.60 (m, 2H, p-aryl), 7.94 (m, 4H, o-aryl).

Tc-99 COMPLEXES OF AMINE OXIMES

D.E. Troutner, K. Aston, and W.A. Volkert

Department of Chemistry, University of Missouri  
Columbia, Missouri 65211, USA

Recent studies by Volkert, et al. (1) have shown significant differences in the chemical and biological properties of complexes of Tc-99m with multidentate amine oxime ligands. These ligands can be represented by the formulas and common names below.



In rodents neither Tc-AO or Tc-BnAO showed the significant brain uptake found with Tc-PnAO (2). Tc-AO was cleared primarily by the kidneys and Tc-PnAO by the liver and intestines. Tc-BnAO was also cleared by the liver and intestines but with greater kidney clearance than Tc-PnAO. As part of an attempt to relate the biological activity of these complexes to their structures, Tc-99 complexes of AO, PnAO, and BnAO were prepared. Tc-EnAO was not attempted since it could not be produced in high-yield with Tc-99m.

Complexes were prepared by reacting 0.03-0.06 mmoles of Tc-99 (spiked with Tc-99m) as  $\text{NH}_4\text{TcO}_4$  with a two or three-fold excess of ligand in 10 to 20 ml of saline solution buffered with 0.1M  $\text{NaHCO}_3$ . Small portions of  $\text{SnCl}_4 \cdot 5\text{H}_2\text{O}$  slurried in saline were added, usually in two-fold excess. The resulting mixture was filtered to remove solids and the filtrate analyzed by acetone and saline ascending solvent paper chromatography and electrophoresis. All complexes moved with the solvent in saline. In acetone, however, Tc-PnAO moved with the solvent, Tc-AO moved only slightly, and Tc-BnAO appeared to have two components, 20-30% remaining at the origin and the rest moving with the solvent. Each complex appeared to be neutral upon electrophoresis and there was evidence for only a few percent of  $\text{TcO}_4^-$  in each. A small portion of each filtrate was extracted from saline with an equal volume of  $\text{CHCl}_3$ . Less than 1% of Tc-AO was extracted, approximately 50% of the Tc-BnAO, and greater than 95% of the Tc-PnAO. Paper chromatography of the Tc-BnAO extracted into  $\text{CHCl}_3$  gave chromatograms similar to those for Tc-PnAO and that remaining in the aqueous fraction gave ones similar to Tc-AO. About 30% of the Tc-BnAO could be back

extracted into saline, but only a few percent of the Tc-PnAO. All of these observations are consistent with previous Tc-99m results for these same complexes (1,3).

No further experiments were done with Tc-AO since its hydrophilic properties were consistent with biodistribution. The filtrates of the other two complexes were extracted with several portions of  $\text{CHCl}_3$  and the solvent allowed to evaporate. The resulting oily solids were taken up in  $\text{CH}_3\text{OH}$ . Both  $\text{CHCl}_3$  and  $\text{CH}_3\text{OH}$  solutions of Tc-PnAO were orange and those of Tc-BnAO were green. Slow evaporation of the  $\text{CH}_3\text{OH}$  solutions after addition of a few drops of water resulted in orange-red crystals of Tc-PnAO but a noncrystalline solid of Tc-BnAO which was reddish brown. The crystal structure of Tc-PnAO has been reported elsewhere (4) and is a distorted square pyramid with a  $\text{TcO}^{3+}$  core, deprotonated amine nitrogens, and a hydrogen bond between the oxime oxygens. A partial characterization of the Tc-BnAO solid was done in order to compare it to Tc-PnAO. Proton NMR in  $d_6$ -DMSO of both solids showed methyl groups at 2.226, 1.409, and 1.369 ppm for Tc-PnAO and 2.222, 1.424, and 1.393 ppm for Tc-BnAO. These are characteristic of amine oxime complexes without ring puckering and suggest a Tc-BnAO structure similar to that of Tc-PnAO. There was also a resonance at 19.33 ppm in agreement with the one found in Co(III) and Rh(III) complexes of BnAO (5) indicating a hydrogen bond between the oxime oxygens. However, there is an IR band at  $\sim 890\text{ cm}^{-1}$  in Tc-BnAO which might indicate a  $\text{TcO}_2^{1+}$  core, while the Tc-PnAO has a band at  $925\text{ cm}^{-1}$ , consistent with the  $\text{TcO}^{3+}$  core found in the crystal. The greater hydrophilicity of the Tc-BnAO might also be due to a  $\text{TcO}_2^{1+}$  core. Attempts are underway to grow Tc-BnAO crystals suitable for X-ray and neutron diffraction determination of its structure.

Tc-AO is a neutral but hydrophilic complex which would be expected to show biodistributions unlike those of Tc-PnAO. Two species of Tc-BnAO are indicated, one with properties similar to Tc-AO and another similar to Tc-PnAO, but significantly more hydrophobic, which would explain biodistributions for Tc-BnAO intermediate between those for Tc-AO and Tc-PnAO.

1. W.A. Volkert, unpublished results.
2. W.A. Volkert, D.E. Troutner, T.J. Hoffman, R.M. Seger and R.A. Holmes, *J. Nucl. Med.* 24, P128 (1983).
3. D.E. Troutner, W.A. Volkert, T.J. Hoffman, and R.A. Holmes, *Int. J. Appl. Rad. and Isotop.*, in press.
4. C.K. Fair, D.E. Troutner, E.O. Schlemper, R.K. Murmann, and M. Hoppe, submitted to *Acta Cryst. C*.
5. E.O. Schlemper and S. Siriparisarnpipat, *Inorg. Chem.*, in press.

SYNTHESIS OF NEW BIS-AMINOETHANETHIOL(BAT) DERIVATIVES:  
POSSIBLE LIGANDS FOR Tc-99m BRAIN IMAGING AGENTS

---

H.F. Kung, C.C. Yu, J. Billings, M. Molnar and M. Blau\*  
Department of Nuclear Medicine, SUNY/Buffalo and VA Medical Center,  
Buffalo, NY 14215 and \*Department of Radiology, Harvard Medical  
School, Boston, MA 02115

Several neutral lipid-soluble Tc-99m bis-aminoethanethiol (BAT) complexes, an  $N_2S_2$  ligand, have been shown to cross the blood-brain barrier (J Nucl Med, March 1984). In order to prepare BAT derivatives for structure-activity relationship study we have developed two versatile synthetic methods which can specifically place substitution groups on one of the carbons between the two nitrogens. By voiding substitution of the N or S positions, the ability to form stable and neutral Tc-99m complex is unchanged.

In the first reaction route (Scheme 1) the cyano and oxime groups on ethyl cyanoglyoxylate-2-oxime (**1**) were simultaneously reduced by catalytic hydrogenation. The ethyl 2,3-diaminoproprionate (**2**) was reacted with 2,2'-dithio-bis-(2-methylpropanal) to give a 10-member ring diimine (**3**). When the diimine was treated with sodium borohydride at 50°C, a free hydroxy derivative (**4**) of BAT was obtained. The diimine (**3**) can also be converted to the amide (**5**) by reacting with concentrated ammonia at room temperature. Subsequent reduction of the amide (**5**) with diborane gave the free amine (**6**). All of the reactions in Scheme 1 gave excellent yield (over 90%), except the last diborane reduction step, which was 60%.

The second route employs the Strecker reaction for preparing  $\alpha$ -aminonitriles (Scheme 2 and 3). Using cyclohexanone (**7**) or 2-methoxybenzaldehyde (**14**) as the starting material, the  $\alpha$ -amino nitrile derivatives can be prepared. After reducing the aminonitriles with lithium aluminum hydride, the diamines (**9** and **16**) were condensed with dialdehydes to give the corresponding diimines (**10** and **17**). The dimercapto and diimine bonds were reduced simultaneously by "Red-Al" to give the desired BAT compounds (**12** and **18**). Compound **18** was treated with boron tribromide, a demethylating agent, to give a phenolic compound (**19**).

By using Sn(II)-PPI or sodium borohydride as the reducing agent, the BAT derivatives were labeled successfully with Tc-99m pertechnetate. The purity of the Tc-99m BAT complexes was > 95% (HPLC, reverse-phase column, acetonitrile: pH 7.0 dimethylglutaric acid buffer). Partition coefficient (P.C.) of these Tc-99m complexes was measured (1-octanol: pH 7.0 Buffer).

The biodistribution in rats (i.v. injection) was evaluated using I-125 iodoantipyrine (IAP), a freely diffusible tracer, as the internal reference. Compounds with a free hydroxyl group (**4** and **19**) showed lower brain uptake, inspite of high P.C.; this may be related to *in vivo* instability of the complexes. High initial brain uptake was observed for three compounds (**6**, **18** and **12**), however, only compound **12** (P.C.=384) showed significant brain retention.

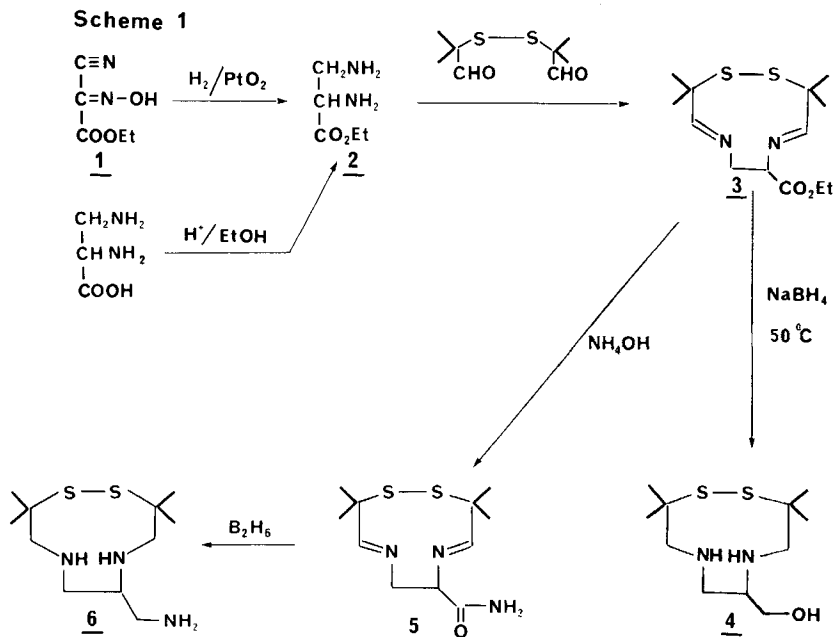


These schemes provide convenient and versatile synthetic routes for preparing BAT derivatives with unsubstituted  $N_2S_2$  ligand. Compounds of this type may be useful as brain imaging agent in themselves or as a basis for further structure-activity relationship study to improve brain uptake and retention.

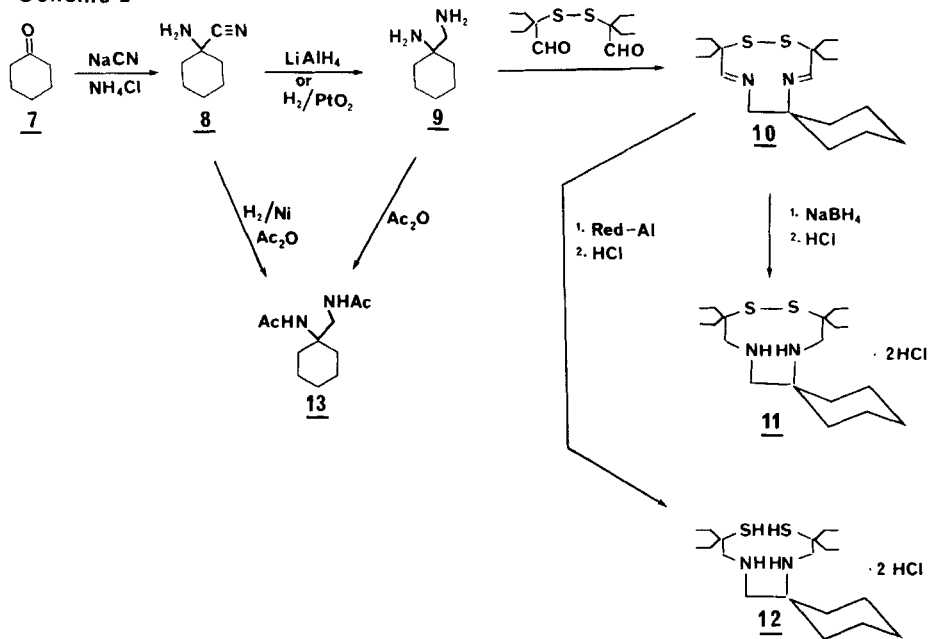
	$R_1$	$R_2$	$R_3$	P.C. <sup>+</sup>	2 Min*	15 Min*	
	<u>4</u>	CH <sub>3</sub>	H	64	0.4(0.3)	0.2(0.5)	
	<u>6</u>	CH <sub>3</sub>	H	47	1.3(1.0)	0.3(0.5)	
	<u>18</u>	CH <sub>3</sub>	H	260	2.3(1.7)	0.3(0.7)	
	<u>19</u>	CH <sub>3</sub>	H	197	0.4(0.3)	0.2(0.4)	
	<u>12</u>	C <sub>2</sub> H <sub>5</sub>			384	2.2(1.1)	0.7(1.2)

\*Total % brain uptake (ratio of Tc-99m BAT/I-125IAP in brain)

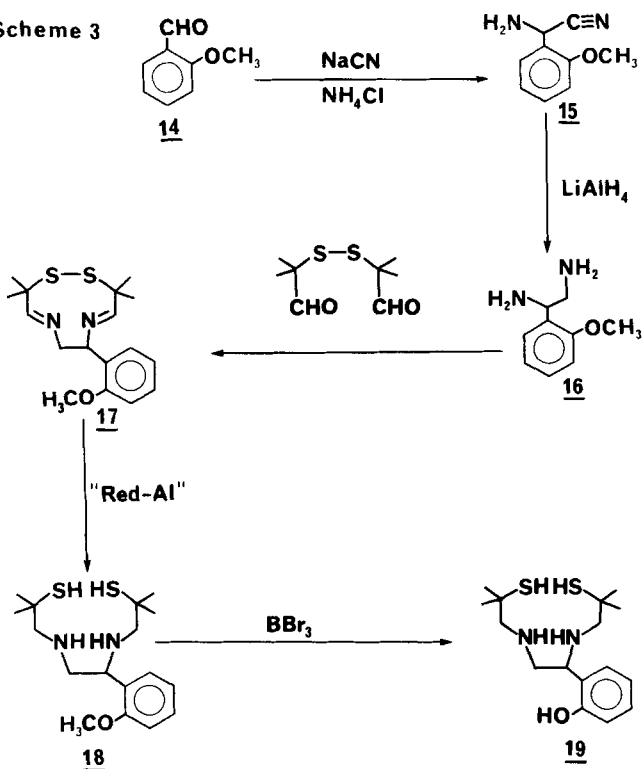
<sup>+</sup>Partition coefficient (1-octanol: pH 7.0 buffer)



Scheme 2



Scheme 3



TECHNETIUM-99m-LABELED PARA AMINOHIPPURIC ACID ANALOG: A NEW RENAL AGENT

L.R. Chervu, B.M. Sundoro and M.D. Blaufox

Department of Nuclear Medicine, Albert Einstein College of Medicine, Bronx, New York 10461.

I-131-iodohippuric acid is the radiopharmaceutical of choice in the evaluation of renal tubular secretory function (1). However, it has the disadvantage of imparting a high absorbed radiation dose to the patient besides having unsuitable energy radiations for gamma camera imaging. A Tc-99m labeled renal agent which is quantitatively secreted by the tubules has been sought unsuccessfully for many years.  $^{99m}\text{Tc}$ -DADS (N,N'-bis(mercaptoacetamido)ethylene diamine)) has been reported as suitable for assessing renal function but it involves considerably complicated procedures for its preparation (2). A PAH analog which possesses functional groups for Tc-99m binding as well as hippurate-like renal secretory properties is reported here.

Of the two PAH analogs prepared, the first compound (N<sup>4</sup>,N<sup>4</sup>-(diacetylamino)-hippuric acid) does not yield a stable complex with Tc-99m. The second, N<sup>4</sup>-(carbonylmethyliminodiacetic acid)-hippuric acid (PAHIDA) is prepared by reacting p-aminohippuric acid with freshly prepared nitrilotriacetic anhydride (1:1) in dry DMF at 100 °C for two hours. After work-up and crystallization from 50:50 acetone/water, the compound is isolated as white crystals with a 60% yield: mp:222-223 °C. The structure is confirmed by MS, NMR and elemental analysis. Tc-99m labeled PAHIDA is successfully achieved at a pH of 5.8 using Sn(II) reduction method. The complex yielded one single and stable radiopharmaceutical established by ITLC and HPLC with >97% radiopurity.

Biodistribution of the Tc-99m PAHIDA is determined in rats at different time intervals and compared with I-131-hippuran and the data are shown in Table. The values of percent administered dose present at 30 minutes post injection in blood, kidney, urine and liver of rats respectively are 6.3± 1.0, 4.4±0.7, 61.3±12.1, and 1.2±0.3 for Tc-99m-PAHIDA and 1.2±0.2, 0.9± 0.2, 64.8±2.0 and 0.9±0.3 for I-131-hippuran. Rat urine analysis by paper chromatography suggests that the agent is excreted intact without any metabolic alteration. Scintigraphic images in rabbits have shown that the Tc-99m complex is rapidly excreted in urine with no significant extrarenal pathway providing excellent renal images. The reported agent satisfies structural requirements for renal secretion (3) owing to the presence of R-CONHCH<sub>2</sub>COOH grouping analogous to hippuran and may have the potential to replace I-131 hippuran for renal studies with high target to background ratio.

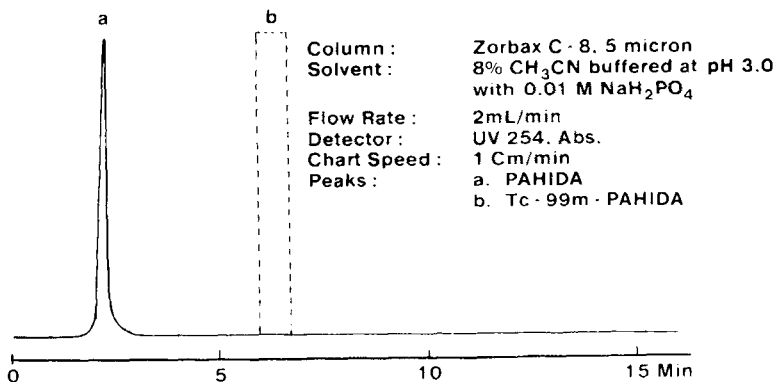
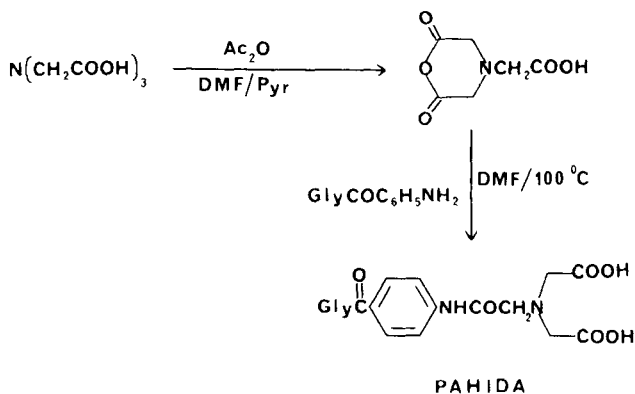
- (1) Chervu L.R. and Blaufox M.D., Sem. Nucl. Med., 12,224 (1982).
- (2) Fritzbeg A.R., Kuni C.C., Klingensmith III W.C.,Stevens J.,and Whitney W.P., J. Nucl. Med. 23, 592 (1982).
- (3) Despoupoulos A., J. Theor. Biol. 8,163(1965).

## ORGAN DISTRIBUTION DATA IN RATS FOR TC-99m-PAHIDA\*

ORGAN	% ADMINISTERED DOSE <sup>@</sup>			
	15 MIN	30 MIN	60 MIN	240 MIN
Blood	9.2±1.1 (3.7±0.4)	6.3±1.0 (1.2±0.2)	2.5±0.6 (0.5±0.1)	1.2±0.2 (0.2±0.0)
Urine	42.0±7.5 (54.5±7.0)	61.3±12.1 (64.8±2.0)	73.1±8.9 (69.7±3.0)	76.5±5.2 (79.0±7.0)
Liver	1.8±0.4 (1.8±0.2)	1.2±0.3 (0.9±0.3)	0.7±0.1 (0.6±0.3)	0.4±0.1 (0.1±0.0)
Kidney	4.1±0.4 (3.7±0.4)	4.4±0.7 (0.9±0.2)	3.2±0.4 (0.6±0.2)	3.5±0.4 (0.1±0.0)

\*<sup>131</sup>I-Hippuran values are shown in parentheses.

@ 6 Animals for each time intervals; Mean value ±1 S.D. are given.

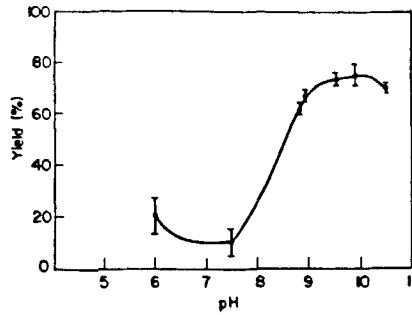
SYNTHESIS OF N<sup>4</sup>-(CARBONYLMETHYLIMINODIACETIC ACID)-HIPPURIC ACID (PAHIDA)

## CRITICAL PARAMETERS AFFECTING Tc-99m LABELING OF HUMAN FIBRINOGEN IN VITRO

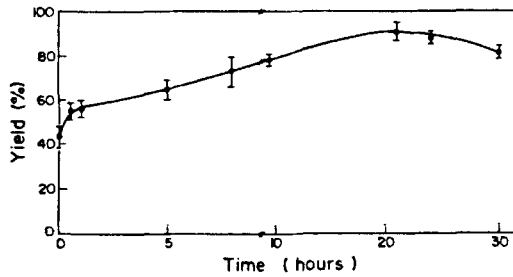
E. Lavie, M. Bitton and S. Mechlis  
Soreq Nuclear Research Centre, Yavne 70600, Israel

This study was undertaken to improve the in vitro labeling conditions for Tc-99m fibrinogen (1-3), which could serve as an important tool in the diagnosis of deep vein thrombosis. The factors which could affect the labeling which were studied were: pH, SnCl<sub>2</sub> and fibrinogen concentrations, pre- and post-labeling incubation times and temperature. Best results were achieved by incubating human fibrinogen (2.5 mg/ml) with SnCl<sub>2</sub> (0.02 mg/ml) at pH 9.8 for 22 hours before adding the TcO<sub>4</sub><sup>-</sup> solution (Fig. 1). This process led to a 90% labeling yield. It was demonstrated by in vitro incubation with plasma that there was no transfer of the label to other plasma proteins. Clottability of the labeled protein was 85% compared to 89% of the native unlabeled fibrinogen. Labeling efficiency was highly dependent on the time of interaction between SnCl<sub>2</sub> and fibrinogen. The yield increased from 50% for zero interaction time to 90% after 22 hours (Fig. 2). Blood clearance studies of the Tc-99m fibrinogen preparation gave results similar to those for I-125 fibrinogen. X-ray fluorescence technique was employed to measure the amount of bound tin at different times before labeling (Fig. 3). It was found that the binding of tin to fibrinogen reached saturation after 20 hours. This demonstrates a strong correlation between the tin-fibrinogen binding and the labeling yield. It is concluded that the conditions described here represent an efficient method for in vitro labeling of fibrinogen.

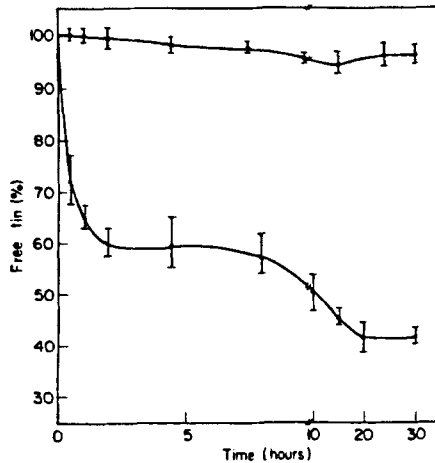
- (1) Wong D.W. and Mishkin F.S., J. Nucl. Med. 16, 343 (1974).
- (2) Harwig S.S.L., Harwig J.F., Coleman R.E. and Welch M.J., J. Nucl. Med. 17, 40 (1976).
- (3) Harwig J.F., Harwig S.S.L., Welch L.D. and Welch M.J., Int. J. Appl. Rad. Isot. 27, 5 (1976).



**Fig. 1.** The effect of final pH on the labeling yield. Experimental conditions: fibrinogen 2.5 mg/ml,  $\text{SnCl}_2$  0.22 mg/ml, temperature  $21^\circ$ . Each point represents mean + S.E. (n=3). Maximum labeling was observed at pH 9.8.



**Fig. 2.** Effect of time of interaction between  $\text{SnCl}_2$  and fibrinogen. Labeling was measured 30 minutes after the addition of  $\text{TcO}_4^-$ . Maximum labeling was achieved after an interaction time of 22 hours.



**Fig. 3.** Binding of tin to fibrinogen with time. Upper curve represents % total Sn (expressed as  $\text{Sn}^{+2}$ ) determined by iodometry and XRF. Lower curve represents % free tin in the solution determined by XRF after separating the supernatant from the protein. Maximum binding (60% of total Sn) was observed after 20 hours interaction between  $\text{SnCl}_2$  and fibrinogen.

SYNTHESIS OF DI-THIOSEMICARBAZONE DERIVATIVES OF ARALKYL CARBOXYLIC ACID AS  $^{99m}\text{Tc}$ -BIFUNCTIONAL RADIOPHARMACEUTICAL

Y.Arano, Y.Magata and A.Yokoyama

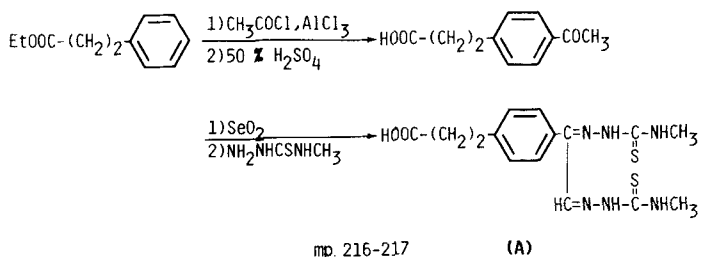
Department Radiopharmaceutical Chemistry, Faculty of Pharmaceutical Sciences, Kyoto University, Sakyo-ku, Kyoto 606, Japan.

Development of technetium- $^{99m}\text{Tc}$  (Tc- $^{99m}$ ) labeled radiopharmaceutical based on the concept of bifunctional radiopharmaceutical (BR) has attracted our attention. Most of the published work has been focused on the synthesis of bifunctional chelating agent (BCA) containing EDTA or DTPA skeleton for the chelating with Ga-67, In-111 (1,2). Our long interest on sulfur containing agent has revealed the satisfactory characteristic of kethoxal bis-thiosemicarbazone (KTS), containing a  $\text{S}\overset{\curvearrowright}{\text{N}}$  coordination, appropriate for the formation of a stable, relatively small and uncharged chelate of Tc- $^{99m}$  (3). Thus, di-thiosemicarbazone (DTS) was selected as basic molecule for the design of new BCAs.

To test the validity of the present approach, synthesis of BCA containing DTS moiety and aralkyl carboxylic acid of various chain length was estimated. In the present work, two carbon (A) and eleven carbon (B) chain length derivatives were synthesized. Their application demonstrated in case (A), by using it as a BCA for coupling macromolecules (human serum albumin, HSA) through the carboxylate group and in case (B) as a representative of a biomolecule derivative, a fatty acid analog of great interest in myocardial studies. Synthesis of these compounds were performed as described in Fig.1 and 2. Namely, after p-carboxyethyl phenylglyoxal or p-carboxyundecyl phenylglyoxal was obtained as (A) or (B) precursor respectively, condensation with N-methylthiosemicarbazide was performed. After recrystallization, pure products were obtained. Applicability of (A) for coupling HSA was easily achieved by the azido method. Excellent in-vivo behavior, comparable to radioiodinated HSA (Fig.3) was obtained, with higher stability and great potential for the labeling of other macromolecules, such as monoclonal antibodies. Using the same labeling reaction but in ethanol, Tc- $^{99m}$  labeling of (B) was achieved with good yield, as detected on TLC (acetone:acetic acid=100:5;  $R_f$ =0.8). Upon dilution with HSA solution, intravenous injection in mice showed promising performance (Table 1). Synthesis of derivatives with diverse chain length is needed for more specific BR (4,5). The gathered results offered good evidence for the great applicability of ligand containing DTS as a basic technetium coordination group for the design of new Tc- $^{99m}$ -BR of biomolecules.

- (1) L.H.DeRiemer, et al. J. Med. Chem. vol.22, 1019 (1979)
- (2) C.H.Paik, et al. J. Nucl. Med. vol.24, 932 (1983)
- (3) A.Yokoyama, et al. J. Nucl. Med. vol.17, 816 (1976)
- (4) C.A.Otto, et al. J. Nucl. Med. vol.22, 613 (1981)
- (5) H.H.Coenen, et al. J. Nucl. Med. vol.22, 891 (1981)

**Synthesis of p-carboxyethyl phenylglyoxal bis(N-methyl thiosemicarbazone)**

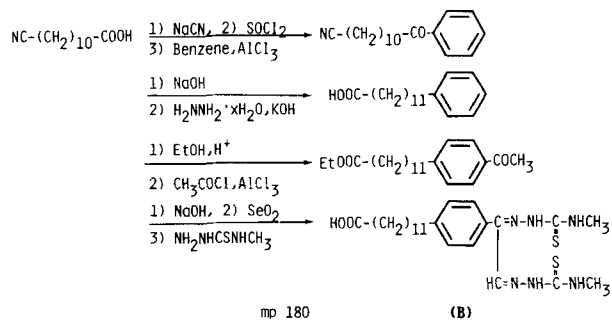


Elemental analysis for  $\text{C}_{15}\text{H}_{20}\text{N}_6\text{O}_2\text{S}_2$

	C	H	N
Calcd.:	47.35	5.30	22.09
Found :	47.30	5.48	22.27

Fig. 1

**Synthesis of p-carboxyundecyl phenylglyoxal bis(N-methyl thiosemicarbazone)**



Elemental analysis for  $\text{C}_{24}\text{H}_{38}\text{N}_6\text{O}_2\text{S}_2$

	C	H	N
Calcd.:	56.90	7.56	16.59
Found :	56.68	7.57	16.42

Fig. 2



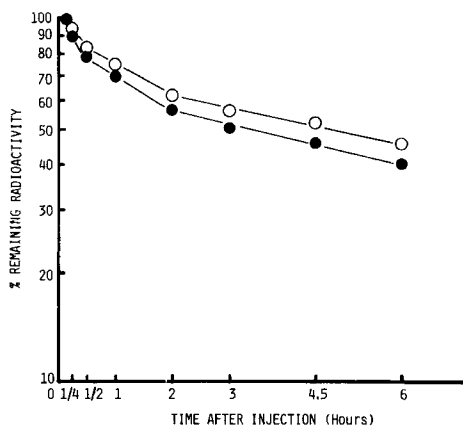


Fig. 3 Blood clearance : each point expressed as percentage of sample taken up at 5 min. in rabbits.

○ — ○ Tc-99m DTS-HSA  
 ● — ● I-131 HSA

**Biodistribution of Radioactivity In Mice After Intravenous Injection of 99m-Tc-Fatty Acid Analog\***

Organ	5 min.	30 min.	60 min.
Blood	21.43 (2.22)	13.78 (1.95)	9.59 (0.99)
Heart	4.10 (0.41)	4.76 (0.63)	5.03 (0.81)
Lung	9.46 (1.31)	7.82 (1.26)	6.78 (1.01)
Liver	18.39 (1.54)	25.70 (4.16)	26.00 (2.85)
Kidney	6.50 (0.75)	6.89 (1.20)	6.04 (0.53)
Intestine	0.73 (0.06)	2.66 (0.45)	3.31 (0.44)
Stomach	0.61 (0.18)	1.60 (0.51)	1.05 (0.25)

\* % Dose/gram organ; average of 5 animals and (s.d.)

Table. 1

## PREPARATION OF Ga-67-DTPA-FIBRINOGEN AND ITS BIODISTRIBUTION IN BALB/C MICE

G. B. Saha and V. Halbleib

College of Pharmacy, University of New Mexico, Albuquerque, NM 87131, USA

Radiolabeling of proteins has been carried out using bifunctional chelates such as EDTA analogues (1,2), DTPA (3,4) and disferoxamine (5). In this work, fibrinogen has been labeled with Ga-67 using DTPA as the chelating agent and its biodistribution has been studied.

Initially, DTPA anhydride was prepared by heating DTPA and acetic anhydride in pyridine at 65°C for 24 hr (6). Fibrinogen was coupled to DTPA by mixing DTPA anhydride and fibrinogen in powder form in a molar ratio of 5:1, and then dissolving the mixture in 0.05 M Hepes buffer, pH 7 (3). DTPA-fibrinogen was separated by Sephadex G-25 column chromatography using Hepes buffer as the eluent. Chelated fibrinogen was labeled with Ga-67 by incubating with 200-500  $\mu$ Ci of Ga-67-Chloride at room temperature for 30 min. Ga-67-DTPA-fibrinogen was further purified by Sephadex column chromatography. Labeling efficiency, stability and clottability were determined by standard techniques. Approximately 3-4  $\mu$ Ci of labeled fibrinogen was injected intravenously in groups of 4 Balb/c mice for each time period of 16, 24, 48 and 72 hr after injection. Mice were sacrificed at these time periods and activities in various organs and blood measured. The per cent administered dose per organ and per gram of organ were calculated from these activities.

Labeling efficiency of Ga-67-DTPA-fibrinogen was about 60-85% and it remained stable for a period of almost 72 hr. Clottability remained constant at nearly 61% for 24 hr, then reducing to about 47% at 48 hr. Blood activity decreased from 6% at 16 hr to 1% at 72 hr. The uptake values did not change much over the period of 16 to 72 hr in most organs. The uptake values (% dose/gram) were: kidneys (28-35%), liver (20-28%), spleen (8-15%), bowel (9-13%), stomach (7-9%), lungs (4-5%), heart (2-3%) and muscle (0.3-1%).

In summary, Ga-67-DTPA-fibrinogen can be prepared with high labeling efficiency, stability and clottability. It demonstrates normal *in vivo* biodistribution in mice and has potential use for detection of thrombi.

- (1) Sundberg M.W., Mears C.F., Goodwin D.A., Diamonti C.J., *J. Med. Chem.* 17, 1304 (1974).
- (2) Wagner S.J., Welch M.J., *J. Nucl. Med.* 20, 428, (1979).
- (3) Hnatowich D.J., Layne W.W., Childs R.L., *Int. J. Appl. Radiat. Isot.* 33, 327 (1982).
- (4) Paik C.H., Murphy P.R., Eckelman W.C., Volkert W.A., Neba R.C., *J. Nucl. Med.* 24, 932 (1983).
- (5) Ohmomo Y., Yokoyama A., Suzuki J., Tanaka H., Yamamoto K., Horiuchi K., Ishii Y., Torizuka K., *Eur. J. Nucl. Med.* 7, 458 (1982).
- (6) Eckelman W.C., Karesh S.M., Reba R.C., *J. Pharm. Sci.* 64, 704 (1975).

## PERCENT DOSE/ORGAN OF Ga-67-DTPA-FIBRINOGEN IN BALB/C MICE

Organ	16 hr	24 hr	48 hr	72 hr
Blood	3.06 $\pm$ 0.94	3.30 $\pm$ 0.55	1.39 $\pm$ 0.18	0.44 $\pm$ 0.23
Heart	0.36 $\pm$ 0.11	0.31 $\pm$ 0.04	0.31 $\pm$ 0.06	0.21 $\pm$ 0.06
Lungs	1.34 $\pm$ 0.29	0.78 $\pm$ 0.10	0.71 $\pm$ 0.04	1.02 $\pm$ 0.50
Spleen	1.11 $\pm$ 0.54	1.69 $\pm$ 0.21	1.99 $\pm$ 0.11	1.82 $\pm$ 0.69
Liver	29.97 $\pm$ 12.11	26.42 $\pm$ 4.66	35.11 $\pm$ 3.72	25.04 $\pm$ 7.73
Kidneys	9.19 $\pm$ 3.99	10.89 $\pm$ 1.12	11.29 $\pm$ 0.55	8.09 $\pm$ 2.02
Muscle	0.37 $\pm$ 0.05	0.34 $\pm$ 0.05	0.06 $\pm$ 0.01	0.06 $\pm$ 0.02
Stomach	3.03 $\pm$ 0.90	2.26 $\pm$ 0.59	2.66 $\pm$ 2.47	3.28 $\pm$ 1.21
Bowel	11.66 $\pm$ 3.02	13.68 $\pm$ 1.92	13.22 $\pm$ 0.76	10.52 $\pm$ 2.08

## PERCENT DOSE/GM OF TISSUE OF Ga-67-DTPA-FIBRINOGEN IN BALB/C MICE

Organ	16 hr	24 hr	48 hr	72 hr
Blood	5.76 $\pm$ 1.24	4.20 $\pm$ 0.48	1.67 $\pm$ 0.08	0.82 $\pm$ 0.26
Heart	2.84 $\pm$ 0.67	2.38 $\pm$ 0.51	2.09 $\pm$ 0.30	1.52 $\pm$ 0.33
Lungs	5.32 $\pm$ 1.38	4.43 $\pm$ 0.74	4.01 $\pm$ 0.33	4.24 $\pm$ 1.59
Spleen	8.32 $\pm$ 3.24	12.94 $\pm$ 2.07	15.21 $\pm$ 1.18	13.89 $\pm$ 2.99
Liver	22.35 $\pm$ 7.30	21.13 $\pm$ 3.82	27.64 $\pm$ 2.24	20.31 $\pm$ 3.55
Kidneys	31.63 $\pm$ 12.84	35.24 $\pm$ 5.95	30.87 $\pm$ 0.87	27.69 $\pm$ 3.38
Muscle	0.95 $\pm$ 0.24	0.81 $\pm$ 0.09	0.63 $\pm$ 0.31	0.30 $\pm$ 0.17
Stomach	7.52 $\pm$ 1.81	6.70 $\pm$ 1.56	6.60 $\pm$ 7.31	8.97 $\pm$ 3.59
Bowel	9.64 $\pm$ 2.50	12.57 $\pm$ 2.03	13.12 $\pm$ 0.75	8.98 $\pm$ 2.02

CLOTTABILITY OF FIBRINOGEN

<u>Time (hr)</u>	<u>Clottable Fibrinogen (%)</u>
1	61.0 $\pm$ 3.6
24	61.7 $\pm$ 1.5
48	46.7 $\pm$ 1.5

FACTORS INFLUENCING RADIOLABELING OF ANTIBODIES WITH  $^{111}\text{In}$ 

C.H. Paik, J.J. Hong, M.A. Ebbert, S.C. Heald, R.C. Reba and W.C. Eckelman<sup>1</sup>  
 Radiopharmaceutical Chemistry Section, The George Washington University Medical  
 Center, Washington, D.C., 20037

The simplest method of labeling antibody (Ab) with  $^{111}\text{In}$  is to conjugate Ab with DTPA via one of three reported acylation methods and subsequently to complex the Ab-DTPA conjugate with  $^{111}\text{In}$ . We have recently reported on the systematic variation of parameters in the first step, the conjugation reaction.<sup>2,3,4</sup> This work concentrates on the radiolabeling procedure.

The theoretical specific activity of  $^{111}\text{In}$  labeled antibody conjugate containing 1 DTPA molecule per Ab is 324 Ci per g Ab (MW=150,000) assuming the formation of a 1:1 complex of  $^{111}\text{In}$  and DTPA. The experimentally obtained specific activity is, however, generally about 100 times less than the theoretical specific activity mainly due to metallic ion contaminants and unfavorable kinetics in cases where the concentration of Ab-DTPA is very dilute. For a maximum incorporation of  $^{111}\text{In}$  to immunologically active antibody DTPA conjugate (sAb-DTPA) it is important to measure the relative reactivity between free DTPA and Ab-DTPA, and between sAb-DTPA and deactivated Ab-DTPA (nAb-DTPA). The first comparison is important because free DTPA contaminating the Ab-DTPA solution might bind all of the  $^{111}\text{In}$  if it is much more reactive. The second comparison is equally important, especially for labeling tumor specific antibodies if appropriate preparative affinity columns to separate sAb-DTPA from nAb-DTPA are not available. In order to obtain the above information, Ab at 8.7 mg/ml ( $5.8 \times 10^{-5}\text{M}$ ) was reacted with cyclic DTPA dianhydride (cDTPAA) at cDTPAA/Ab ratios of 1, 5, 20 and 40 in 0.1M bicarbonate buffer at pH 8.3. Using a titration method with  $\text{InCl}_3$  containing a tracer amount of  $^{111}\text{In}$ , the above reaction was determined to produce 0.14, 1.3, 5.1 and 10.8 DTPA molecules per sAb, and 0.15, 1.8, 5.4 and 10.8 DTPA molecules per nAb. The percentage of sAb remaining after the above reactions based on UV peak intensities was 89%, 89%, 76% and 62% respectively. This indicates an inverse relationship between DTPA conjugation and immunologic activity of Ab. These results disagree with the hypothesis that nAb contains a much larger number of DTPA per Ab than sAb. The reaction of no-carrier-added  $^{111}\text{In}$  with the reaction mixtures from the molar ratios of 1, 5, 20 and 40 gave radiochemical yields of 4%, 17%, 27% and 21% for the respective Ab-DTPA. These are the radiochemical yields in the presence of free DTPA. This indicates that Ab-DTPA containing an average of 1.4, 5.1, and 10.8 DTPA molecules per Ab is more reactive than that containing 0.14 DTPA; and is about as reactive as free DTPA. The percentage of  $^{111}\text{In}$  activity incorporated into sAb-DTPA from the reactions at the above molar ratios were 84%; 74%; 71% and 53% of the activities incorporated into the total Ab-DTPA. These are similar to the percentage activities based on UV peak intensities given above. This indicates that the reactivities of sAb-DTPA and nAb-DTPA from the same conjugation reactions are similar.

In conclusion, attempts at producing high specific activity radiolabeled antibodies are counterbalanced by decreasing immunologic activity but  $^{111}\text{In}$  does distribute among unconjugated DTPA, sAb-DTPA and nAb-DTPA on a near statistical basis at these concentrations. These data define the factors necessary to produce high specific activity, immunologically active Ab-DTPA- $^{111}\text{In}$ .

- (1) Present Address: Department of Nuclear Medicine, Clinical Center, National Institutes of Health, Bethesda, MD 20205
- (2) Paik, C.H., Murphy, P.R., Eckelman, W.C. et al: J. Nucl Med 24:932, 1983
- (3) Paik, C.H., Ebbert, M.A., Murphy, P.R., et al: J. Nucl Med 24, 1158, 1983
- (4) Paik, C.H., Lassman, C.R., Murphy, P.R., et al: Hybridoma 2, 248, 1983

Table 1

DTPA conjugation to Ab from the reactions at various cDTPA to Ab ratios

$\frac{\text{cDTPAA}}{\text{Ab}}$	%SAb UV Method	$\frac{\# \text{In Atoms}}{\text{sAb}}$	$\frac{\# \text{In Atoms}}{\text{nAb}}$	$\frac{\# \text{In Atoms}}{\text{Total Ab}}$
--	91(88-95) <sup>a</sup>	--	--	--
1	89(86-94)	0.14(0.10-0.16)	0.15(0.10-0.17)	0.14
5	89(88-90)	1.3 (1.2-1.3)	1.8 (1.7-1.9)	1.4
20	76(63-81)	5.1 (4.2-6.0)	5.4 (3.8-6.6)	5.2
40	62(55-66)	10.8 (8.6-13.8)	10.8 (9.0-12.1)	10.8

<sup>a</sup> The percentage of active antibody in the stock anti human serum albumin antibody solution.

The concentration of antibody used for the reaction was 8.7 mg/ml.

The data are average numbers of triplicate to quintuplicate experiments.

Table 2

Relative reactivities of DTPA and Ab-DTPA toward  $^{111}\text{In}$ 

$\frac{\text{cDTPAA}}{\text{Ab}}$	$\frac{\text{Ab-Conjugated DTPA}}{\text{Ab}}$	$\frac{\text{Ab-DTPA}^{\text{a}}}{\text{cDTPAA}}$	Ab-DTPA- $^{111}\text{In}^{\text{b}}$	Relative reactivity <sup>c</sup>
1	0.14	14%	4%	29%
5	1.4	28%	17%	61%
20	5.2	26%	27%	103%
40	10.8	27%	21%	78%

<sup>a</sup> The percentage yield of DTPA conjugation to Ab. It was obtained by dividing column two by column one.

<sup>b</sup> No-carrier-added labeling yield.

<sup>c</sup> The reactivity of Ab-DTPA relative to DTPA.

Table 3

The percentage labeling of the antibody DTPA conjugate with no-carrier-added  $^{111}\text{In}$ .

$\frac{\text{cDTPAA}}{\text{Ab}}$	% Active Ab <sup>a</sup>	Ab-DTPA- $^{111}\text{In}$	
		Affinity Chrom. <sup>b</sup>	TLC <sup>c</sup>
--	91(88-95) <sup>d</sup>	---	---
1	84(80-89)	4(2-9)	13.5(4-23)
5	74(72-76)	17(15-19)	32 (29-35)
20	71(67-77)	27(17-37)	45 (33-58)
40	53(39-64)	21(17-23)	39 (31-43)

<sup>a</sup> Determined based on  $^{111}\text{In}$  activity associated with sAb.

<sup>b</sup> The percentage of  $^{111}\text{In}$  activity incorporated to total antibody DTPA conjugate when reacted with the reaction mixture. The percentage was determined based on  $^{111}\text{In}$  associated with the antibody fractions from the affinity-gel filtration column.

<sup>c</sup> The percentage was based on TLC analysis.

<sup>d</sup> The percentage of active antibody in the stock solution. The data are the average number of triplicate to quintuplicate experiments.

**BIFUNCTIONAL CHELATING AGENTS BEARING BROMOACETAMIDE OR ISOTHIOCYANATE GROUPS: PREPARATION, CONJUGATION TO ANTIBODIES, DETERMINATION OF YIELD, AND RADIOLABELING**

C.F. Meares, D.A. Goodwin, M.J. McCall, D.I. Reardan and C.I. Diamanti  
Chemistry Department, University of California, Davis, California 95616.

Monoclonal antibodies tagged with radioactive metal chelates have considerable potential for imaging and therapy (1,2,3,4). We have investigated the reactions of three different monoclonal antibodies with bromoacetamidobenzyl-EDTA ("BABE," prepared according to ref. 5) and isothiocyanatobenzyl-EDTA ("CITC," prepared by reaction of aminobenzyl-EDTA with thiophosgene in 3N HCl). The conjugation procedure which we favor involves incubation of the antibody ( $> 20 \mu\text{g}/\mu\text{l}$ ) at pH 9,  $37^\circ\text{C}$ , in 0.15 M sodium phosphate buffer for 2 hr with either a 10 fold molar excess of BABE or a 3 fold excess of CITC. A preliminary measure of the extent of conjugation is made by treating an aliquot of the reaction mixture with carrier-free  $^{57}\text{Co}^{++}$  and separating free chelates from antibody-bound chelates with thin-layer chromatography. When the desired number of chelates (1 to 2) per antibody is obtained, the reaction is stopped and the buffer changed to 0.1 M citrate, pH 6, by a simple 2-min centrifugation through a Sephadex G-50-80 column (6). At this point, the number of antibody-bound chelating groups can be accurately determined by titration of an aliquot with a standardized cobalt solution. The product is then frozen and stored. When needed an aliquot of chelate-tagged antibody ( $> 10^{-5}$  M chelating groups) in 0.1 M citrate, pH 6, is thawed and mixed with an equal volume of column-purified  $^{111}\text{InCl}_3$  in 0.1 M citrate, pH 5. Radiolabeling is complete in 5-10 min. Studies of monoclonal antibodies against mouse B cells, mouse lymphoma, or human transferrin receptor show excellent retention of biological activity by conjugates bearing an average of 1-2 chelates per antibody.

- (1) Khaw B.A., Fallon J.T., Strauss H.W., Haber E., *Science*, **209**, 295 (1980).
- (2) Scheinberg D.A., Strand H., Gansow O.A., *Science*, **215**, 1511 (1982).
- (3) Rainsbury R.M., Westwood J.H., Coombes R.C., Neville A.M., Ott R.J., Kalirai T.S., McCready V.R., Gazet J-C., *Lancet*, 934 (Oct. 22, 1983).
- (4) Hnatowich D.J., Layne W.W., Childs R.L., Lanteigne D., Davis M.A., Griffin T.W., Doherty P.W., *Science*, **220**, 613 (1983).
- (5) DeRiemer L.H., Meares C.F., Goodwin D.A., and Diamanti C.I., *J. Labelled Comp. and Radiopharm.*, **XVIII**, 1517 (1981).
- (6) Penefsky H.S., *Meth. in Enzymology*, **LVI**, 527 (1979).

N-SUCCINYLDSEFFERIOXAMINE B: A NEW COMPOUND FOR LABELLING OF PROTEINS AND FOR ASSESSING RENAL FUNCTION

J.D.M. Herscheid and A. Hoekstra

Radio-Nuclide Centre(RNC) of the Free University

P.O.Box 7161, 1007 MC Amsterdam, The Netherlands

Since proteins labelled with iodine often provide products with in vivo instability many centres are investigating the possible use of bifunctional chelates coupled to proteins which would rapidly bind with a choice of radionuclides. However, coupling procedures with 1-ethyl-3-(3-dimethylamino-propyl) carbodiimide (EDC) or glutaraldehyde often lead to a significant increase in protein loss (1), due to intra- and inter-molecular coupling with nucleophilic groups on the protein itself.

We have developed a new method for preparing desferrioxamine B(DF)-protein chelates. DF is reacted with succinic anhydride to give N-succinyl-desferrioxamine B(SDF) which can subsequently be converted with dicyclohexyl carbodiimide into a cyclic anhydride as determined by IR-spectroscopy. It is known that such active esters couple very well with the lysine residues of proteins, which was confirmed by the preparation of the BSA-SDF complex.

In addition, it appeared that free  $^{67}\text{Ga}$ -SDF is excreted very fast by the kidneys. Since its chemical structure resembles the structure which is assumed to be obligatory for tubular secretion (2), the potencies of  $^{67}\text{Ga}$ -SDF as a renal function agent were tested in rats and rabbits and compared with the biokinetics of [ $^{131}\text{I}$ ]-o-iodohippuric acid(OIH).

The results of the biodistribution and renographic studies (Table 1 and 2) indicate that renal excretion of  $^{67}\text{Ga}$ -SDF is very fast, in rats even faster than OIH. No marked effect of probenecid on the excretion rate of either  $^{67}\text{Ga}$ -SDF or OIH could be found. However, it is clear that this Gallium-67 labelled complex might be valuable as a renal scanning agent.

(1) Gy. A. Janoki et. al., Int. J. Appl. Radiat. Isotop., 34, 871 (1983).

(2) A. Despopoulos, J. Theoret. Biol., 8, 163 (1965).



Table 1. Biodistribution of  $^{67}\text{Ga-SDF}$  and  $^{131}\text{I-OIH}$  in  $n$  rats, as percentage of injected dose per gram of tissue ( $\pm$  s.d.).

	$^{131}\text{I-OIH}$	$^{67}\text{Ga-SDF}$		
		20 min. ( $n=4$ )	20 min. ( $n=5$ )	60 min. ( $n=2$ )
Blood	0.38(0.23)	0.51(0.06)	0.05(0.01)	0.009(0.001)
Kidney	3.36(1.66)	2.69(1.21)	0.39(0.03)	0.23(0.01)
Spleen	0.14(0.06)	0.12(0.01)	0.022(0.001)	0.009(0.001)
Liver	0.39(0.18)	0.13(0.01)	0.029(0.006)	0.013(0.005)
Stomach	0.16(0.08)	0.07(0.02)	0.023(0.003)	0.003(0.001)
Intestine	0.14(0.05)	0.18(0.03)	0.15(0.03)	0.14(0.04)
Lung	0.21(0.13)	0.32(0.03)	0.040(0.004)	0.017(0.003)

Table 2. Renogram values of  $^{131}\text{I-OIH}$  and  $^{67}\text{Ga-SDF}$  for rats or rabbits ( $\pm$  s.d.)

	$^{131}\text{I-OIH}$	$^{131}\text{I-OIH}$	$^{67}\text{Ga-SDF}$	$^{67}\text{Ga-SDF}$
	$n$	Probenecid $n$	$n$	Probenecid $n$
<u>Rat</u>	$n=5$	$n=3$	$n=4$	$n=5$
$T_{\text{max}}$ (min.)	2.1(0.3)	2.4(0.7)	1.7(0.2)	2.2(0.3)
Bladder <sup>†</sup>	29(5)	18(4)	53(9)	40(9)
Blood <sup>‡</sup>	0.38(0.23)	0.71(0.24)	0.51(0.06)	0.48(0.17)
<u>Rabbit</u>	$n=8$	$n=8$	$n=8$	$n=8$
$T_{\text{max}}$ (min.)	3.5(0.8)	3.4(0.7)	4.4(1.0)	3.6(0.5)
Bladder <sup>†</sup>	47(4)	42(5)	33(6)	32(5)
Blood <sup>‡</sup>	0.016(0.003)	0.020(0.004)	0.112(0.020)	0.087(0.017)

† percent injected dose

‡ percent injected dose/gram

IN-111-MONOCYTES AND IN-111-PMN: RADIOPHARMACEUTICALS FOR INFARCTION AND INFLAMMATORY DISEASE DETECTION

C.J.Mathias, D.Schwartz, P.Needleman, M.J.Welch

The Edward Mallinckrodt Institute of Radiology, Washington University School of Medicine, St. Louis, MO 63110 U.S.A.

Recent observations have described the presence of specific types of cells in organ tissue that has been damaged in some way.<sup>1</sup> The migration of leukocytes to regions of tissue inflammation and/or infarction has been well established, but the characterization of specific leukocyte subpopulation kinetic properties has not been established *in vivo*.<sup>2</sup> White blood cells (WBC) radiolabeled with an imageable isotope could be useful to evaluate the cell kinetics in various animal models. Isolation of particular subpopulations was difficult and finally accomplished by applying leukocyte rich plasma (LRP) to two sequential ficoll density gradients as shown. (Figure 1) The subpopulations of mononuclear leukocytes and polymorphonuclear leukocytes can be extracted from the gradient, pelleted by diluting with saline, and radiolabeled with In-111-8-hydroxyquinoline as previously described.<sup>2</sup> In-111-8-hydroxyquinoline (In-111-oxine) was used without comparison to other ligands since 1) it readily incorporates into the isolated cells, and 2) the chemotactic stimulation described elsewhere<sup>3</sup> when oxine is present was not a consideration in the animal models utilized.

From 60-120ml of whole rabbit blood  $3 \times 10^{10}/\text{mm}^3$  and  $1 \times 10^7/\text{mm}^3$  polymorphonuclear leukocytes (PMN) can be isolated. The labeling efficiency with In-111-oxine is, of course, related to the total cell mass isolated since the labeling mechanism seems to be primarily passive diffusion. When PMN were to be isolated more whole blood was obtained (80-120ml) in order to acquire a suitable number of cells for radiolabeling. The labeling efficiency was more variable when PMNs were radiolabeled (since the total cell mass is significantly less) than when the monocytes were radiolabeled; however, direct documentation of a relationship between cell mass and labeling efficiency has not been established due to difficulties in obtaining reliable cell counts. Although several routine methods of cell counting were attempted, a non-esterase specific stain (positive for monocytes, negative for PMNs) was ultimately the most specific identification technique available and the cell counting is highly variable due to complications from the density gradient. Labeling efficiencies, varied from 45-98% for monocytes and 9-65% for PMNs, were directly related to the variation in total cell mass based on observation of total pellet volume.

The animal model utilized was hydronephrosis in rabbits which has been shown to accumulate leukocytes during inflammatory changes.<sup>1</sup> The radiolabeled cells were administered at various times after hydronephrosis was induced (by left ureter obstruction at the level of the bladder). The contralateral (right) kidney (CLK) was the individual control in each case. The migration of the radiolabeled cells was monitored by scintigraphic imaging and ultimate biodistribution measured *in vitro* at 72 hours after hydronephrosis was induced. The hydronephrotic kidney accumulated  $2.4 \pm 0.3$  times the amount of radioactivity of that in the CLK. (Figure 2)

- (1) Okegawa T., Jonas P.E., DeSchryver K., Kawasaki A., Needleman P., *J.Clin. Invest.* 71, 81 (1983).
- (2) Weiss E.S., Ahmed S.A., Thakur M.L., Welch M.J., Coleman R.E., Sobel B.E., *Am.J. Cardiol.* 40, 195 (1977).
- (3) Mathias C.J., Heaton W.A., Welch M.J., Douglas P.G., Kelly J.D., *Int. J. Appl. Rad. Isot.* 32, 651 (1981).

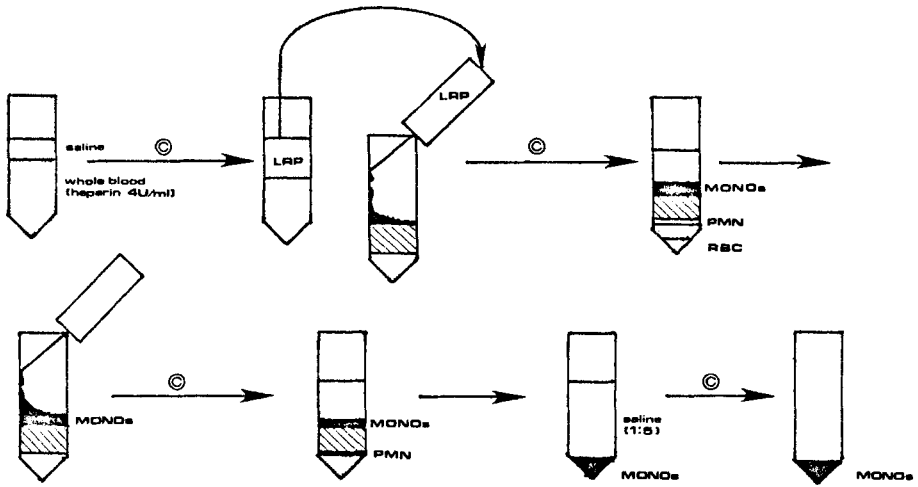


Figure 1. Schematic representation of monocyte and PMN isolation.  
 © represents centrifugation step.

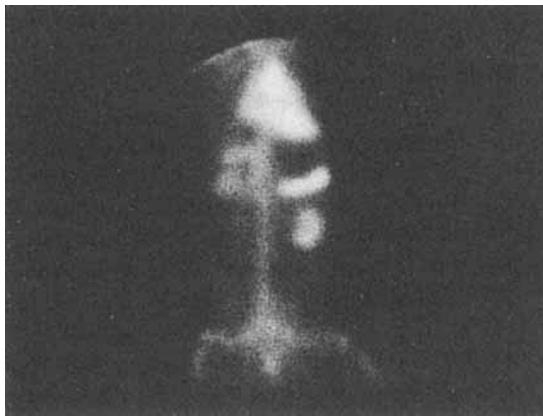


Figure 2. Scintigram obtained immediately after injection of In-111-monocytes. The left kidney (HNK) has marked uptake of radioactivity as compared to the right kidney (CLK) which is normal.

GALLIUM-67 BINDING TO TUMOR CELLS IN VITRO: ROLE OF ATP AND GLYCOPROTEINS

---

S. Vallabhajosula, H. Lipszyc and S.J. Goldsmith  
 Andre Meyer Department of Physics-Nuclear Medicine, The Mount Sinai Medical  
 Center, New York, New York 10029, USA.

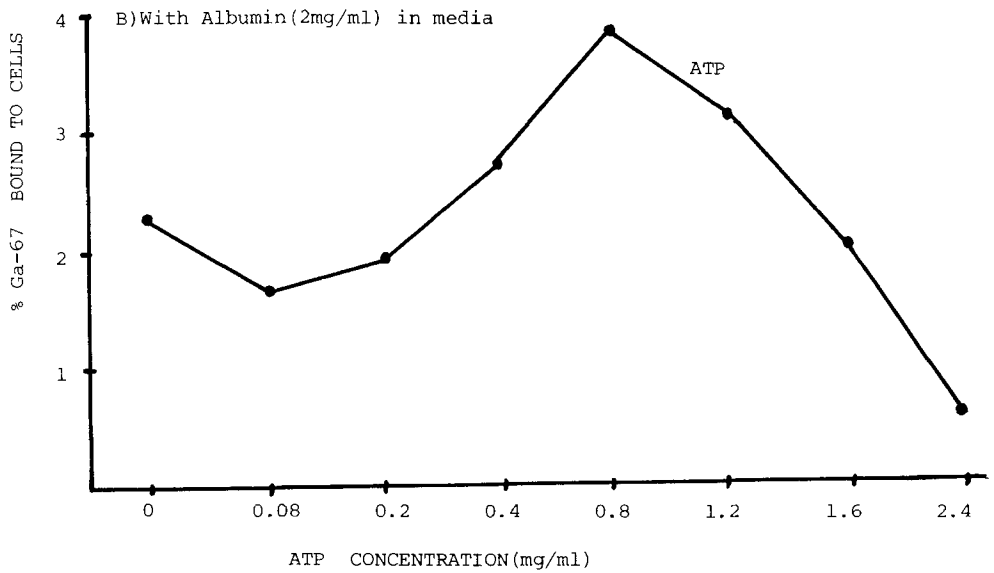
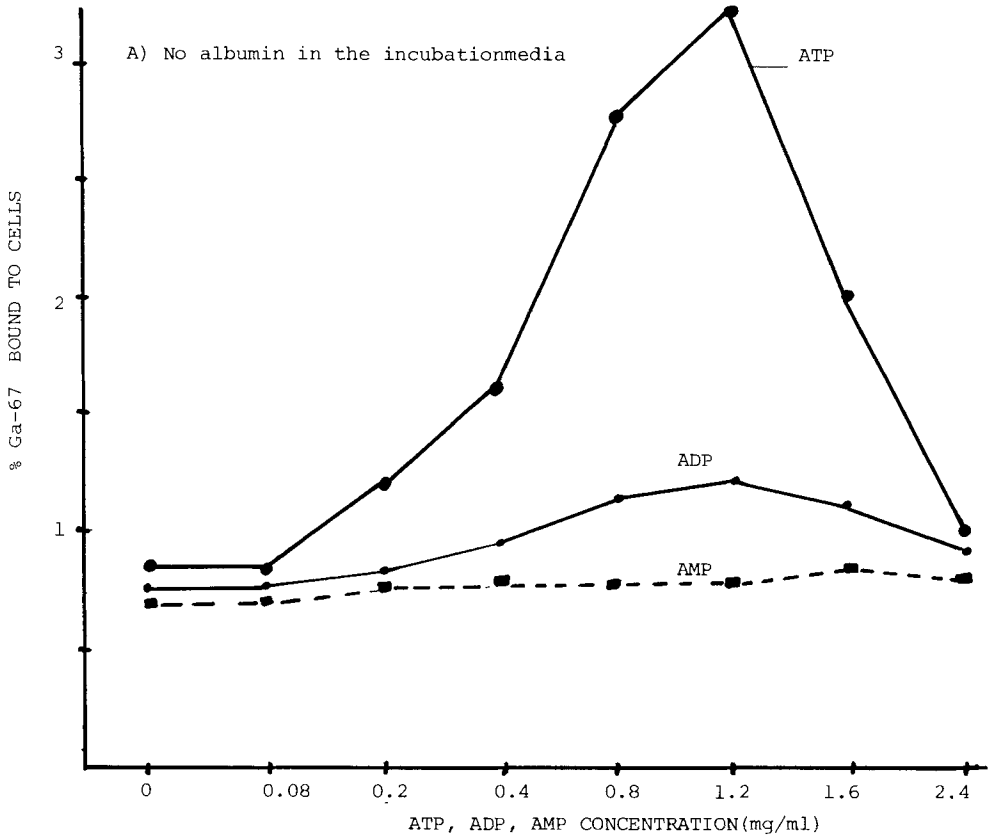
The iron-binding glycoproteins, transferrin and lactoferrin have been shown to promote the uptake of Ga-67 by tumor cells under in vitro experimental conditions (1,2). The processes which facilitate the transfer of radiogallium from glycoprotein to intracellular binding sites, however, are not clearly understood. Larson et al (1) proposed that  $^{67}\text{Ga}$ -transferrin complex is taken up intact into the tumor cell through transferrin receptors on the cell membrane. In an in vivo tumor model Hayes et al (3) observed a reduction in the tumor uptake of Ga-67 when bound to transferrin. While evaluating the role of glycoproteins on tumor uptake of Ga-67, we have observed that Ga-67 also binds to polystyrene culture tubes in the presence of transferrin or lactoferrin (5). Approximately  $10^{13}$  glycoprotein molecules bind per tube. When albumin was added to incubation media to reduce Ga-67 non-specific binding, the glycoprotein enhancement of radiogallium uptake by tumor cells was dependent upon albumin level, decreasing in absolute uptake as albumin concentration is increased suggesting that glycoprotein binding to the tumor cells is non-specific (4). Weiner et al (6) have recently shown that Ga-67 binding to transferrin and lactoferrin was reduced in the presence of ATP due to the formation of  $^{67}\text{Ga}$ -ATP complex. ATP is a membrane active substrate and is not transported into the cell. Thus we have studied the effect of ATP on the uptake of Ga-67 alone and  $^{67}\text{Ga}$ -glycoprotein complex by the tumor cells.

Burkitt's lymphoma cells grown in tissue culture were incubated with  $^{67}\text{Ga}$ -citrate in 0.02M MOPS and saline buffer, pH 7.0 at  $37^{\circ}\text{C}$  for 2 hrs. The binding of Ga-67 to the cells increases with increasing ATP concentration of upto 1.2mg/ml (0.8+3.2%) and decreased thereafter. However, ADP and AMP did not show any significant promotion of Ga-67 uptake by the cells. This biphasic response of ATP effect on Ga-67 uptake by the cells was observed in the presence of albumin (2mg/ml) in the incubation media. Binding of Ga-67 to tumor cells was studied at various concentrations of lactoferrin in the incubation media and also with and without ATP (2mg/ml). The maximum enhancement of Ga-67 uptake by the cells observed at 80ug/ml of lactoferrin was totally abolished in the presence of ATP. In addition, Ga-67 activity bound to cells in the presence of lactoferrin was almost completely removed by washing the cells with saline containing ATP.

These results demonstrate that cellular uptake of Ga-67 in glycoprotein free media may be promoted by the formation of  $^{67}\text{Ga}$ -ATP complex. The cell associated Ga-67 activity in the presence of glycoproteins is decreased by ATP, suggesting that  $^{67}\text{Ga}$ -glycoprotein complex was bound to cell membrane and not necessarily incorporated into the tumor cell. In the light of these data, caution is required in interpreting cell culture experiments which have not directed attention to non-specific cell-protein interaction.

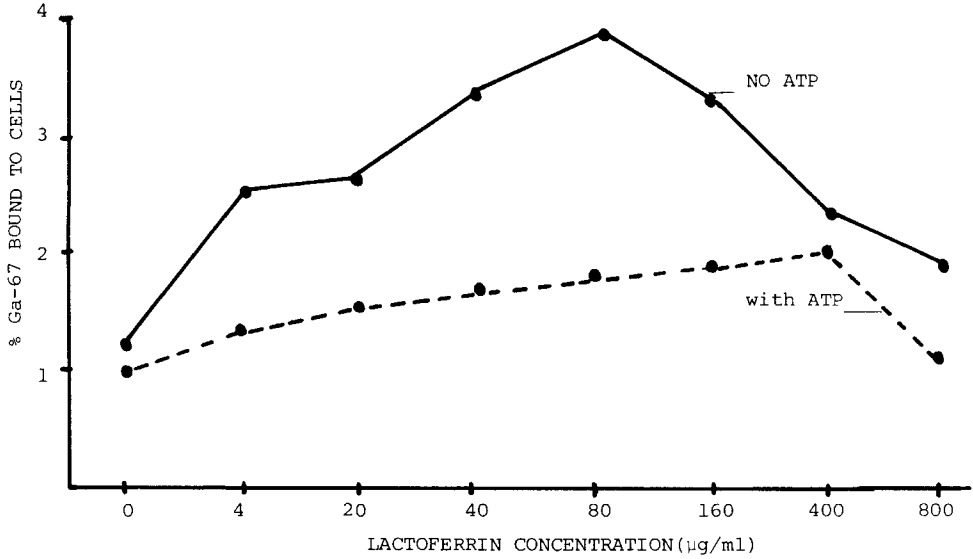
- (1) Larson S.M., Rasey J.S., Allen D.R., Grunbaum Z., J. Natl. Cancer. Inst. 64, 41 (1980)
- (2) Vallabhajosula S., Lipszyc H., Goldsmith S.J., Ohnuma T., J. Nucl. Med. 22, p50 (1981).
- (3) Hayes R.L., Rafter J.J., Byrd B.L., Carlton J.E., J. Nucl. Med. 22, 325 (1981).
- (4) Vallabhajosula S., Goldsmith S.J., Lipszyc H., Chahinian A.P., Ohnuma T., Eup. J. Nucl. Med. 8, 354 (1983).
- (5) Vallabhajosula S., Goldsmith S.J., Eup. J. Nucl. Med. 8, 223 (1983).
- (6) Weiner R.E., Schreiber G.J., Hoffer P.B., J. Nucl. Med. 24, 608 (1983).

EFFECT OF ATP, ADP AND AMP ON THE UPTAKE OF GALLIUM-67 BY TUMOR CELLS

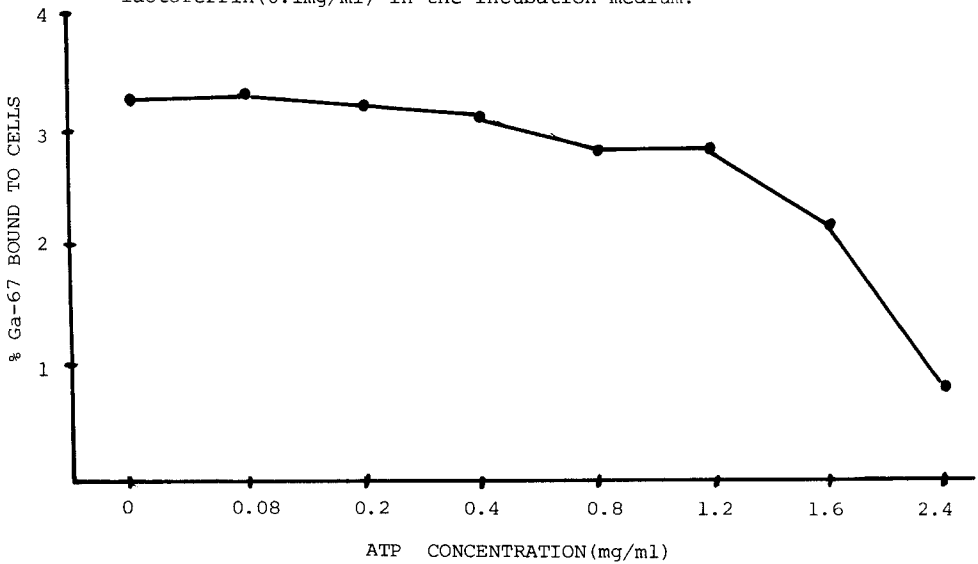


EFFECT OF ATP AND LACTOFERRIN ON GALLIUM-67 UPTAKE BY TUMOR CELLS

A) Ga-67 uptake as a function of lactoferrin concentration with and without ATP in the incubation media.



B) Ga-67 uptake as a function of ATP concentration with lactoferrin (0.1mg/ml) in the incubation medium.



$^{169}\text{Yb}$ -COMPLEXES VERSUS  $^{67}\text{Ga}$ -CITRATE IN TUMOR LOCALIZATION

G.V.S. Rayudu, M.E. Abril and E.W. Fordham  
Department of Radiology and Nuclear Medicine, Rush University  
Medical Center, Chicago, IL. 60612, U.S.A.

The tumor localizing agents have been classified into five types(1): (a) cations, (b) antibiotic agents, (c) antibody type agents, (d) metabolites/miscellaneous agents, and (e) DNA/RNA synthesis inhibitors. In the area of cations; Ga-67(2), lanthanides(3), lanthanides and actinides(4,5), representative metal citrates(6), and various gallium complexes(7), have been evaluated for tumor specificity. In this communication, thirteen complexes of Yb-169 were evaluated in Sarcoma-180 bearing mice and the results were compared to those of  $^{67}\text{Ga}$ -citrate.

The complexes were prepared by adding 10 mg of each complexing agent-containing solution of: acetic, citric, dimethyl lactic, amino acetic(glycine), gluconic, glycolic, lactic, dipicolinic, diethylene triamine pentaacetic acid(DTPA), ethylene diamine tetraacetic acid (EDTA), n-hydroxy ethylethylene diamine triacetic acid(HEDTA), nitrilo triacetic acid(NTA), and triethylene tetraamine hexaacetic acid(TTHA), to high specific activity  $^{169}\text{Yb}$ -chloride and adjusting the pH to 6. The final Yb-169 complexes were bacteria filtered. Aliquots, including that of commercially available  $^{67}\text{Ga}$ -citrate, were injected into S-180 tumor bearing ICR strain female mice. The biodistribution values studied at 2 days post i.v. as expressed in percent of injected dose per gram and per organ are presented in Tables I and II.

The results suggest that the acetic, citric, dimethyl lactic, glycolic, aminoacetic, lactic, and gluconic complexes were comparable to  $^{67}\text{Ga}$ -citrate while dipicolinic, DTPA, EDTA, HEDTA, NTA, and TTHA were inferior to  $^{67}\text{Ga}$ -citrate as they form strong complexes with Yb-169 and clear from the tumor as well as from whole body.

Additional obvious advantages of  $^{169}\text{Yb}$ ( $T_{1/2}=32\text{d}$ ) over  $^{67}\text{Ga}$ ( $T_{1/2}=3.2\text{d}$ ) are: i) Long shelf life for convenient availability; ii) Slight bone uptake which will help as a reference to locate tumors; iii) Reactor produced Yb-169 has world wide availability when compared to cyclotron produced Ga-67; and iv) Less soft tissue background when compared to Ga-67.

- (1) Rayudu G.V.S., Formulation of Radiotracers, Proceedings of the Second Int. Symposium on Radiopharmacology, 2, 334-345, (1981).
- (2) Edwards C.L., and Hayes R.L., J. Nucl. Med., 10, 103-105, (1969).
- (3) Hisada K., and Ando A., J. Nucl. Med., 14, 615-617, (1973).
- (4) Rayudu G.V.S., Fordham E.W., Ramachandran P.C., Friedman A.M., and Sullivan J.C., J. Nucl. Med., 15, 526, (1974).
- (5) Rayudu G.V.S., Fordham E.W., Ramachandran P.C., Sullivan, J.C., and Friedman, A.M., Int. J. Nucl. Med. and Bio., 2, 44-45, (1975).
- (6) Rayudu G.V.S., Clark P., Hong K., Ali A., and Fordham E.W., Radioactive Metal Citrates in Tumor Localization, Proc. of the 3rd World Congress in Nuclear Medicine and Biology, 3, Vol I, 673, (1982).
- (7) Rayudu G.V.S., Abril M.E., Ali A., Fordham E.W., and Rajan K.S.,  $^{67}\text{Ga}$  Complexes Versus  $^{67}\text{Ga}$ -Citrate in Tumor Localization, Proc. of the 3rd World Congress in Nuclear Medicine and Biology, 3, Vol I, 670, (1982).

TABLE I. BIODISTRIBUTION OF  $^{169}\text{Yb}$ -COMPLEXES AND  $^{67}\text{Ga}$  IN TUMOR BEARING MICE  
 % PER GRAM AT 2 DAY PIV (Mean  $\pm$  S.D. of 5 Animals)

	DIPICOLINIC				GLUCONIC ACID				NPA		TTHA	
	ACETATE	CITRIC ACID	DIMETHYL LACTIC ACID	GLYCINE	GLYCOLIC ACID	LACTIC ACID	67Ga-CITRATE	DTPA	EDTA	HEDTA	NPA	TTHA
Blood	0.12 $\pm$ 0.03	0.12 $\pm$ 0.04	0.11 $\pm$ 0.03	0.07 $\pm$ 0.02	0.13 $\pm$ 0.06	0.09 $\pm$ 0.02	0.55 $\pm$ 0.17					
Heart	0.71 $\pm$ 0.27	0.66 $\pm$ 0.15	0.42 $\pm$ 0.08	0.49 $\pm$ 0.17	0.39 $\pm$ 0.10	0.53 $\pm$ 0.10	0.64 $\pm$ 0.14					
Liver	3.91 $\pm$ 0.48	3.51 $\pm$ 1.33	3.63 $\pm$ 0.35	3.70 $\pm$ 1.11	3.67 $\pm$ 1.03	3.55 $\pm$ 0.94	5.90 $\pm$ 3.15					
Lung	1.10 $\pm$ 0.28	1.31 $\pm$ 0.39	1.08 $\pm$ 0.14	1.18 $\pm$ 0.38	1.22 $\pm$ 0.41	1.11 $\pm$ 0.24	1.31 $\pm$ 0.38					
Kidney	9.60 $\pm$ 4.67	7.85 $\pm$ 3.90	5.16 $\pm$ 1.19	6.31 $\pm$ 1.78	5.14 $\pm$ 1.52	5.89 $\pm$ 1.97	5.53 $\pm$ 0.61					
Stomach	0.87 $\pm$ 0.44	1.01 $\pm$ 0.40	0.67 $\pm$ 0.15	1.00 $\pm$ 0.35	0.68 $\pm$ 0.19	1.02 $\pm$ 0.49	1.69 $\pm$ 0.94					
Muscle	0.44 $\pm$ 0.17	0.77 $\pm$ 0.25	0.33 $\pm$ 0.07	0.45 $\pm$ 0.20	0.29 $\pm$ 0.11	0.44 $\pm$ 0.21	0.27 $\pm$ 0.09					
Bone	32.74 $\pm$ 7.19	33.81 $\pm$ 3.01	36.35 $\pm$ 4.49	31.43 $\pm$ 12.47	28.24 $\pm$ 8.45	32.15 $\pm$ 7.93	5.90 $\pm$ 0.03					
Brain	0.06 $\pm$ 0.02	0.06 $\pm$ 0.02	0.04 $\pm$ 0.02	0.05 $\pm$ 0.02	0.04 $\pm$ 0.01	0.04 $\pm$ 0.02	0.09 $\pm$ 0.01					
Tumor	4.68 $\pm$ 0.42	4.97 $\pm$ 1.33	3.29 $\pm$ 1.80	3.67 $\pm$ 0.91	3.75 $\pm$ 0.72	3.02 $\pm$ 1.04	3.03 $\pm$ 1.40					
	DIPICOLINIC				GLUCONIC ACID				NPA		TTHA	
	DTPA	EDTA	HEDTA	NPA	TTHA							
Blood	0.12 $\pm$ 0.09	0.01 $\pm$ 0.006	0.005 $\pm$ 0.003	0.06 $\pm$ 0.02	0.07 $\pm$ 0.06	0.03 $\pm$ 0.005	0.05 $\pm$ 0.02					
Heart	0.33 $\pm$ 0.10	0.05 $\pm$ 0.006	0.04 $\pm$ 0.03	0.55 $\pm$ 0.07	0.05 $\pm$ 0.05	0.08 $\pm$ 0.05	0.15 $\pm$ 0.06					
Liver	2.16 $\pm$ 0.47	0.11 $\pm$ 0.04	0.20 $\pm$ 0.09	3.35 $\pm$ 1.19	0.41 $\pm$ 0.12	0.32 $\pm$ 0.08	0.26 $\pm$ 0.06					
Lung	0.68 $\pm$ 0.18	0.05 $\pm$ 0.03	0.04 $\pm$ 0.03	1.18 $\pm$ 0.17	0.11 $\pm$ 0.04	0.14 $\pm$ 0.06	0.09 $\pm$ 0.07					
Kidney	4.13 $\pm$ 4.19	0.69 $\pm$ 0.29	0.81 $\pm$ 0.21	5.90 $\pm$ 2.52	1.47 $\pm$ 0.46	1.08 $\pm$ 0.53	1.71 $\pm$ 0.76					
Stomach	0.38 $\pm$ 0.16	0.13 $\pm$ 0.17	2.20 $\pm$ 4.17	0.97 $\pm$ 0.37	0.37 $\pm$ 0.61	0.08 $\pm$ 0.02	0.07 $\pm$ 0.04					
Muscle	0.35 $\pm$ 0.10	0.02 $\pm$ 0.008	0.02 $\pm$ 0.008	0.35 $\pm$ 0.09	0.04 $\pm$ 0.02	0.06 $\pm$ 0.03	0.04 $\pm$ 0.02					
Bone	33.36 $\pm$ 5.34	0.10 $\pm$ 0.04	1.88 $\pm$ 0.18	40.61 $\pm$ 5.86	6.55 $\pm$ 1.62	6.74 $\pm$ 0.76	1.03 $\pm$ 0.25					
Brain	0.04 $\pm$ 0.02	0.01 $\pm$ 0.008	0.02 $\pm$ 0.006	0.05 $\pm$ 0.01	0.02 $\pm$ 0.01	0.01 $\pm$ 0.005	0.03 $\pm$ 0.01					
Tumor	0.93 $\pm$ 0.06	0.04 $\pm$ 0.00	0.05 $\pm$ 0.009	2.84 $\pm$ 0.96	0.16 $\pm$ 0.12	0.27 $\pm$ 0.11	0.36 $\pm$ 0.45					



TABLE II. BIODISTRIBUTION OF  $^{169}\text{Yb}$ -COMPLEXES AND  $^{67}\text{Ga}$  IN TUMOR BEARING MICE  
 % PER ORGAN AT 2 DAY PIV (Mean  $\pm$  S.D. of 5 Animals)

	ACETATE	CITRIC ACID	DIMETHYL LACTIC ACID	GLYCINE	GLYCOLIC ACID	LACTIC ACID	$^{67}\text{Ga}$ -CITRATE
Blood	0.15 $\pm$ 0.03	0.14 $\pm$ 0.05	0.14 $\pm$ 0.03	0.10 $\pm$ 0.03	0.20 $\pm$ 0.08	0.13 $\pm$ 0.03	0.97 $\pm$ 0.03
Heart	0.06 $\pm$ 0.02	0.05 $\pm$ 0.008	0.03 $\pm$ 0.005	0.05 $\pm$ 0.02	0.04 $\pm$ 0.01	0.04 $\pm$ 0.005	0.06 $\pm$ 0.01
Liver	4.31 $\pm$ 0.98	3.73 $\pm$ 0.87	3.87 $\pm$ 0.22	4.03 $\pm$ 0.97	4.89 $\pm$ 0.92	3.62 $\pm$ 0.51	10.33 $\pm$ 5.54
Lung	0.18 $\pm$ 0.07	0.18 $\pm$ 0.07	0.15 $\pm$ 0.03	0.19 $\pm$ 0.07	0.21 $\pm$ 0.06	0.16 $\pm$ 0.04	0.22 $\pm$ 0.07
Kidney	2.19 $\pm$ 0.69	1.70 $\pm$ 0.69	1.28 $\pm$ 0.30	1.64 $\pm$ 0.37	1.56 $\pm$ 0.38	1.48 $\pm$ 0.47	1.59 $\pm$ 0.07
Stomach	0.27 $\pm$ 0.20	0.34 $\pm$ 0.29	0.16 $\pm$ 0.05	0.25 $\pm$ 0.17	0.22 $\pm$ 0.08	0.27 $\pm$ 0.08	0.57 $\pm$ 0.37
Muscle	3.40 $\pm$ 0.88	5.67 $\pm$ 1.75	2.70 $\pm$ 0.61	3.67 $\pm$ 1.22	2.67 $\pm$ 0.86	3.68 $\pm$ 1.56	3.03 $\pm$ 1.04
Bone	60.21 $\pm$ 10.95	58.08 $\pm$ 5.44	68.36 $\pm$ 5.80	61.40 $\pm$ 14.54	61.95 $\pm$ 14.33	63.27 $\pm$ 10.54	22.80 $\pm$ 0.98
Brain	0.03 $\pm$ 0.005	0.02 $\pm$ 0.009	0.017 $\pm$ 0.01	0.02 $\pm$ 0.008	0.018 $\pm$ 0.007	0.02 $\pm$ 0.009	0.02 $\pm$ 0.00
Tumor	6.66 $\pm$ 1.39	5.17 $\pm$ 1.21	4.37 $\pm$ 1.59	4.36 $\pm$ 2.97	4.17 $\pm$ 1.20	4.45 $\pm$ 0.53	7.40 $\pm$ 3.24

	DTPA	EDTA	GLUCONIC ACID	HEDTA	NTA	TTHA
Blood	0.16 $\pm$ 0.12	0.01 $\pm$ 0.006	0.004 $\pm$ 0.002	0.08 $\pm$ 0.06	0.06 $\pm$ 0.03	0.06 $\pm$ 0.03
Heart	0.03 $\pm$ 0.01	0.004 $\pm$ 0.001	0.003 $\pm$ 0.002	0.05 $\pm$ 0.01	0.004 $\pm$ 0.003	0.009 $\pm$ 0.002
Liver	2.16 $\pm$ 0.52	0.11 $\pm$ 0.03	0.18 $\pm$ 0.02	3.75 $\pm$ 1.31	0.36 $\pm$ 0.06	0.47 $\pm$ 0.20
Lung	0.10 $\pm$ 0.04	0.006 $\pm$ 0.003	0.007 $\pm$ 0.008	0.16 $\pm$ 0.04	0.01 $\pm$ 0.004	0.03 $\pm$ 0.01
Kidney	1.15 $\pm$ 1.34	0.18 $\pm$ 0.07	0.19 $\pm$ 0.03	1.36 $\pm$ 0.24	0.30 $\pm$ 0.08	0.31 $\pm$ 0.11
Stomach	0.15 $\pm$ 0.06	0.05 $\pm$ 0.07	0.69 $\pm$ 1.37	0.24 $\pm$ 3.07	0.21 $\pm$ 0.41	0.04 $\pm$ 0.03
Muscle	2.94 $\pm$ 0.77	0.18 $\pm$ 0.04	0.15 $\pm$ 0.04	3.10 $\pm$ 0.98	0.30 $\pm$ 0.17	0.62 $\pm$ 0.23
Bone	64.29 $\pm$ 4.32	0.18 $\pm$ 0.05	3.39 $\pm$ 0.55	83.10 $\pm$ 15.09	10.92 $\pm$ 2.12	18.00 $\pm$ 6.63
Brain	0.02 $\pm$ 0.008	0.005 $\pm$ 0.004	0.007 $\pm$ 0.003	0.02 $\pm$ 0.005	0.007 $\pm$ 0.003	0.005 $\pm$ 0.001
Tumor	1.74 $\pm$ 0.24	0.07 $\pm$ 0.05	0.08 $\pm$ 0.03	3.10 $\pm$ 1.63	0.20 $\pm$ 0.12	0.47 $\pm$ 0.33

AUTORADIOGRAPHIC AND SCINTIGRAPHIC STUDIES OF TIN-CONTAINING COMPOUNDS IN NORMAL ANIMALS AND IN ANIMAL MODELS OF BONE DISEASE

Z. H. Oster, P. Som, S.C. Srivastava, G.E. Meinken, H.L. Atkins, F. F. Knapp, Jr., T. A. Butler and A. B. Brill

Medical Department, Brookhaven National Laboratory, Upton, New York 11973, USA

Although tin is included in most Tc-99m labeling kits its effect and metabolism are poorly understood. Thus it was noticed that in addition to acting as a reducing agent, a change in the behaviour of a compound can be affected by varying the Tc: Tin ratios (1,2) and that the oxidation state of tin is of great importance (3). The present is a study of the bone binding properties of Sn-117m stannic and stannous MDP and DTPA in well defined oxidation states in normal animals and in some animal models mimicking human disease.

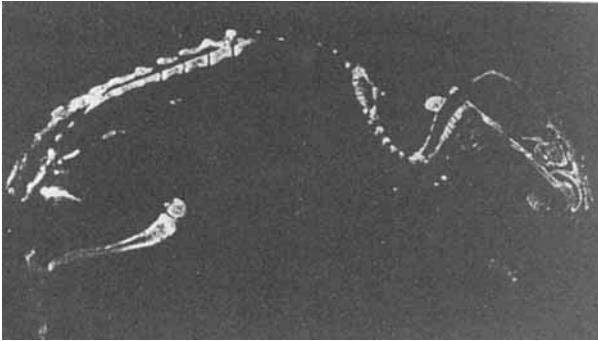
Sn-117m was produced in the Oak Ridge National Laboratory high flux reactor by the following reaction:  $\text{Sn-116} (n,\gamma)\text{Sn-117m}$  and Sn-117m(2+) and (4+)DTPA and MDP were prepared as described elsewhere (4). The Tc-99m DTPA and MDP were prepared from commercially available sources. Tissue distribution studies and whole body autoradiography were performed in Swiss albino (BNL strain) mice and in Fischer rats. A scintigraphic comparison of Sn-117m(4+)DTPA and Tc-99m(Sn+2)MDP was performed in dogs. Models of fracture, osteomyelitis and ischemic muscle lesions were produced in rabbits and the effect of hypervitaminosis A was studied in Fischer rats. Nude mice bearing osteosarcoma of human origin (5) were also studied.

The non-phosphate Sn-117m(4+)DTPA showed the highest bone uptake with lowest uptake in soft tissues. Increased deposition was observed at sites of fracture, osteomyelitis and in ischemic muscle lesions. In hypervitaminosis A, decreased skeletal uptake was noticed. Human osteosarcoma in nude mice showed intense uptake in the tumor, forming a spiculated pattern.

The biological similarity of the non-phosphate Sn-117m(4+)DTPA and Tc-99m(Sn2+)MDP suggests that tin may bind to bone phosphate similarly to the exchange binding when the latter is administered. Sn-117m(4+)DTPA has very good imaging properties because of its 158.6 KeV gamma rays, but its long half-life (14.03 d) makes it suitable only for imaging of long term follow-up periods. The use of Sn-117m(4+)DTPA for therapy of bone tumors should be considered because of (a) its high deposition and persistence in cortical bone as compared to bone marrow, (b) the abundance of short-range Auger and conversion electrons may cause less bone marrow radiation as compared to P-32, and (c) the whole body radiation is also less than that of P-32 which emits high-energy (1.7 MeV) beta rays.

- (1) Lin T.H., Khentigan A., and Winchell H.S.: A  $^{99\text{m}}\text{Tc}$ -chelate substitute for organoradiomercurial renal agents. *J Nucl Med* 15: 34-35, 1974.
- (2) Oster Z.H., Som P., Gil M.C., et al.  $^{97}\text{Ru}$ -DMSA for delayed renal imaging. *Radiology* 141: 185-190, 1981.
- (3) Srivastava S.C., Meinken G., Smith T.D., et al. Problems associated with stannous  $^{99\text{m}}\text{Tc}$  radiopharmaceuticals. *Int J Appl Radiat Isot* 28: 83-95, 1977.
- (4) Srivastava S.C., Meinken G.E., Richards P., et al. The development and in-vivo behavior of tin-containing radiopharmaceuticals I: Chemistry, preparation and distribution in small animals. In preparation, 1984.
- (5) Eilon G, Perkins J, and Viola MV: Characteristics of a calcitonin-responsive cell line derived from a human osteosarcoma. *Cancer Res* 43:327-332, 1983.

Work performed under Contract No. DE-AC02-76CH00016 with the United States Department of Energy.



Autoradiograph of rat following I.V. injection of Sn-117m(4+)DTPA. Intense uptake in cortical bone and lack of activity in bone marrow is evident.



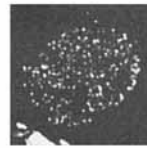
Scintiphotos of a dog 24 hrs after Sn-117m(4+)DTPA. Notice high uptake in bone as compared to soft tissues.



5d  
C A

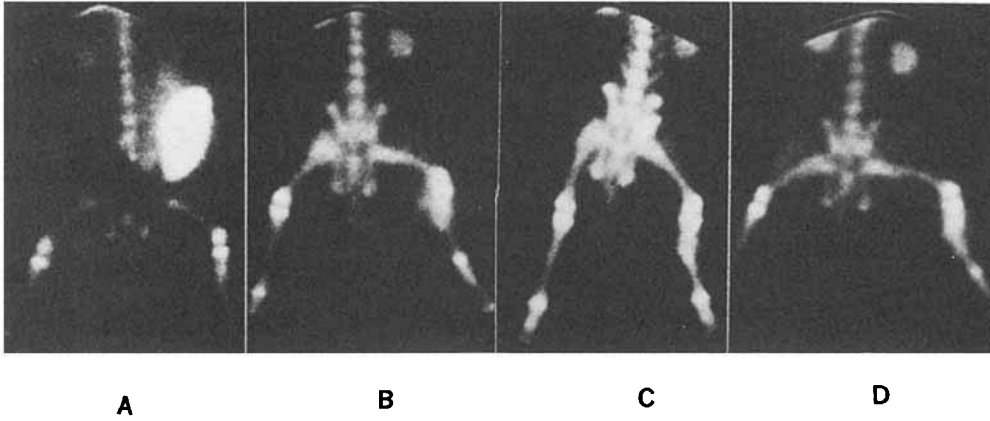


8d  
C A



Scintiphotos of control (C) and vitamin A treated rats (A) for 5 and 8 days. Notice decreased uptake in A as compared to C and high uptake in gangrenous tails.

Autoradiograph of human osteogenic sarcoma transplanted to nude mouse. The uptake of Sn-117m(4+)DTPA is non-uniform forming a spiculated pattern.



Scintiphotos of rabbit with fracture 3 hrs after Tc-99m MDP (A) and 24 hrs after Sn-117m(4+)DTPA (B). Scintiphotos of rabbit with osteomyelitis 3 hrs after Tc-99m MDP(C) and 24 hrs after Sn-117m(4+)DTPA. Although the uptake patterns are similar with the two compounds, higher uptake is noticed in the femur with osteomyelitis.

TABLE 1. LESION TO NORMAL BONE RATIOS IN RABBITS

	Fracture				Osteomyelitis			
	3 hrs	24 hrs	48 hrs	8 days	3 hrs	24 hrs	48 hrs	8 days
Tc-99m(Sn2+)MDP	1.75				2.54			
Sn-117m(4+)DTPA	1.90	3.72	3.45	2.99	3.06	3.92	3.36	2.52

TABLE 2. COMPARATIVE RADIATION DOSIMETRY OF Sn-117m(4+)DTPA AND P-32 IN SELECTED SITES AND WHOLE BODY (WB)

Organs and WB	Sn-117m(4+)DTPA Dose(rad/mCi)	P-32-Phosphate
Bone	21.0	10-50
Bone Marrow	1.6	20-40
Whole Body	0.35	8-10
Excretory Organs	1.0	2-5

EVALUATION OF ADSORBENTS FOR THE OSMIUM-191/IRIDIUM-191m ULTRASHORT-LIVED RADIONUCLIDE GENERATOR SYSTEM

C. Brihaye\*, T. A. Butler and F. F. Knapp, Jr., Nuclear Medicine Group, Oak Ridge National Laboratory, Oak Ridge, TN 37830, U.S.A.

The Os-191/Ir-191m generator system has several important advantages including the short half-life ( $T_{1/2} = 4.96$  sec) of the Ir-191m daughter which minimizes the absorbed radiation dose received by the patient. In addition, the half-life of the Os-191 parent ( $T_{1/2} = 15.4$  d) could make the useful life of the generator several weeks. A description of an Os-191/Ir-191m separation by ion exchange techniques was published in 1956 (1). Later, a generator designed for medical purposes was developed which used the AG1X8 anion exchanger resin as the osmium(IV) adsorbent (2). The latest design of this generator, first described in 1980 (3), employs the AGMP-1 resin loaded with osmium(VI). Iridium-191m obtained from this system has been used effectively for the evaluation of intracardiac shunts in children (4,5) and for the determination of left ventricular ejection fractions in adults (6). The goal of the present studies was to evaluate potential new adsorbents for this system with the objective of achieving higher yields of Ir-191m and lower Os-191 breakthrough over a period of several weeks.

A systematic evaluation of adsorbents included 39 inorganic materials broadly classified as oxides (nine), antimonates (seven), ferro-ferricyanides (eight), phosphates (six), sulfides (three), and other materials (six), including the organic anion-exchanger AGMP-1. Os-191 species in oxidation states (VI), potassium tetrachloroosmate,  $K_2[OsO_2(Cl)_4]$ ; (IV), potassium hexachloroosmate,  $K_2OsCl_6$ ; and (III), potassium hexathiocyanatoosmate,  $K_3Os(SCN)_6$ , were prepared as shown in Scheme I. Uptake was measured on the adsorbents by a batch equilibration method where 0.25 g of exchanger was added to 5 ml of radioactive osmium solution. After 15 h of continuous agitation, the solution was centrifuged and the activity of 1 ml of solution was measured. The exchangers showing high Os-191 uptake were further evaluated as adsorbents by determining Ir-191m yield and Os-191 breakthrough by elution studies. The exchangers having a high uptake of Os-191 were equilibrated with Os-191 by the same procedure and transferred into 1 ml syringes provided with a glass wool plug. The elution of Ir-191m was tested with three potentially injectable solutions: 0.9% NaCl-0.1 M HCl, 0.9% NaCl-0.01 M HCl, and 5% glucose. For elution tests, 5 ml volumes of these solutions were passed rapidly (about 5 sec) through the columns.

Because of the ultra-short half-life of Ir-191m (4.96 sec) an analytical procedure was developed to accurately determine the yield of the Ir-191m. The high levels of Ir-191m cannot be measured immediately after elution by a NaI(Tl) detector system because of excessive dead time. A waiting period of several half-lives is thus allowed to reduce the count rate. The remaining Ir-191m is counted until essentially all has decayed (at least 40 sec, 8 half-lives). By using standardized geometrical factors and digital timers, accurate and reproducible values can be obtained. The % yield of Ir-191m and Os-191 breakthrough are calculated as follows:

$Y (\%) =$  Percent yield of Ir-191m eluted from the column based on the equilibrium amount associated with the Os-191 adsorbed at the time of elution.

---

\*Present address: University of Liege, Cyclotron Research Center, Liege, Belgium

Research sponsored by the Office of Health and Environmental Research, U.S. Department of Energy under contract W-7405-eng-26 with the Union Carbide Corporation.

$$Y (\%) = \frac{(^{191m}\text{Ir}) - (^{191}\text{Os}) \times \lambda^{191m} \times f \times 100}{\epsilon \times I_0 \times A(^{191}\text{Os}) \times 3.7 \times 10^4 \times e^{-\lambda^{191m} t_w}}$$

B (%) Breakthrough percentage of Os-191 eluted with the Ir-191m based on the Os-191 on the adsorbent at the time of elution.

$$B (\%) = \frac{(^{191}\text{Os}) \times 100 \times f}{t_c \times \epsilon \times I_0 \times 3.7 \times 10^4 \times A(^{191}\text{Os})}$$

A(<sup>191</sup>Os) = <sup>191</sup>Os adsorbed on the column at the time of elution in μCi

λ<sup>191m</sup> = Decay constant of Ir-191m = 0.140 sec<sup>-1</sup>

ε = Efficiency of the detection system at 130 keV

I<sub>0</sub> = Intensity of the 130 keV gamma ray from <sup>191</sup>Os/<sup>191m</sup>Ir is 0.259

t<sub>w</sub> = Waiting time (sec) before counting the Ir-191m

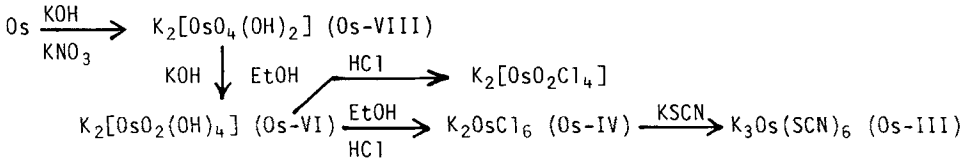
t<sub>c</sub> = Counting time (sec) to measure the Os-191 content

f = Experimentally determined geometrical factor for activities measured at different distances or different volumes.

(<sup>191</sup>Os) = Counts of Os-191 detected in t<sub>c</sub> seconds. It is convenient to use the same counting time for determination of Ir-191m and Os-191

(<sup>191m</sup>Ir) = Ir-191m counts, after t<sub>w</sub> for at least 8 half-lives (40 sec)

The results of the elution measurements are summarized in Tables 1-3 and indicate that the AGMP-1 is the best system tested. Because of the attractive properties of Ir-191m for a variety of clinical applications, other osmium compounds and additional adsorbents should be evaluated.



Scheme I

- (1) Campbell, E. C., and Nelson, F. J. *Inorg. Chem.*, **3**, 233 (1956).
- (2) Yano, Y. and Auger, H. O. *J. Nucl. Med.*, **9** (1), 2 (1967).
- (3) Cheng, C., Treves, S., Samuel, A., and Davis, M. A. *J. Nucl. Med.*, **21**, 1169 (1980).
- (4) Treves, S., Cheng, C., Samuel, A., Lambrecht, R., Babchyc, B., Zimmerman, R., and Norwood, N. *J. Nucl. Med.*, **21** (12), 1151 (1980).
- (5) Treves, S., "Iridium-191m: Clinical Usefulness of Ultrashort-Lived Radionuclides in Nuclear Cardiology," International Symposium on Single Photon Ultrashort-Lived Radionuclides, Washington, D.C., May 9-10, 1983, U.S. Department of Energy, in press.
- (6) Heller, G. V., "Potential for Iridium-191m", *ibid.*

Table 1. Iridium-191m Elution Yield (%) and Osmium-191 Breakthrough (%) from Exchangers Loaded with Potassium Tetrachloroosmate(VI).

Exchanger	Ir-191m Yield (%)			Os-191 Breakthrough (%)		
	0.9% NaCl -0.1 M HCl	0.9% NaCl -0.01 M HCl	5% Glucose	0.9% NaCl -0.1 M HCl	0.9% NaCl -0.01 M HCl	5% Glucose
Hydrated tin(IV) oxide	<0.01	<0.01	<0.01	0.15	0.04	9.10 <sup>-3</sup>
Hydrated titanium oxide	<0.01	<0.01	<0.01	0.51	0.12	0.03
Hydrated manganese dioxide	<0.01	<0.01	<0.01	9.10 <sup>-3</sup>	<3.10 <sup>-4</sup>	<3.10 <sup>-4</sup>
Hydrated zirconium oxide	<0.01	<0.01	<0.01	0.23	0.07	0.01
Copper ferrocyanide	1.4	1.7	0.8	0.13	0.02	0.15
Zirconium ferrocyanide	0.3	0.2	<0.01	0.02	0.02	0.08
AGMP-1	35.8	37.2	4.3	0.05	1.4	0.008

Table 2. Iridium-191m Elution Yield (%) and Osmium-191 Breakthrough (%) from Exchangers Loaded with Potassium Hexachloroosmate(IV).

Exchanger	Ir-191m Yield (%)			Os-191 Breakthrough (%)		
	0.9% NaCl -0.1 M HCl	0.9% NaCl -0.01 M HCl	5% Glucose	0.9% NaCl -0.1 M HCl	0.9% NaCl -0.01 M HCl	5% Glucose
Hydrated tin(IV) oxide	0.03	<0.01	<0.01	0.61	0.21	0.06
Hydrated titanium oxide	0.12	0.14	0.03	0.52	0.81	0.22
Hydrated ferric(III) oxide	0.71	0.67	0.06	0.8	0.1	0.2
Hydrated zirconium oxide	0.1	0.1	0.09	0.12	0.08	0.09
Hydrated chromium oxide	<0.01	<0.01	0.7	1.16	0.23	0.15
Acid alumina	<0.01	1.4	0.06	0.8	0.4	6.10 <sup>-3</sup>
Lead sulfide	<0.01	<0.01	<0.01	3.10 <sup>-3</sup>	5.10 <sup>-3</sup>	1.10 <sup>-3</sup>
Pertitanic acid	0.45	0.21	0.19	0.71	0.13	0.46
AGMP-1	2.5	1.6	1.4	0.06	4.10 <sup>-3</sup>	3.10 <sup>-3</sup>

Table 3. Iridium-191m Elution Yield (%) and Osmium-191 Breakthrough (%) from Exchangers Loaded with Potassium Hexathiocyanatoosmate(III).

Exchanger	Ir-191m Yield (%)			Os-191 Breakthrough (%)		
	0.9% NaCl -0.1 M HCl	0.9% NaCl -0.01 M HCl	5% Glucose	0.9% NaCl -0.1 M HCl	0.9% NaCl -0.01 M HCl	5% Glucose
Hydrated tin(IV) oxide	<0.01	<0.01	<0.01	1.6	1.4	0.2
Hydrated titanium oxide	2.2	<0.01	<0.01	4.9	2.3	0.06
Hydrated ferric(III) oxide	<0.01	<0.01	<0.01	0.6	1.5	0.03
Hydrated manganese oxide	1.8	1.0	<0.01	0.4	0.2	0.4
Hydrated zirconium oxide	0.04	<0.01	<0.01	1.9	3.1	0.03
Acid alumina	<0.01	3.7	<0.01	1.9	4.1	0.01
Zirconium ferrocyanide	1.7	<0.01	<0.01	0.8	1.5	0.1
Lead sulfide	0.9	0.7	<0.01	1.7	1.1	0.05
AGMP-1	0.4	0.04	<0.01	0.07	0.1	0.06

## DEVELOPMENT AND EVALUATION OF RADIORUTHENIUM LABELED DIISOPROPYL HIDA AND BROMOTRIMETHYL HIDA FOR DELAYED STUDIES OF THE BILIARY TRACT

S.C. Srivastava and G.E. Meinken

Medical Department, Brookhaven National Laboratory, Upton, New York 11973.

Whereas the various technetium-99m-labeled HIDA derivatives are the agents of choice for hepatobiliary imaging studies (1), there are situations (e.g., neonatal hepatitis, biliary atresia, etc.) that require delayed studies, and where use of a longer-lived tracer is necessary. Ruthenium-97-labeled PIPIDA (p-isopropyl HIDA) and BIDA (p-butyl HIDA) were developed and proposed as replacements for  $^{131}\text{I}$ -Rose Bengal in view of the latter agent's various drawbacks, and the excellent imaging properties of ruthenium-97 (2-4).

This study was carried out to label two newer generation ligands, DISIDA (2,6-diisopropylphenylcarbamoylmethyl iminodiacetic acid) and bromotrimethyl HIDA (3-bromo-2,4,6-trimethylphenylcarbamoylmethyl iminodiacetic acid), with ruthenium-103 and to evaluate the biodistribution of the labeled agents in mice. These compounds, labeled with  $^{99\text{m}}\text{Tc}$ , have been shown to display superior hepatobiliary specificity, rapid transit, negligible renal excretion, and resistance to competition by elevated bilirubin levels (5,6).

In all labeling experiments, ruthenium-103 was used for convenience. The method typically was as follows. To a 2 ml solution of 10-20 mg ligand in pH 5, 0.05 M sodium acetate, 25  $\mu\text{l}$  ruthenium-103 chloride (in HCl) was added with mixing. The pH was checked and adjusted to 5 if necessary. The mixture was then heated by immersing in a boiling water bath for 60 min. Radiochemical purity was determined using the following chromatographic systems:  $\mu\text{-C}_{18}$  reverse-phase TLC in 0.05 M pH 5 phosphate in 70% methanol; silica gel TLC in 0.05 M pH 7 phosphate in 70% methanol; and micropolyamide TLC in 100% methanol. Ruthenium-103 acetate, pH 5, heated for 60 min at 100°, was used as a control. Silica gel TLC provided the best separations. The desired complexes were obtained in >95% labeling yields using the above procedure.

The ruthenium-103 chloride solution contained both Ru(III) and Ru(IV). Conversion to Ru(III) was accomplished by refluxing in ethanol overnight. However, no significant difference (in vitro or in vivo) was observed in the behavior of the complexes when prepared with either of the two ruthenium species, possibly due to the eventual preponderance of Ru(III) in the final product. In subsequent experiments, no effort was made to convert Ru(IV) to Ru(III) prior to the labeling reactions.

Biodistribution studies were performed in normal BNL mice after injecting the appropriate agent (0.2 ml) i.v. via the tail vein. The animals were sacrificed at 5, 30 and 120 minutes post injection and the tissue samples counted for activity. Typical data are summarized in Table I. The distribution was very similar to the corresponding  $^{99\text{m}}\text{Tc}$ -labeled agents. High hepatic uptake and negligible renal excretion resulted with both DISIDA and bromotrimethyl HIDA. The uptake kinetics and hepatic transit times were however, slightly different. When the Disofenin kit (New England Nuclear) containing tin was used, blood clearance as well as clearance from the other tissues was more rapid.

Results of this study suggest that ruthenium-97-labeled DISIDA and bromotrimethyl HIDA could be potentially useful agents for delayed studies of the hepatobiliary system.

- (1) Loberg M.D., Nunn A.D. and Porter D.N., "Nuclear Medicine Annual", New York, Raven Press, 1981, pp 1-33.
- (2) Schachner E.R., Gil M.C., Atkins H.L., et al., J. Nucl. Med. 22, 352 (1981).
- (3) Schachner E.R., Gil M.C., Som P., et al., J. Nucl. Med. Commun. 4, 94 (1983).



- (4) Srivastava S.C., Richards P., Som P., et al., "Frontiers in Nuclear Medicine", Heidelberg, Springer-Verlag, 1980, pp 123-133.  
 (5) Klingensmith W., Fritzberg A.R., Spitzer V.M., et al., "Nuclear Medicine and Biology", Pergamon, Paris, 1982, pp 1596-1599.  
 (6) Nunn A.D., Loberg M.D. and Conley R.A., J. Nucl Med. 24, 423 (1983).

Table 1. Tissue Distribution of  $^{103}\text{Ru}$ -Labeled Acetate, Diisopropyl HIDA and Bromotrimethyl HIDA in mice ( $n=3$ )<sup>1</sup>

Compound	Time, min	Percent dose per organ						
		Blood	Liver	Gut	Kidney	Spleen	Muscle	Bone
Acetate	5	13.20	10.20	7.32	3.77	0.27	16.60	6.85
	30	8.46	8.91	7.76	2.13	0.27	10.60	6.93
Diisopropyl-HIDA	5	2.14	19.42	68.30	0.67	0.03	2.71	0.76
	30	0.98	6.69	86.92	0.17	0.01	1.44	0.46
Diisopropyl-HIDA with tin (Disofenin kit)	5	1.85	23.70	60.60	1.05	0.04	2.81	1.00
	30	0.28	2.60	92.80	0.19	0.01	0.48	0.14
Bromotrimethyl-HIDA	5	4.62	24.78	52.57	0.81	0.08	5.04	6.84
	30	1.55	4.06	87.35	0.32	0.03	1.80	0.53

<sup>1</sup>Results shown (percent dose per organ) are the average of 3 mice. Blood, bone and muscle were assumed to constitute 7, 10 and 43% of body wt. respectively. Standard deviations are omitted for the sake of clarity. The average whole body recovery of activity was  $97.2 \pm 2.7\%$  for all compounds (at 5 to 120 min), except for acetate (80% at 5 min, 59% at 30 min, and 54% at 120 min).

**Acknowledgments.** Ligands used in this study were kindly provided by New England Nuclear (Disofenin, DISIDA), and Squibb (bromotrimethyl HIDA). This research was supported by the U.S. Department of Energy under Contract #DE-AC02-76CH00016.

A SINGLE-STEP  $^{99m}\text{Tc}$ -SULPHUR COLLOID, FREEZE-DRIED KIT: FORMULATION AND BIOKINETIC EVALUATION

A.M. AL-Hilli , N.H.Agha, I.F.AL-Jumaili and H.M. AL-Azzawi.  
Nuclear Research Centre, Radioisotope Production Department, P.O.Box 765  
Baghdad-Iraq

Technetium- $^{99m}$  sulphur colloid is a well known radiopharmaceutical for imaging the liver and spleen (1,2). The formation of currently used  $^{99m}\text{Tc}$ -sulphur colloids is usually involve the treatment of different reagents comprising the preparation with technetium in multiple-steps including heating to obtain the labelled colloid prior to medical application. However, this work presents a formulation of preformed sulphur colloid, freeze-dried kit to be directly labelled with technetium without any further treatment. The formulation of the kit is based upon the binding of stannous-tin with sulphide ions released from heating thioacetamide (3) at acidic condition, using carboxy methyl cellulose (CMC) as a hydrophilic stabilizer (4). The amounts of tin (II) sulphur precolloid and stabilizer in the kit are equivalent to 0.125 mg  $\text{SnCl}_2$  , 0.050 mg thioacetamide and 2.5 mg CMC.

The quantities of the reactants and the conditions of the reaction have been chosen from the study of the labelling kinetics of the preparation to achieve a high yield of  $^{99m}\text{Tc}$ -sulphur colloid. Gelchromatography Column Scanning (GCS) method (5,6) was applied for the determination of the reduced  $^{99m}\text{Tc}$ -colloid, free pertechnetate and  $^{99}\text{Tc}$ -sulphur colloid. The pH of the preparation was found to be the most prominent factor affecting the yield of sulphur colloid. The optimal value has been determined to be between 3.0 to 3.5 . Since at higher pH level the yield of the labelled sulphur colloid was significantly decreased. This is probably due to partial dissociation of the tin (II) sulphur precolloid in the preparation resulting in increasing the amounts of reduced  $^{99m}\text{Tc}$ -colloid and free pertechnetate, as shown in the Figure, using the GCS-method. It is suggested that the dissociation of tin (II) sulphur precolloid would influence the blood clearance and liver uptake kinetics.

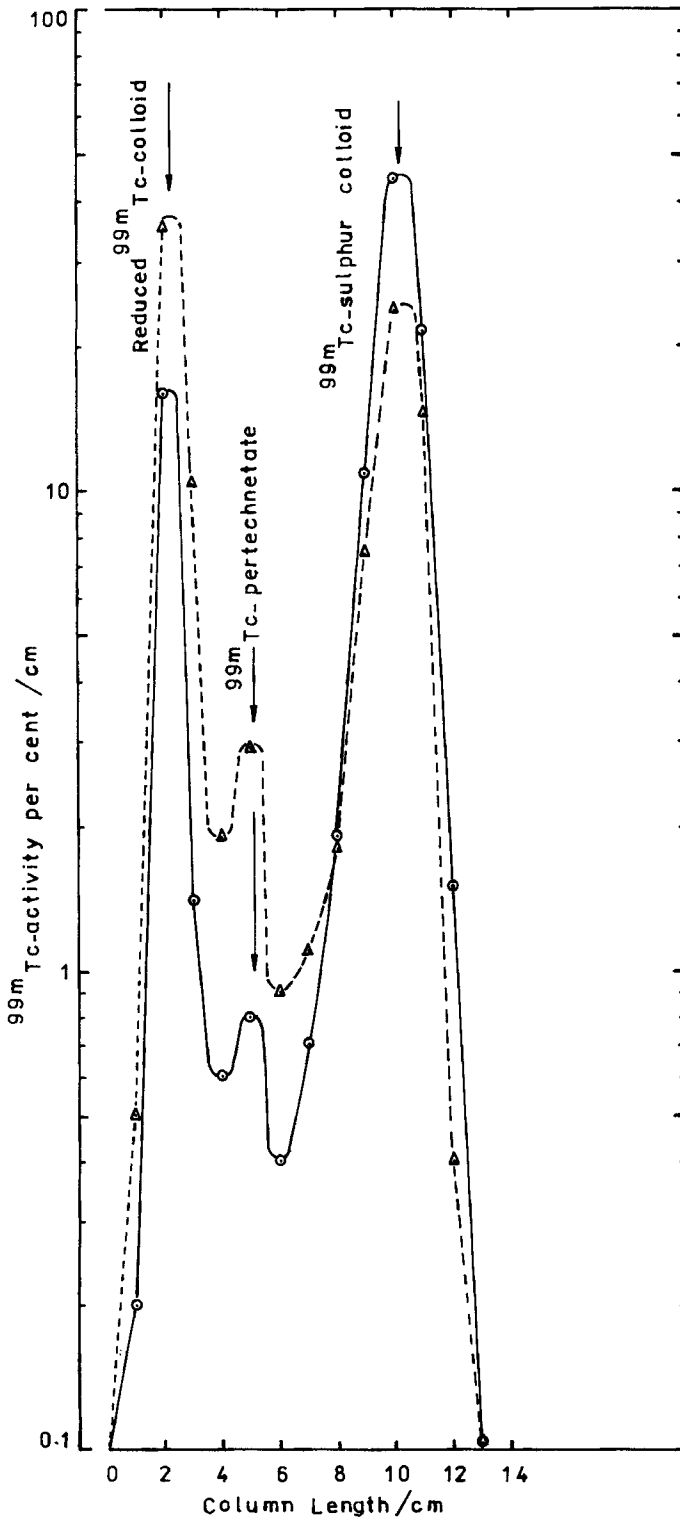
The blood clearance data of the labelled colloid in rabbits showed that the biological half-times of the fast and slow components were 3 and 67 min. respectively. The in vivo organ distribution results in mice as a function of pH are summerized in the table. The high percentage of administered activity accumulated in the liver indicates a high colloid yield with optimal size particles, since the negligible activity detected in both kidneys and gut confirms the in vivo stability of sulphur colloid preparation of pH 3.5. The insignificant activity observed in the lungs reveals the excellent hydrophilic properties of CMC.

$^{99m}\text{Tc}$ -sulphur colloid kit has been clinically evaluated on normal subjects. The results showed rapid blood clearance and high liver uptake of the radiopharmaceutical with normal surrounding tissue background

- (1) Patton D.D., Garcia E.N. and Webber M.M., Amer. J. Roentgenol. Rad. Therapy and Nucl. Med., 97, 380 (1966).
- (2) Haney T.A., Ascino I., Gigliotti J.A., Gusmano E.A. and Bruno J.A., J.Nucl. Med., 12, 64 (1970) .
- (3) Andres E., Ann. Rev. Nucl. Sc., 9, 203 (1959).
- (4) Stern H.S., McAfee J.G. and Subramanian G., J.Nucl. Med., 7, 665 (1966).
- (5) Persson R.B.R., In proc. Int. Symp. Radiopharmaceuticals, 1974. Atlanta, Ga, USA. Soc. Nucl. Med. (N.Y.), 228 (1975).
- (6) Persson R.B.R., Strand S.E. and Knoos T., J. Radioanal Chem., 43, 275 (1978).

Table of organ distribution results of  $^{99m}\text{Tc}$ -sulphur colloid preparations in mice obtained at 20 min. post injection.

organ	% admin.dose / organ at pH value:	
	3.5	4.2
Blood	1.4	6.3
Liver	90.5	65.5
Spleen	2.3	1.1
Lungs	0.5	0.5
Kidneys	0.6	2.8
Gut	1.0	3.5



The Figure shows the GCS-profiles of  $^{99m}\text{Tc}$ -sulphur colloid preparations at pH 3.5 O—O and pH 4.2  $\Delta$ — $\Delta$  .

THE RADIOCHEMICAL QUALITY CONTROL OF  $^{99m}\text{Tc}$ -PHYTATE AND THE EFFECT OF GAMMA RADIATION (2.5 Mrad) ON Sn-PHYTATE KITS TO BE LABELLED WITH  $^{99m}\text{Tc}$  FOR LIVER SCANNING

M.A.A.Al-Janabi , Z.M.Yousif, Y.F.Shafiq,  
M.H.S.Al-Hissoni and B.M.Al-Allak.

Radioisotope Production Department, Nuclear Research Centre, Tuwaitha,  
Baghdad, Iraq.

Subramanian et al (1) have pointed out the application of  $^{99m}\text{Tc}$ -phytate in clinical diagnosis. Authors have prepared this radiopharmaceutical and applied it in nuclear medicine (2). Some authors have clinically compared  $^{99m}\text{Tc}$ -phytate with other liver scanning agents (3,4). We have studied many parameters related to Sn-phytate kits to be labelled with  $^{99m}\text{Tc}$  and found underestimated radiochemical yields using Sephadex G-25 gel chromatography (5). It is intended in this paper to through light on this point by a proper choice of technique for the analysis of  $^{99m}\text{Tc}$ -phytate.

We have applied various gel chromatographic media and we recommend the GCS method for the radiochemical analysis of  $^{99m}\text{Tc}$ -phytate using Sephadex G-10 and 0.9% NaCl as eluent. This technique is rapid and reliable.

Authors have studied the effect of ionizing radiation on medicinal preparations. It was reported that absorbed radiation doses of 2.5 Mrad are sufficient for obtaining preparation sterility with a high coefficient of safety (6).

With respect to Sn-phytate kits, the irradiation (2.5 Mrad) did not affect neither the radiochemical yield of  $^{99m}\text{Tc}$ -phytate nor the stability of Sn-phytate. The organ distribution in mice was affected by irradiation. The table shows slight decrease in liver uptake with higher radiocolloid deposition in the spleen. Irradiated and non-irradiated Sn-phytate kits give rise to similar human images for both liver and spleen using radiocolloid formed in vivo or in vitro. The radiocolloid deposition in the spleen in mice is not reflected in humans. Species differences through some light on the study of radiocolloid distribution.

- (1) Subramanian G., McAfee J.G., Mehter A., Blair R.J. and Thomas F.D. J.Nucl. Med. 14 , 459 (1973).
- (2) Sewatkar A.B., Noronha O.P.D., Ganatra R.D. and Glenn H.J. Nucl-Med. (Stuttgart) 14, 46 (1975) .
- (3) Akisada M. and Miyamae T. Radioisotopes 24, 626 (1975) .
- (4) Arzoumanian A., Rosenthal L., Seto H. J. Nucl. Med. 18, 118 (1977) .
- (5) Al-Janabi M.A.A., Ali Heyam Y. and Al-Salem A.M. First European Symposium on Radiopharmacy and Radiopharmaceuticals, Elsinore , Denmark (1983) .
- (6) Barelko E.V., Babakina G.S., Berezovskaya I.V., Degilova V.S. , Piruzyan L.A., Pomortseva N.V., Solyanina I.P., Sukhamov V.V., Talrose V.L., Tyrina E.A. and Tsibulskaya M.I. Chim. Farm. J.7.94 (1977).

Organ distribution of  $^{99m}\text{Tc}$ -phytate in mice 30 min. after intravenous administration using irradiated (2.5 Mrad) and non-irradiated Sn-phytate kits

Organ	% of injected dose	
	A	B
Liver	90.98	86.30
Spleen	2.09	5.38
Lungs	0.55	0.26
Kidneys	0.64	0.50

A : non-irradiated kits

B : irradiated kits

MECHANISTIC ASPECTS OF THE TECHNETIUM- $^{99m}\text{Tc}$ -TIN-RBC LABELING REACTIONS

S.C. Srivastava, R.F. Straub and P. Richards

Medical Department, Brookhaven National Laboratory, Upton, New York 11973.

This study was undertaken to elucidate mechanistic aspects of the in-vitro method (including BNL kit method) for labeling red blood cells (RBC) with technetium- $^{99m}\text{Tc}$ . The role of various contributing factors in the  $^{99m}\text{Tc}$ -Sn-RBC system, although addressed earlier, has not been clearly established (1-3). Following parameters were investigated in detail: (i) kinetics of tin uptake by RBC using various  $\text{Sn}^{2+}$  complexes; (ii) effect of plasma and other suspending media; (iii) role of oxidation and chelation on removal of plasma tin; (iv) kinetics of  $^{99m}\text{Tc}$  uptake into "tinned" RBC and the effect of carrier  $^{99}\text{Tc}$  on labeling yields; (v) sites of attachment of tin and technetium within the RBC; and (vi) the long-term in-vivo retention of tin.

Of the many ligands studied, citrate (cit) and glucoheptonate were most effective in transporting tin into the RBC. Stannous cit kits labeled with Sn-117m or Sn-113 and containing 2, 15, and 50  $\mu\text{g}$  tin were studied further. The tin uptake was dependent upon blood sample volume, tin content of kits, and temperature. The uptake was very rapid within the first 10 min and then slowly increased up to 2 hr. Little or no uptake resulted when the kits contained stannic tin. Typical results are described in Table 1. The uptake of  $^{99m}\text{TcO}_4^-$  by the tinned RBC depended on the extracellular  $\text{Sn}^{2+}$  concentration. Removal of plasma  $\text{Sn}^{2+}$  before  $^{99m}\text{TcO}_4^-$  addition (either by centrifugation or by adding  $\text{NaOCl}$  + EDTA to sequester and oxidize  $\text{Sn}^{2+}$  to  $\text{Sn}^{4+}$ ) resulted in >95%  $^{99m}\text{Tc}$ -labeling of RBC in 5-15 min. When carrier  $^{99}\text{Tc}$  was present, labeling efficiency improved with increased tin content of RBC. Using a 15  $\mu\text{g}$  tin cit kit + 3 ml blood, or a 50  $\mu\text{g}$  kit + 1 ml blood, >95% labeling yields were obtained, with  $^{99m}\text{TcO}_4^-$  solutions containing  $^{99}\text{Tc}$  equivalent to 300-400 mCi of  $^{99}\text{Mo}$  decay. Addition of EDTA after the tinning step caused an outward shift in the RBC vs plasma  $\text{Sn}^{2+}$  concentration. However, when plasma tin was oxidized to  $\text{Sn}^{4+}$ , EDTA did not cause a significant RBC tin loss. In the whole blood labeling procedure (4), following the tinning of RBC,  $\text{NaOCl}$  had to be added first and then EDTA in order to provide >95% incorporation of  $^{99m}\text{Tc}$ . Reversed order of addition gave poor labeling.

Results on the distribution of tin and  $^{99m}\text{Tc}$  in plasma and within the cell components are shown in Table 2. The RBC-associated tin is distributed between membrane and hemoglobin very similarly to  $^{99m}\text{Tc}$ . The binding of  $^{99m}\text{Tc}$  to hemoglobin appears to have a greater ionic character than most metal-protein complexes. The tag is labile to dilution with water, to low ionic strength solutions at neutral pH, and dissociates in an electrical field. In-vivo stability of  $^{99m}\text{Tc}$ -RBC is attributable to the cell membrane that maintains high hemoglobin concentration within the cell and considerably slows the outward migration of reduced technetium species. Experiments with double-labeled RBC in dogs ( $^{51}\text{Cr}$  labeling followed by labeling same cells with  $^{99m}\text{Tc}$ ) gave intravascular  $^{99m}\text{Tc}/^{51}\text{Cr}$  ratios of 1.0, 0.96, 0.89 and 0.54 at 0.25, 2, 4, and 25.5 hr respectively, following injection. These results demonstrate that the  $^{99m}\text{Tc}$  label slowly leaves the circulation ( $t_{1/2}$  20-35 hr depending on the labeling method). Since  $^{51}\text{Cr}$  loss was found to be negligible, technetium labeling does not damage the RBC. Data in dogs (Fig. 1) showed that the EDTA treatment of tinned cells conferred greater in-vivo stability on the label. Blood clearance  $t_{1/2}$  was longest for  $^{99m}\text{Tc}$ -RBC prepared using the whole blood method. Also, following a single tin pyrophosphate injection as in the in-vivo labeling procedure, significant retention of tin (using Sn-117m labeled kits) was demonstrated even after 6 weeks.

Results from this study support the following conclusions: (i) stannous ion complexed with citrate and many other ligands diffuses into the RBC and becomes bound mostly to hemoglobin; (ii) pertechnetate diffuses freely in and out of RBC; (iii) inside the "tinned" RBC, pertechnetate gets reduced and bound predominantly to the  $\beta$ -globin chain of hemoglobin; (iv) stannic tin as well as reduced

technetium species are generally not transported across the RBC membrane; (iv) extracellular  $\text{Sn}^{2+}$  prematurely reduces pertechnetate, thus inhibiting the entry of technetium into RBC and thereby causing low labeling yields; (vi) tin is retained by the RBC for a long period; and (vii) in-vitro labeling with  $^{99\text{m}}\text{Tc}$  does not damage the RBC.

- (1) Srivastava S.C. and Chervu L.R., *Semin. Nucl. Med.*, 1984 (in press).
- (2) Dewanjee M.K. and Rao S.A., "Nuclear Medicine and Biology", Pergamon, Paris, 1982, p. 1894.
- (3) Billingham M.W. and Waddell T.L., *Int. J. Appl. Radiat. Isotopes* 34, 607 (1983).
- (4) Srivastava S.C., Babich J.B. and Richards P., *J. Nucl. Med.* 24, P128 (1983).

Table 1. Tin Uptake by Red Blood Cells Following Incubation of Whole Blood with Stannous Citrate Kits (N = 2-10)<sup>1</sup>

Sn in kit, µg	Blood volume			
	1 ml		4 ml	
	5 min	30 min	5 min	20 min
2	-	-	0.28	-
15	1.84 ± 0.18	3.47 ± 0.12	4.34 ± 0.54	5.72 ± 0.67
50	5.89 ± 1.93	10.15 ± 0.50	14.51 ± 4.72	13.59

<sup>1</sup>Tin content of RBC in µg after incubation (22°) with tin citrate kits labeled with Sn-117m or Sn-113. The kits also contained in addition to tin, 3.67 mg trisodium citrate, dihydrate, and 5.5 mg dextrose. Cells were separated and washed 2x with saline before counting for the radioactivity.

Table 2. Uptake and Distribution of Tin and Technetium into Various Blood components (% of total, N=10)<sup>1</sup>

Fraction or Component	Tin ( $^{117\text{m}}\text{Sn}$ or $^{113}\text{Sn}$ )	Technetium ( $^{99\text{m}}\text{Tc}$ )
RBC - Membrane	5.7 ± 2.9	1.7 ± 0.3
Non-membrane	18.3 ± 5.1	94.8 ± 2.0
Heme	-	17.3 ± 6.5
Globin	-	77.4 ± 9.7
Total	25.7 ± 0.3	96.5 ± 2.0
Plasma	73.3 ± 4.2	2.7 ± 1.7
Saline wash (2x2ml)	2.1 ± 0.7	0.6 ± 0.3

<sup>1</sup>Average typical results from a number of observations. Tin citrate kits (including Sn-117m or Sn-113 labeled kits) containing varying amounts of tin, and 3 ml blood were used. Whole blood procedure was followed with 15 and 50 µg kits.



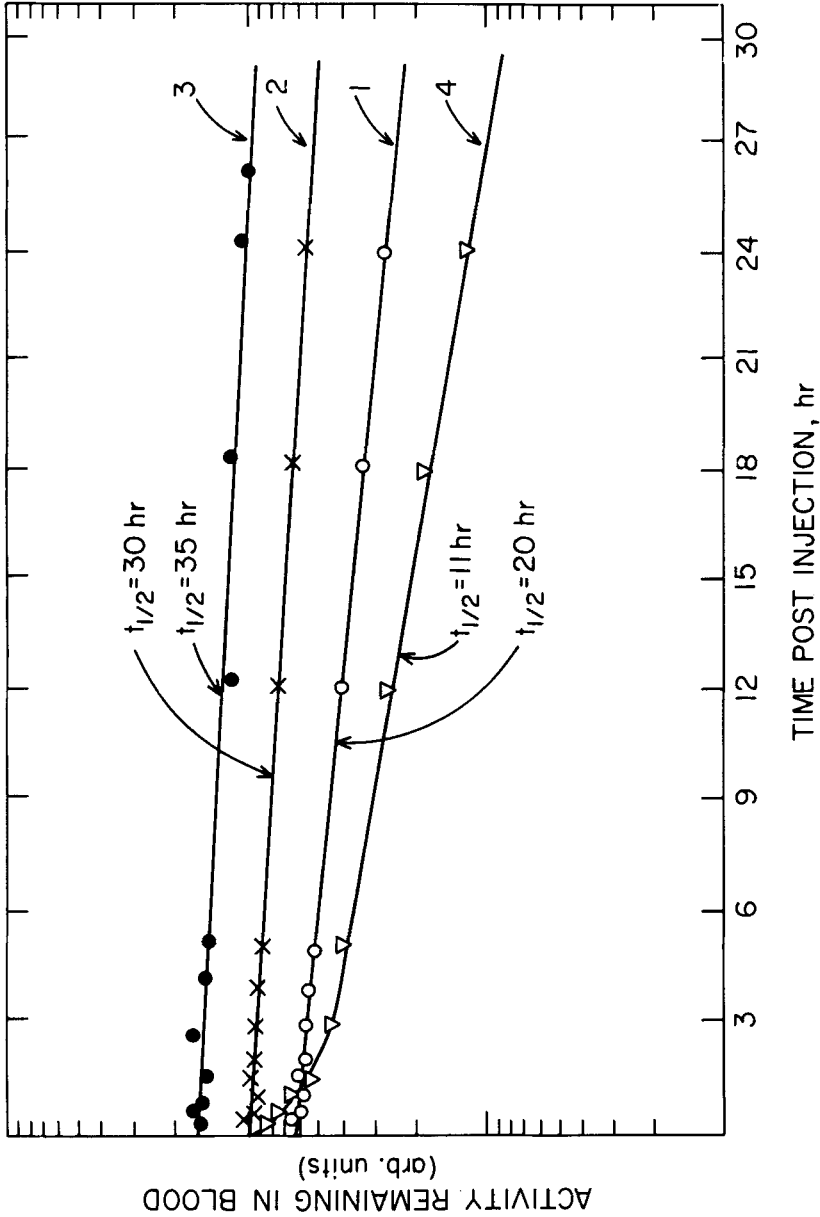


Figure 1. Blood clearance curves of in-vitro labeled  $^{99m}\text{Tc}$ -RBC in asplenic dog. Curves 1 (normal) and 4 (heat-damaged), saline dilution after tinning. Curve 2 (normal), EDTA dilution after tinning. All using 2 µg tin citrate kit and cell separation prior to  $^{99m}\text{TcO}_4^-$  addition. Curve 3, whole blood procedure using 50 µg tin citrate kit (NaOCl + EDTA after tinning).

INTRACELLULAR DISTRIBUTION OF RADIONUCLIDES AND TURNOVER OF RED CELLS LABELED WITH CR-51, IN-111, and TC-99M IN DOGS.

S.T. Mackey, M.K. Dewanjee, S. Chowdhury and H.W. Wahner  
Mayo Clinic and Foundation, Rochester, Minnesota 55905.

The effect of intracellular distribution of Cr-51, In-111, and Tc-99m-radionuclides on clearance rates of labeled red cells was studied sequentially in five mongrel dogs. Saline washed red cells from citrated dog blood were labeled with 51-Cr-chromate (50  $\mu$ Ci), Tc-99m pertechnetate (10 mCi) in vitro, ( $\text{Sn}^{2+}$ : 8  $\mu$ g/ml of packed RBC) in vivo and modified in vivo (in vivitro) and In-111-tropolone (500  $\mu$ Ci). In Cr-51-labeling, free chromate was removed by the addition of 50 mg of ascorbic acid per 10 ml of packed red cells and administered intravenously. The distribution of radionuclides in labeled cells was measured by hypotonic lysis of red blood cells in 0.015 M phosphate buffer. The effect of anticoagulant, heparin and acid-citrate-dextrose (ACD) on the binding to membrane and hemoglobin was also investigated. The membrane was separated from hemoglobin by ultracentrifugation at 100,000 G for two hours at 4°C (Beckman L8-55) and membrane filtration (0.45  $\mu$ M cellulose acetate); RBC membrane was washed three times to free of hemoglobin. Blood clearances of in vivo labeled Tc-99m red blood cells (30  $\mu$ g  $\text{Sn}^{2+}$ /kg) and in vitro labeled Tc-99m, Cr-51, and In-111 red blood cells were determined by serial blood sampling (15 samples in four days for Tc-99m, 25 samples in 14 days for In-111 and 30 samples in 30 days for Cr-51 radionuclides). The red blood cell distribution (%) of the radionuclides and mean exponential red blood cell survival time in days and the major blood clearance component (%) are shown in Table 1 and Figure 1, respectively. The proposed model of transport of pertechnetate and stannous ion through RBC membrane is shown in Figure 2.

Heparin anticoagulant increases Tc-99m binding to hemoglobin more than ACD. Red blood cells labeled with Tc-99m had the highest clearance rate. Previous studies underestimated the amount of Tc-99m bound to membrane proteins. In-labeled red blood cells have a faster blood clearance than Cr-red blood cells. This change in blood clearance of Tc-99m, In-111, and Cr-51 labeled red blood cells may be due to the change in the distribution of radionuclides on the membrane and hemoglobin. More membrane binding may lead to faster turnover rate.

- (1) Sachs J.R., Knauf P.A., and Dunham P.B., "The Red Blood Cell", Academic Press, New York (1975).
- (2) Cantley L.C. and Aisen P., J. Biol. Chem., 254, 1781-1784 (1979).
- (3) Atkins H.L., Eckelman W.C., Klopper J.F., and Richards P., Radiology, 106, 357-360 (1973).
- (4) Pavel D.G., Zimmer A.M., and Patterson V.N., J. Nucl. Med., 18, 305-308 (1977).
- (5) Dewanjee M.K., J. Nucl. Med., 15, 703-707 (1974).
- (6) Dewanjee M.K. and Wahner H.W., Radiology, 132, 711-716 (1979).
- (7) Dewanjee M.K., Rao S.A., and Penniston J.T., Fourth Int. Symp. on Radio-pharmaceutical Chem., Julich, August 23-27, 1983, pp.193-195.
- (8) Rao S.A. and Dewanjee M.K., Eur. J. Nucl. Med., 7, 282-285 (1982).

Table 1 RBC survival time with Cr-51, In-111, and Tc-99m labeled RBC in dogs and distribution in membrane and hemoglobin

Label	L.E.(%)	Recovery(%)	$T_{1/2}$ (D)	Membrane(%)	Hemoglobin(%)
Cr-51 RBC (in vitro:ACD)	95±4	85±8	29±4	9±3	91±4
In-111 RBC (in vitro:ACD)	86±12	77±12	16±3	60±6	40±3
Tc-99m RBC (in vitro:ACD)	87±10	38±9	5±3	58±9	40±7
Tc-99m RBC (in vivo:Heparin)	76±15	51±16	7±2	29±5	64±7
Tc-99m RBC (in vivitro) Heparin	90±4			12±4	88±3
ACD (NIHA)	92±5			37±7	63±7

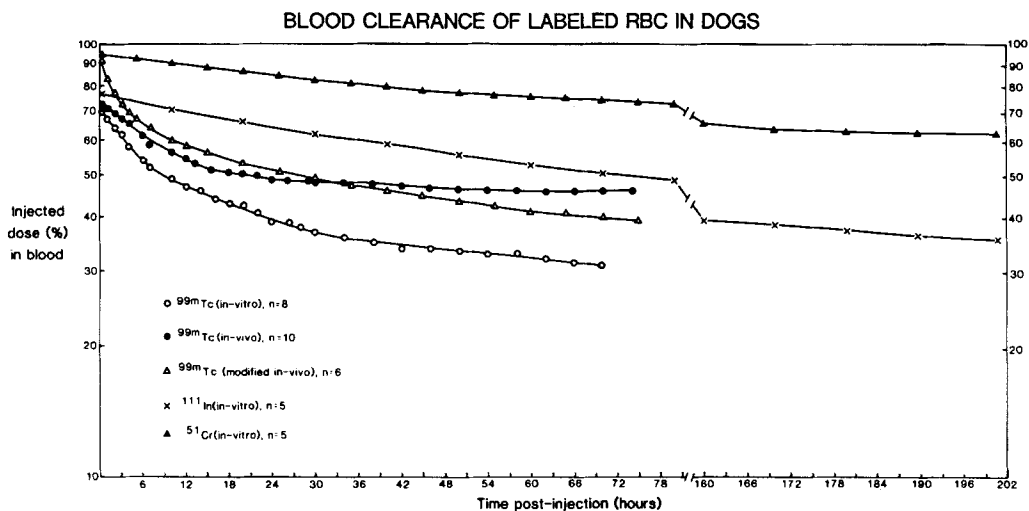


Fig. 1. Blood clearance of Cr-51, In-111, and Tc-99m labeled red blood cells in dogs

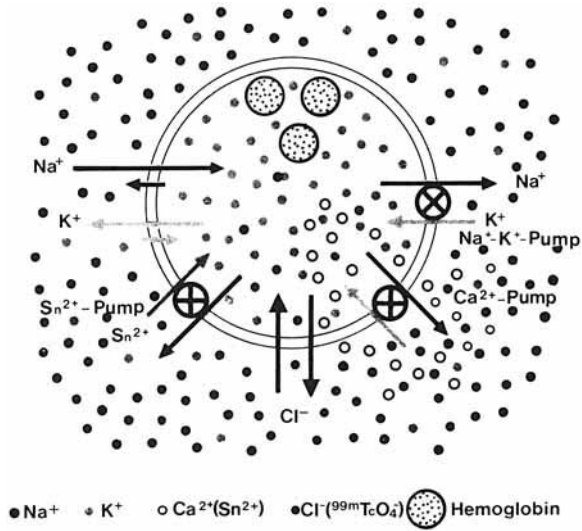


Fig. 2. Proposed model of transport of pertechnetate and stannous ion through RBC membrane

TECHNETIUM (+1, +3, AND +5) COMPLEXES BY LIGAND EXCHANGE FROM HEXAKIS(S-THIOUREA) TECHNETIUM (+3) AND OXO-TETRAKIS-(S-TETRAMETHYLTHIOUREA)TECHNETATE (+5)

M.J. Abrams, D. Brenner, A. Davison and A.G. Jones

Department of Chemistry, Massachusetts Institute of Technology, Cambridge, MA 02139.

We have reported previously on the utility of the complex hexakis-(S-thiourea) technetium (+3) as a synthetic intermediate in the preparation of the known complexes *trans*-[dichlorobis(diphos)]technetium(+3) and *hexakis*-(*t*-butylisonitrile)technetium(+1) in aqueous media (1-3). These studies have now been extended to include complexes containing the ligands dimethylthiourea (dmu) and tetramethylthiourea (tmtu).

In 2N HCl the pertechnetate ion reacts with dmu and tmtu to yield complexes of Tc(+3) and Tc(+5), respectively (2,4). The Tc(+3) complex  $[Tc(dmu)_6](PF_6)_3$  was isolated as bright red needles and characterized by elemental analysis, IR and optical spectroscopy, conductance, and magnetic susceptibility. All of these data are consistent with a formation of the cation as a dmu analog of  $[Tc(tu)_6]^{+3}$  (2). Tmtu, on the other hand, does not form a simple hexa-coordinate species under these conditions. Instead, the reddish orange oxotechnetium(+5) complex  $[TcO(tmtu)_4](PF_6)_3$  was isolated.

Both this and the original Tc(+3) thiourea (tu) complex have been used as synthetic precursors for other species beyond those reported previously. For example, with the thiocyanate ligand, the  $[Tc(tu)_6]^{3+}$  forms the known complex  $[Tc(NCS)_6]^{3-}$  in 62% yield (2). Also with the trimethylphosphite ligand, the new technetium (+1) cation  $[Tc(P(OCH_3)_3)_6]$  was isolated in a 31% yield as the white hexafluorophosphate salt. This species was characterized by elemental analysis, IR and optical spectroscopy, conductance,  $^1H$  and  $^{31}P$  NMR spectroscopy and field desorption mass spectrometry (FDMS). The latter clearly showed a strong signal at  $m/z$  843, corresponding to the parent cation (2,3).

The complex  $[TcO(tmtu)_4]^{3+}$  similarly was used as an intermediate for the preparation of the known (Tc(+5) species  $[trans-TcO_2(py)_4]^+$ , isolated in high yield as its hexafluorophosphate salt. Also, prepared *in situ* from  $TcO_4$ , the tmtu complex reacts in ethanolic base with  $N,N'$ -ethylenebis(2-mercaptoacetamide) to form the  $[TcO(ema)]^{-1}$  anion, which was isolated as its tetraphenyl arsonium salt (61% yield) (2,3).

From these results, it is clear that these two thiourea complexes can be used very effectively as labile intermediates at carrier added levels in the search for new chemistry in oxidation states +5, +3, and +1.

- (1) Abrams M.J., Davison A., Brodack J.W., Jones A.G., Faggiani R., and Lock C.J.L., Proc. 4th Int. Symp. on Radiopharm. Chem., Julich FRG, 1982, p.321.
- (2) Abrams M.J., Ph.D. Thesis, Massachusetts Institute of Technology, May, 1983.
- (3) Abrams M.J., Davison A., Faggiani R., Lock C.J.L., and Jones A.G., Inorg. Chem. (in press).
- (4) Abrams M.J., Brenner D., Davison A., Jones A.G., Inorg. Chim. Acta (in press).
- (5) Kuzina A.F., Oblova A.A., and Spitsyn V.I., Russ. J. Inorg. Chem. 17, 1377 (1972).

Oxotetrakis(tetramethylthiourea)technetium(+5) hexafluorophosphateAnalysis for  $C_{20}H_{48}F_{18}N_8OP_3S_4Tc$ :

	C	H	N	S
calculated	22.26	4.49	10.39	11.89
found	22.28	4.52	10.34	11.93

Optical spectrum ( $CH_3CN$ ):

520 nm ( $\epsilon = 1.2 \times 10^3 \text{ L mol}^{-1} \text{ cm}^{-1}$ ), 393 ( $5.9 \times 10^3$ )  
 256 ( $6.3 \times 10^4$ )

IR spectrum (KBr):  $Tc = O$  975  $\text{cm}^{-1}$  (s)Conductivity ( $CH_3CN$ ,  $10^{-3}M$ )  $\Lambda_M = 419 \text{ ohm}^{-1} \text{ cm}^2 \text{ mol}^{-1}$ Hexakis(trimethylphosphite)technetium(+1) hexafluorophosphateAnalysis for  $C_{18}H_{54}F_6O_{18}P_7Tc$ :

	C	H	P
calculated	21.87	5.52	21.93
found	22.06	5.35	21.78

Melting point:  $> 115^\circ \text{ C dec.}$ Optical spectrum ( $CH_3CN$ ): 212 nm ( $\epsilon = 2.2 \times 10^4$ )

Infrared spectrum (KBr):

2945(m), 2840(m), 1460(m), 1170(m), 1050(vs)  
 845(s), 770(s), 690(s), 535(s)

Conductivity ( $CH_3CN$ ,  $10^{-3} M$ ):  $\Lambda_M = 136 \text{ ohm}^{-1} \text{ cm}^2 \text{ mol}^{-1}$  $^1H$  nmr ( $CDCl_3$ ): 3.63 ppm (sharp multiplet)

$^{31}P\{^1H\}$ nmr( $CDCl_3$ ): dectet 266.8-41.1 ppm ( $J_{TcP}$  910 Hz;  $^{99}Tc$ ,  $I = 9/2$ )  
 septet -86.4 to -203.5 ( $J_{PF}$  708 Hz)

FDMS(+):  $m/z = 843(s) [Tc(P(OCH_3)_3)_6]^+$

SKELETAL UPTAKE PROPERTIES OF Tc-99m-LABELED MULTIDENTATE PHOSPHONATE LIGANDS

W. A. Volkert, J. Simon, D. A. Wilson, B. Edwards, E. H. McKenzie, P. Oberle and R. A. Holmes  
Dept. of Radiology, University of Missouri; Nuclear Medicine Service, Veterans Hospital, Columbia, Mo. 65211.

Phosphonate ligands complexed to Tc-99m are used for skeletal imaging studies in essentially all Nuclear Medicine laboratories. Bidentate phosphonates (e.g., MDP, HMDP, PyP or HEDP) are most frequently utilized but have multiple forms in aqueous solutions with heterogeneous skeletal uptake characteristics [1, 2].

The phosphonate compounds chosen for this study have multiple phosphate groups ( $n \geq 4$ ) per molecule and are excellent scale inhibitors. Two basic types of ligands were chosen for this study; Tetramethylenephosphonate derivatives of organic molecules (Figure 1) and multiphosphonated derivatives of ammonia based starburst polymers.\* The presence of multiple phosphate groups and their large size should favor the formation of Tc-99m-chelates with a single species in solution. Of the large ligands studied, tetramethylenephosphonated(bis) aminomethylnorbornane (TPNB) and tetramethylenephosphonated (bis) aminomethyldicyclopentadiene (TPDCPD) exhibited skeletal uptake characteristics in rats that were similar to Tc-99m-MDP (Table 1). While the Tc-99m-complexes with phosphonated starburst polymers had selective bone uptake, they did not localize in bone to the same extent as Tc-99m-MDP (Table 1). All ligands readily formed stable chelates in yields exceeding 90-95% in saline by Sn(II) reduction of Tc-99m-pertechnetate in the presence of excess ligand. Electrophoresis and paper chromatography indicate that each of the chelates are present as primarily one negatively charged species which are stable for  $\geq$  one hour in air saturated aqueous solutions.

Tc-99m-TPNB and TPDCPD exhibited total skeletal uptake in rabbits at 3 hours post injection that was quite high (Table 2). As in rats, the rapid blood clearance of both chelates compare favorably with Tc-99m-MDP. This factor accounts for their comparably high bone to blood (B/B1) and bone to muscle (B/M) ratios (Table 2). Tc-99m-TPNB, in fact, has B/B1 and B/M ratios not significantly different than Tc-99m-MDP. Scintiphotos of 5 kg rabbits injected with Tc-99m-TPNB showed skeletal images that were not visibly different than Tc-99m-MDP. As was the case in rats, there was no significant localization of activity in tissues or organs other than in the skeleton or bladder.

In conclusion, the skeletal imaging qualities of Tc-99m-TPNB and Tc-99m-DCPD, despite their large size, are similar to Tc-99m-MDP in both rats and rabbits. In addition to considerations of their diagnostic potential, their skeletal selectivity, rapid blood clearance, good stability and presumed chelate purity suggests they may form useful therapeutic agents if chelated with various particulate emitting radionuclides [3, 4].

\*Methylenephosphonate Derivatives of  $\text{NH}_3$ -based Starburst Polymers

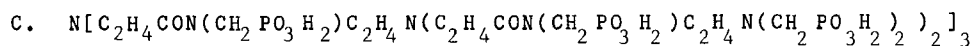
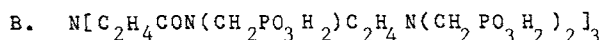
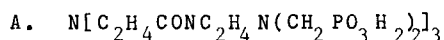


Table 1. Biodistribution of Tc-99m-Tetrakisphosphonate Chelates in Unanesthetized Rats at 2 Hours Post-Injection. Body weight = 160-205 gms. n=5

Organ (a)	Percent Dose/Organ		
	Tc-99m-TPNB	Tc-99m-TPDCPD	Tc-99m-MDP
Skeleton (b)	41.7±2.5	35.9±2.7	39.4±7.3
Blood	0.23±0.04	0.35±0.09	0.27±0.10
Urine	63.1±1.9	57.6±2.2	50.9±1.10
			27.0±4.0
			0.46±0.25
			60.6±0.8
			63.4±2.9
			24.2±4.1
			0.52±0.19
			56.9±16.9
			26.0±3.3
			0.49±0.13
			63.4±2.9
			54±15
			165±68
			50±21
			107±58

Ratios (c)

(a) Other organs (incl. liver, intestines, stomach, heart) had minimal Tc-99m activity with all three chelates (i.e.<0.5% injected dose per 1% body weight).

(b) Total skeletal uptake was estimated by multiplying the % dose in the femur by 25.

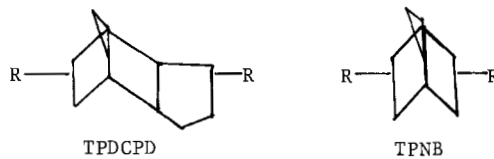
(c) The ratios were calculated from the values of the percentage dose per gram.

TPNB = Tetramethylenephosphonated Norbornane  
 TPDCPD = Tetramethylenephosphonated Dicyclopentadiene



1. Pinkerton, T. C., Ferguson, D. L., et al., *Int. J. Appl. Radiat. Isotopes*, **33**, 907 (1982).
2. Libson, K., Deutsch, E., et al., *J. Nucl. Med.*, **24**, P23, 1983.
3. Weinenger, J., Ketring, A. R., et al., *J. Nucl. Med.*, **24**, P23, 1983.
4. Som, P., Srivastava, S., et al., *J. Nucl. Med.*, **23**, P78, 1982.

Figure 1. Tetramethylenephosphonate Derivatives



R =  $\text{CH}_2\text{N}(\text{CH}_2\text{PO}_3\text{H}_2)_2$

TPDCPD = Tetramethylenephosphonated-diaminomethylcyclopentadiene

TPNB = Tetramethylenephosphonated diaminomethylnorbornane

Table 2. Biodistribution of Tc-99m-tetraphosphonate Chelates in Unanesthetized Rabbits at 3 Hours Post-Injection ( $n \geq 6$ ).

<u>Organ</u>	<u>Tc-99m-TPNB</u>	<u>Tc-99m-TPDCPD</u>	<u>Tc-99m-MDP</u>
<b>% Administered Dose per 1% body wt.<sup>(a)</sup></b>			
Femur	5.3±0.7	4.5±0.5	5.7±0.8
Liver	0.07±0.02	0.14±0.06	0.11±0.03
Muscle	0.03±0.02	0.04±0.02	0.05±0.03
Blood	0.10±0.03	0.20±0.11	0.13±0.06
<b>% Dose/Organ</b>			
Skeleton <sup>(b)</sup>	38.7±6.6	36.7±3.2	52.4±11
Blood <sup>(c)</sup>	0.57±0.18	0.96±0.13	0.82±0.38
<b>Ratios</b>			
Femur/Blood	53±11	30±17	49±25
Femur/Muscle	186±19	132±54	166±84

(a) Woodward, H. Q., et al., *J. Nucl. Med.*, 16:958, 1975.

(b) Percent Femur Uptake x 20 (Jelenko, C., et al., *Am. J. Vet. Res.*, 32:1637, 1971).

(c) % Dose in total blood assumes blood vol. is 6.5% x body wt.

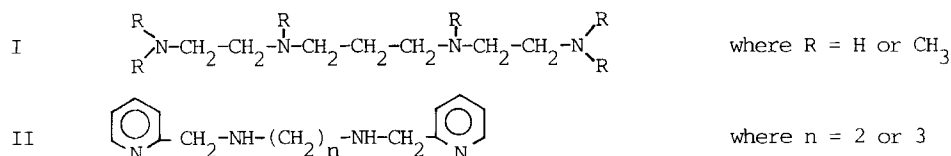
(d) Ratios obtained from % ID/gm data.

CATIONIC COMPLEXES OF Tc-99 AND Tc-99m WITH LIGANDS CONTAINING FOUR NITROGEN  
DONOR ATOMS: CHEMICAL AND BIOLOGICAL PROPERTIES

P.Bläuenstein, P.A.Schubiger, J.Müller, O.Gasser, G.Pfeiffer, G.Anderegg,  
K.Zollinger, Z.Proso

Swiss Federal Institute for Reactor Research, CH-5303 Würenlingen, Switzerland

Two types of ligands (=L) containing four nitrogen donor atoms were investigated with Tc-99 and Tc-99m:



The Tc-99 complexes were analysed with IR- and UV/VIS-spectroscopy and elemental analysis. Electrophoreses and paperchromatography was done on both isotopes.

The ligands of type I usually form pure cationic complexes with less than 10% impurities (e.g. TcO<sub>2</sub>). The IR absorption found at about 800 cm<sup>-1</sup> is typical for the O = Tc = O moiety of Tc(V) complexes (1). UV/VIS spectra are similar to that of the ethylenediamine complex (2). Elemental analysis of the complexes with hexafluorophosphate as counterion and the migration distance during electrophoreses are in agreement with the general formula TcO<sub>2</sub>L<sup>+</sup>.

Protein binding of the complexes investigated with human serum albumine and chromatography with Sephadex G25 was found to be much lower than with other radiopharmaceuticals (3). The biological investigation with Wistar rats chiefly shows a rapid clearance through the kidneys where 50% of the activity is excreted within 30 min after administration.

Type II ligands exhibit more intricate properties. Only 50 to 80% are found to form a similar cationic complex as described above, while the remainder of Tc forms a neutral complex. This uncharged complex does not migrate during electrophoreses but is found at rf = 1 using paper chromatography with acetonitrile/water. This complex is not yet clearly identified, but seems to be similar to the cationic complex, except for an additional OH<sup>-</sup> group bound to Tc, yielding TcO<sub>2</sub>OHL.

(1) S.A.Zuckman, G.M.Freeman, D.E.Troutner, W.A.Volkert, R.A.Holmes, D.G.VanDerveer, E.K.Barefield, *Inorg.Chem.*, 20,2386(1981).

(2) M.E.Kastner, M.J.Lindsay, M.J.Clarke, *Inorg.Chem.*, 21,2037(1982).

(3) C.Schümichen, *Third Int.Symp.Radiopharmacology*, p.66(1983).

NEW MYOCARDIAL IMAGING AGENT :  $^{99m}\text{Tc}$ -COMPLEX OF 3-(p-TRIMETHYL-AMINOETHYL)PHENYL-PROPANE-2,3-DIONE-BIS(N-METHYL-THIOSEMICARBAZONE)

---

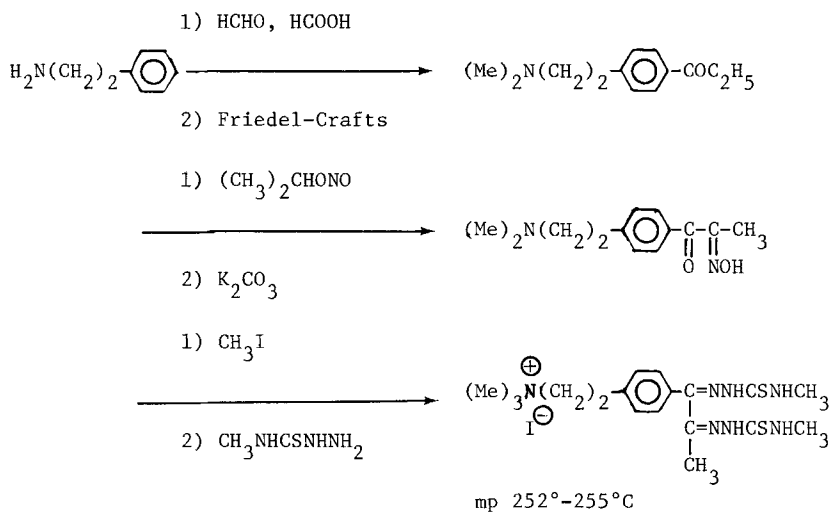
T.Hosotani, A.Yokoyama, Y.Arano, K.Horiuchi, K.Torizuka, Y.Ishii

Dept. Radiopharmaceutical Chemistry, Faculty of Pharmaceutical Sciences, Kyoto University, Sakyo-Ku, Kyoto 606, Japan.

Usefulness of di-thiosemicarbazone (DTS) derivatives as agent for the development of Bifunctional Radiopharmaceutical (BRP) offered good criteria for more specific technetium containing radiopharmaceutical drug design. Based on the myocardium affinity shown by radioiodinated phenylalkylamine derivatives (1,2,3), development of phenylalkylamine DTS derivatives has been achieved in our laboratory. In this approach, as previously reported, the presence of lipophilic benzene ring along with a basic group attached to the chelating molecule DTS provided good basis for the synthesis of primary and tertiary amine derivatives, p-PA-DTS, p-DPA-DTS (4).

In our further pursuit for BRP with higher myocardium localization, synthesis of a quaternary phenylalkylamine DTS derivative was considered of interest. Also, being aware of possible thioketo-thioenol tautomerism in these DTS derivatives, exploitation of this equilibrium for the labeling reaction with  $^{99m}\text{Tc}$  was studied. Synthesis of this new derivative as shown in Fig.1 was carried out through general dimethylation and acylation reaction. Thereafter, reacted with freshly prepared isopropyl nitrite and the crude product after purification, subjected to methylation. Then after the addition of N-methyl-thiosemicarbazide at 1:2 molar ratio and purification, a highly pure product, a 3-(p-trimethyl-aminoethyl)phenylpropane-2,3-dione-bis(N-methyl-thiosemicarbazone)(p-TPA-DTS) was obtained. Studies on the tautomeric equilibrium, derived on a very specific labeling method in ethanol, using the stannous chloride reaction. Very high labeling efficiency (80-90%) of a  $^{99m}\text{Tc}$ -p-TPA-DTS, with great stability upon aqueous dilution was registered by TLC (10%  $\text{NH}_4\text{AcO}:\text{MeOH}=1:1$ , Rf:0.22.  $\text{TcO}_4^-$ , if any Rf:0.8-0.9). Using the present method, efficient labeling of  $^{99m}\text{Tc}$ -p-PA-DTS,  $^{99m}\text{Tc}$ -p-DPA-DTS was also obtained (Rf:0.38 and 0.30). Mice (ddy) biodistribution study showed high heart radioactivity uptake with every derivative tested, but the highest heart/blood ratio of 4.74 (3hr) was achieved with p-TPA-DTS (Table 2). Diverse organ biodistribution and utilization of these new DTS derivatives by the myocardium is discussed based on the structural differences of ligands, as well as, the differences in the Tc coordination environment elicited through the presence of tautomeric equilibrium.

Fig 1 SYNTHESIS OF p-TPA-DTS



Micro analysis (%) ; Found: C=40.32, H=5.62, N=18.23

Calc.: C=40.37, H=5.67, N=18.31

Table 1 BIODISTRIBUTION OF RADIOACTIVITY IN MICE AFTER INTRAVENOUS  
INJECTION OF  $^{99\text{m}}\text{Tc-p-TPA-DTS}$

	% Injected dose per gram tissue*			
	5 min	30 min	60 min	180 min
Blood	3.79 (0.38)	1.53 (0.14)	0.76 (0.08)	0.38 (0.08)
Heart	3.99 (0.55)	2.60 (0.68)	2.22 (0.22)	1.80 (0.20)
Lung	4.03 (2.01)	1.73 (0.34)	1.14 (0.25)	0.58 (0.19)
Liver	26.42 (4.21)	27.72 (4.72)	21.56 (1.51)	16.18 (2.17)
Kidney	20.82 (2.55)	21.12 (2.39)	13.79 (2.39)	8.39 (0.39)
Stomach	0.57 (0.21)	0.68 (0.14)	0.70 (0.15)	0.95 (0.09)

\* Mean  $\pm$  1 s.d. for 5 animals each point.

Injection vehicle = 50/50 (98% ethanol) / (normal saline).

Injection volume = 0.05 ml.

Table 2 TARGET/NON TARGET ORGAN RATIO\* AS A FUNCTION OF TIME

		5 min	30 min	60 min	180 min
H/B1 ratio	p-PA-DTS <sup>†</sup>	1.87	2.44	2.12	—
	p-DPA-DTS <sup>‡</sup>	2.93	2.48	2.55	—
	p-TPA-DTS	1.05	1.70	2.92	4.74
H/Lu ratio	p-PA-DTS	0.50	0.38	0.17	—
	p-DPA-DTS	0.38	0.22	0.26	—
	p-TPA-DTS	0.99	1.50	1.95	3.10
H/Li ratio	p-PA-DTS	0.19	0.15	0.11	—
	p-DPA-DTS	0.51	0.18	0.12	—
	p-TPA-DTS	0.15	0.09	0.10	0.11

\* Calculated from mean % dose/g of heart/mean % dose/g of Blood, Lung, or Liver.

<sup>†</sup>p-PA-DTS : p-phenethylamino-propane-2,3-dione-bis(N-methyl-thiosemicarbazone)

<sup>‡</sup>p-DPA-DTS : 3-(p-N,N-dimethylaminoethyl)phenylpropane-2,3-dione  
bis-(N-methyl-thiosemicarbazone)

- (1) Wieland D.M., et al.: J. Nucl. Med., 22, 22–31, 1981.
- (2) Counsell R.E., et al.: J. Nucl. Med., 15, 991–996, 1974.
- (3) Burns H.D., et al.: J. Nucl. Med., 21, 875–879, 1980.
- (4) Yokoyama A., et al.: Technetium in Chemistry and Nuclear Medicine.  
Cortina International, Verona, 125–127, 1983.

DEPENDENCE OF THE QUALITY OF BONE IMAGE ON THE CHEMICAL NATURE OF  
TECHNETIUM-99M SPECIES PRESENT IN THE RADIOPHARMACEUTICAL

S.K. Shukla, G.B. Manni and C. Ciprinai

Istituto di Cromatografia, C.N.R. Casella Postale 10,  
I-00016 Monterotondo Stazione (Roma), Italy

A variety of benign and malignant disorders can be easily managed if detected at an early stage. Bone imaging has now become the third most frequently performed procedure (1) in nuclear medicine for non-invasive study of many abnormal conditions, e.g., 1) primary or secondary bone lesions, 2) origin of bonepain not detected by radiological methods, 3) evolution of bone alterations (e.g., Paget's disease, bone tuberculosis, osteomyelitis, osteoporosis, etc.), 4) evolution and consolidation of recent fractures, 5) articular inflammations, 6) site of lesions in the case of positive brain scans, and 7) selection of bone biopsy area, etc. The major advantages of the radionuclidic bone imaging include: high sensitivity to early bone disease prior to radiographic or enzymatic changes can be appreciable; low false-negatives and false-positives; and suitability as a screening procedure.

Since the introduction in 1975 (2) of technetium-99m methylenediphosphonate (Tc-99-MDP), the use of previously employed radionuclides Sr-85, Sr-87m, and F-18 for bone imaging has been abandoned because of its widespread availability at low cost, ease of preparation, low radiation risk and high quality of bone image. More recently other technetium-99m diphosphonates have been synthesized (3) and their suitability as bone imaging agent examined. Of these only technetium-99m hydroxymethylenediphosphonate (Tc-99m-HMDP) and technetium-99m 1,2-dicarboxypropane-3,3-diphosphonate (Tc-99m-DPDP) have found clinical application. Many comparative studies of the quality of bone image obtained with different technetium-99m diphosphonates have been reported (3,4) with commercially available kits. We have examined chromatographically and electrophoretically the chemical nature of technetium-99m species present in Tc-99m-HMDP, Tc-99m-MDP, and Tc-99m-DPDP prepared following the instructions of the kit suppliers and have reached the following conclusions:

- 1) The stability of technetium-99m diphosphonates at room temperature varies in the order:  
Tc-99m-DPDP >> Tc-99m-MDP > Tc-99m-HMDP.

Tc-99m-HMDP has to be used within 1 hour after its synthesis, Tc-99m-MDP up to 2 hours and Tc-99m-DPDP up to 4 hours for getting high bone-to-soft tissue and lesion-to-bone radioactivity ratio. The imaging has to be performed accordingly after about 1 hour, 2 hours and 4 hours with the three diphosphonates because of their stability, which is responsible for slower bone uptake of the radionuclide.

- 2) The technetium-99m species present in the three diphosphonates are similar in their chromatographic and electrophoretic behaviour. They are: hydrolyzed technetium-99m species containing tin, the pertechnetate-99m ion and the technetium-99m diphosphonate. The former two technetium-99m species are responsible for soft tissue uptake of the radionuclide and give poor quality images. High quality skeletal image is obtained only with chromatographically pure technetium-99m diphosphonate.
- 3) For the synthesis of the technetium-99m diphosphonates the kit suppliers recommend the volume of technetium-99m eluate from 2 to 10 ml to be added to each vial. Our quality control of the diphosphonate obtained by adding different volumes of the eluate showed that optimal volume is less than 3.5 ml. With

this precaution the technetium-99m diphosphonate preparation is generally pure and the quality of the bone image is high.

We have also synthesized tin-free Tc-MDP and studied its chemical and biological properties. A comparative study of the two Tc-99m-MDP's, obtained with Sn(II) as a reducing agent for the pertechnetate-99m ion and with chromatographically pure technetium-99m(IV), will be presented.

From the available evidence on the nature of technetium-99m in bone imaging agents and on the quality of the bone image obtained from them a mechanism of the radionuclide uptake in the bone has been suggested.

- (1) McIntyre A.B., Paras, P. and Grant R.C., *J. Nucl. Med.* 21, P42 (1980).
- (2) Subramanian G., McAfee J.G., Blair R.J., Kalifelz F.A. and Thomas F.D., *J. Nucl. Med.* 16, 744 (1975).
- (3) Fogelman I., *Eur. J. Nucl. Med.* 7, 506 (1982).
- (4) Subramanian G., McAfee J.G., Thomas F.D., Feld T.A. Zapf-Longo C. and Palladino E., *Radiology* 149, 823 (1983).

EVALUATION OF HIPDM FOR LUNG IMAGING USING IN VIVO AND IN VITRO SINGLE PASS MULTIPLE INDICATOR DILUTION TECHNIQUES

D.N. Abrams, I. Ahmed, S.F.P. Man and A.A. Noujaim Faculty of Pharmacy, U of A, Edmonton, Alberta, Canada.

The metabolic function of the pulmonary endothelium may be compromised during lung injury and the extraction efficiency and retention of the appropriate radiotracer could reflect the extent of the injury. Recently, HIPDM, a brain perfusion agent which demonstrated high lung uptake in experimental animals, was proposed as a possible agent for indexing lung metabolic function (1,2).

An *in vivo* animal model (3) has been adapted in an effort to correlate the blood extraction data derived from a single pass multiple indicator dilution (SPMID) experiment with the  $\gamma$ -camera lung kinetics data obtained during imaging. In brief, the external jugular vein of 8 dogs was cannulated to allow a direct injection of the test substrate (HIPDM) into the right heart and a second canula was placed in the carotid artery from which the effluent blood was sampled every 0.6 sec as it left the lung. In this technique, two indicators are necessary, one of which traces the intravascular route (Tc-99m-Sulfur Colloid). This tracer does not permeate the lung and is used as the reference radiotracer to which the test substrate may be compared. The fractional extraction of HIPDM was calculated (4) from the difference between the instantaneous blood concentrations of the reference and test radiotracers at time  $t$ , as defined by the following equation:

$$E(t) = (1 - C_p(t)) / C_r(t) \quad (1)$$

where  $C_p$  and  $C_r$  are the fractional concentrations of the test and reference compounds respectively. In addition, the cumulative extraction ( $E$ ) can be calculated from the area under the curves of the fractional concentration versus time curves (Figure 1) using equation 2:

$$\int_0^t E(dt) = \int_0^t (C_r(dt) - C_p(dt)) / C_r(dt) \quad (2)$$

During the sampling period following injection,  $\gamma$ -images were also recorded every 0.25 sec using either a PHO-Gamma IV/ADAC or a GE-400 T imaging system, whereby information on both reference and test substrates was recorded (Figure 2). The imaging data was analyzed using the method of Syrota et al(5) whereby the curves are normalized so that the peak value is set at 1.

The effect of oleic acid and radiation induced lung injury has been evaluated using this technique. We feel that this technique will prove valuable for evaluating future radiopharmaceuticals designed for assessing lung metabolic integrity.

(1) Pistolesi M., Fazio F. Marini G, et al, J. Nucl. Med. Allied Sci. 27, 180 (1983).

(2) Kung H.F., Trampusch K.M. and Blau M., J. Nucl. Med. 24, 66 (1983).



(3) Abrams D.N., Man S,F.P., Noujaim A.A. and Wasburn L.C., presented at the "Third International Symposium on Radiopharmacology" in Freiburg, West Germany, Sept 21-25, 1983.

(4) Rickaby D.A., Linehan J.H., Bronikowski T.A. and Dawson C.A., J. Appl. Physiol.: Respirat. Environ. Exercise Physiol. 51, 405 (1981).

(5) Syrota A., Pascal D., Crouzel M. and Kellersholm C., J. Nucl. Med. 22, 145 (1981).

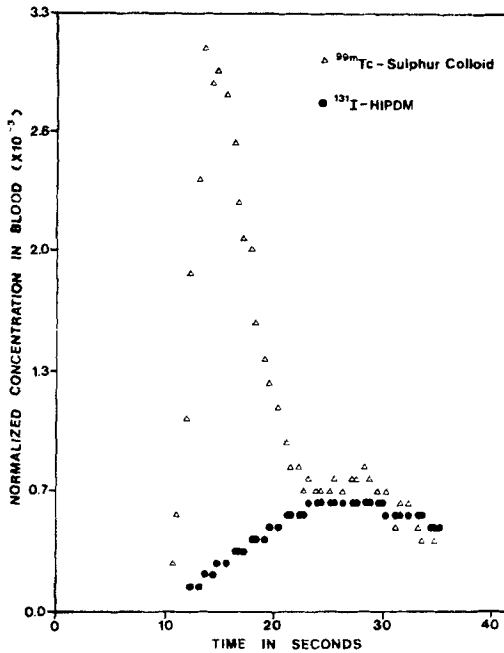


FIG. 1 BLOOD CONCENTRATION CURVE FROM A SPMD EXPERIMENT

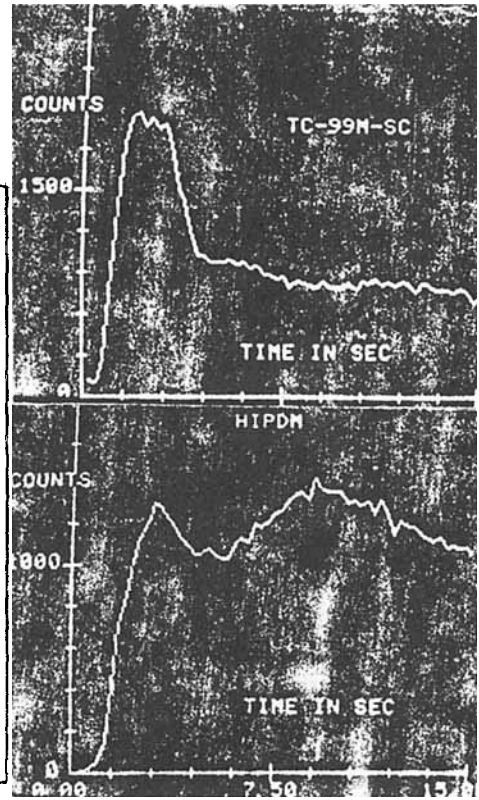


Fig. 2 GAMMA CAMERA TIME - ACTIVITY CURVES

RAPID NO CARRIER ADDED RADIOLABELLING USING ORGANOMERCURY COMPOUNDS

F.P.Charleson, R.J.Flanagan, E.I.Synnes and L.I.Wiebe  
Merck Frosst Canada., P.O.Box 1005, Pointe Claire - Dorval, Quebec, Canada. H9R 4P8.

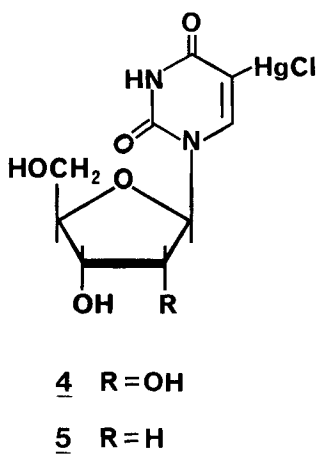
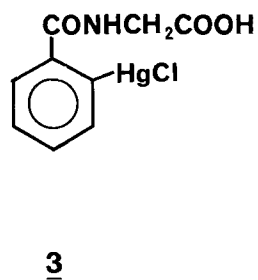
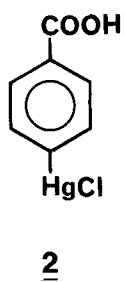
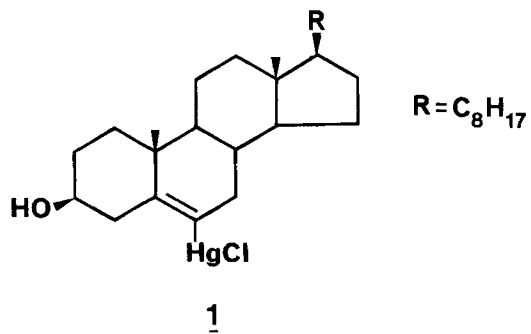
The recent interest in the use of short lived radioisotopes for labelling organic molecules has resulted in a number of methods based on the reaction of zero-valent halogens with carbon skeletons containing heteroatoms. Some of the heteroatoms used to date are Boron (1), Thallium (2) and Tin (3). The difficult step in these procedures is the introduction of the heteroatom into the carbon framework. We have chosen to investigate the use of mercury as an alternative to these methods because of the more comprehensive chemistry available for the synthesis of organomercury compounds.

Organomercury compounds are readily prepared from a variety of precursors, including aliphatic halides (4), olefinic halides (5), aromatic amines (6), olefins (7) and heterocycles (8). Using these methods we have prepared 6-chloromercuricholest-5-en-3- $\beta$ ol (1), 4-chloro mercuribenzoic acid (2), 2-chloromercurihippuric acid (3), 5-chloromercuriuridine (4) and 5-chloromercuri-2'-deoxy-uridine (5). All of these compounds undergo rapid quantitative reaction with iodine ( $I_2$ ) in a variety of organic solvents ranging in polarity from hexane to methanol. The reaction takes place instantly at room temperature. The same reaction can be carried out using polarized halogens such as iodine monochloride, in which case the electropositive halogen becomes attached to the carbon and the electronegative halogen leaves with the mercury. A similar but slightly slower reaction takes place for bromine. In the case of vinylic organomercury compounds care must be taken to avoid an excess of bromine or addition to the double bond occurs. Again, bromine attached to electronegative atoms reacts smoothly in good yield. With chlorine the only viable reaction is the use of chlorine gas as N-chloro species do not react with the carbon mercury bond. This is of great importance in the use of N-chloro compounds such as Chloramine-T for oxidizing iodide to iodine monochloride. In the case of vinylic organomercury compounds there is serious competition between cleavage of the carbon mercury bond and addition of chlorine to the double bond and as a result trichloro compounds are often formed. O-chloro compounds do react with the carbon mercury bond but the scope of this reaction is more limited. To date we have not observed any reaction of electropositive fluorine species with the carbon mercury bond.

We have used the reaction of organomercury compounds with iodine to prepare compounds labelled with [ $^{125}I$ ], [ $^{127}I$ ] and [ $^{131}I$ ]. In all cases the starting materials were the appropriate organomercury compound and sodium iodide. Various oxidizing agents such as Chloramine-T, N-chlorosuccinimide and Iodogen were used to convert the iodide to iodine monochloride. Typical labelling yield were greater than 90%. Separation of the reaction mixture by HPLC gave the corresponding no-carrier-added product. A similar procedure has been carried out for [ $^{77}Br$ ] and [ $^{82}Br$ ] sodium bromide.

In summary, organomercury compounds, because of their ease of synthesis and rapid reaction with iodine and bromine, offer distinct advantages over organoboron and organotin compounds. They are very stable to hydrolysis, do not react with atmospheric oxygen and are readily prepared from a large variety of precursors.

1. G.W.Kabalka and E.E.Gooch, *J.Org.Chem.* **45**, 3578, (1980)
2. D.L.Gilliand, G.P.Basmadjian, A.P.Marchand, G.H.Hinkle, A.Earlywine and R.D.Ice, *J.Radioanal.Chem.* **15**, 7 (1978)
3. M.J.Adam, B.D.Pate, T.J.Ruth, J.M.Berry and L.D.Hall, *J.Chem.Soc.Chem.Comm.* 733, (1981)
4. W.Kitching, B.F.Hegarty and D.Doddrel, *J.Organometal.Chem.*, **21**, 29, (1970)
5. A.N.Nesmeyanov, A.E.Borisov and N.V.Novikova, *Dokl.Akad.SSSR*, **94**, 289, (1954)
6. A.N.Nesmeyanov, L.G.Makarova and I.V.Polovyanyuk, *Z.obsc.Chim.*, **35**, 681, (1965)
7. R.H.Levin and M.A.Spielman, *J.Am.Chem.Soc.*, **62**, 920, (1940)
8. R.G.Smith, H.E.Ensley and H.E.Smith, *J.Org.Chem.*, **37**, 4430, (1972)
9. D.E.Bergstrom and J.L.Ruth, *J.Carb.Nucleos.Nucleot.* **4**, 257, (1977)



## SYSTEMATIC STUDY OF NO-CARRIER-ADDED RADIOBROMINATION AND RADIOIODINATION VIA DEMETALLATION OF GROUP IV METALLATED ARENES

S.M. Moerlein and H.H. Coenen

Institut für Chemie 1 (Nuklearchemie), KFA Jülich GmbH,  
D-5170 Jülich, FRG

Halodemetalation reactions involving trialkyl group IV metal arenes have been successfully applied by several workers to introduce no-carrier-added (n.c.a.) radiobromine and radioiodine into aromatic rings regiospecifically with high yields (1-4). We have synthesized a series of trimethylarylsilicon, -germanium, and -tin compounds substituted at the para position to compare under identical reaction conditions their relative reactivity toward electrophilic bromine and iodine and suitability as precursors for labelling radiopharmaceuticals.

Para-substituted trimethylarylmethyl compounds [ $p\text{-X-C}_6\text{H}_4\text{-M(CH}_3)_3$ ; X = NO<sub>2</sub>, CF<sub>3</sub>, Br, F, H, CH<sub>3</sub>, OCH<sub>3</sub> and M = Si, Ge, Sn] were synthesized in 45-95% yield, purified by fractionation, and chemically characterized. Radiohalogenation reactions were carried out at 25 °C in sealed reaction vessels containing n.c.a. <sup>77</sup>Br<sup>-</sup> or <sup>131</sup>I<sup>-</sup>, dichloramine-T (DCT) oxidizing agent, organometallic compound, and solvent. Use of DCT (5) as the oxidizing agent allowed for halogenation reactions to be carried out in a homogeneous solution with a variety of solvents, including methanol, chloroform, acetonitrile, and carbon tetrachloride. Products were analyzed using radio-HPLC and radio-GC.

Radiochemical yields for n.c.a. halodemetalation was quantitative and very rapid for M = Sn in all solvents tested. For M = Ge, the solvent affected the kinetics as well as the radiochemical yields attained, but in polar solvents high yields were obtained within 10 min (Fig. 1). For M = Si, radiochemical yields were low with these reaction conditions (Fig. 2).

For M = Sn and Ge, high radiochemical yields were obtained with DCT concentrations as low as 10<sup>-3</sup> M. A slight decrease in yield was found for electron-withdrawing substituents X. Electron-donating substituents did not significantly increase yields for M = Si.

From the rapid kinetics, lack of solvent effect, and relatively small influence of para substituents, it was concluded that halodestannylation is the most convenient labelling technique. However, the greater chemical stability and lower toxicity of organogermanium and organosilicon compounds are advantages which make the synthesis of these precursors useful in some labelling situations.

- (1) Hanson R.N., Tonnesen G.L., McLaughlin W.H., Bloomer W.E., and Seitz D.E., *J. Lab. Comp. Radiopharm* **18**, 128 (1981).
- (2) Adam M.J., Ruth T.J., Pate B.D., and Hall L.D., *J. Chem. Soc., Chem. Commun.* 625 (1982).
- (3) Wilbur D.S., Anderson K.W., Stone W.E., and O'Brien H.A., *J. Lab. Comp. Radiopharm.* **19**, 1171 (1982).
- (4) Moerlein S.M., in: *Proceedings of the Third Symposium on the Medical Application of Cyclotrons*, Turku, Finland, June 13-16, 1983, in press.
- (5) Coenen H.H., Petzold G., and Stöcklin G., *J. Lab. Comp. Radiopharm.* **19**, 1580 (1982).

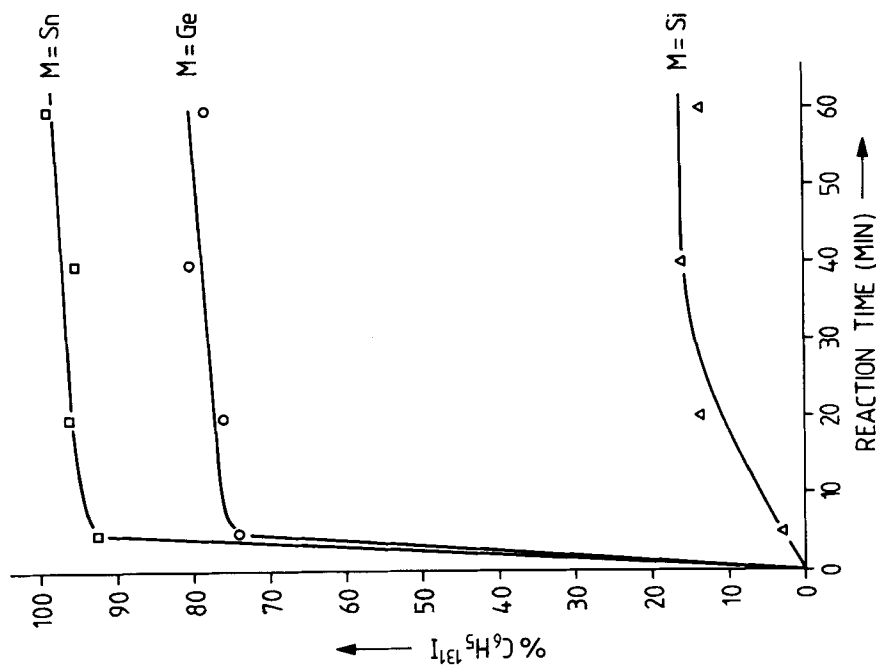


Fig. 2. N.C.A. iodometallation of trimethylphenylmetal (IV) compounds in methanol at R.T.

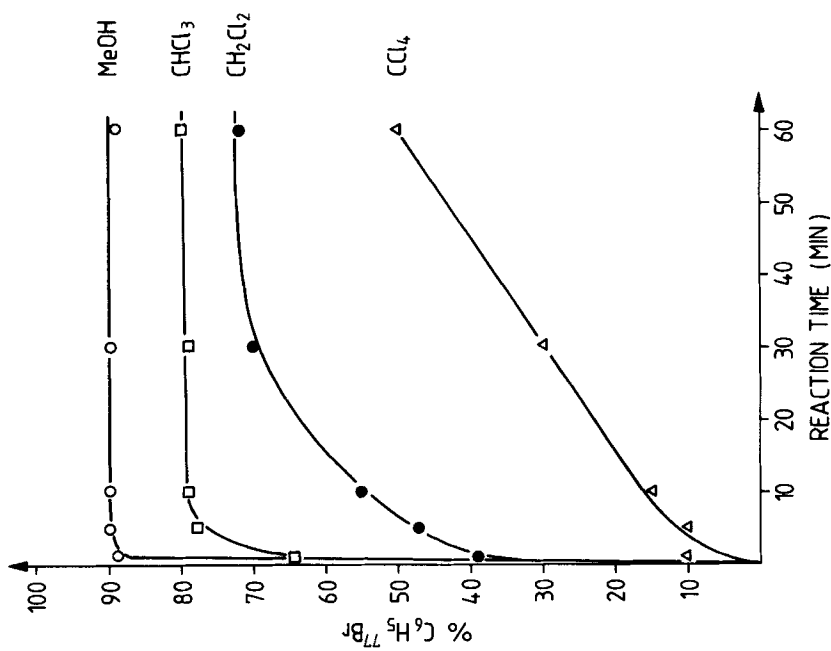


Fig. 1. N.C.A. bromodegermylation of trimethylphenylgermanium in various solvents at R.T.

POSITRON AND GAMMA LABELED PHENTERMINE ANALOGS AS POTENTIAL  
BRAIN PERFUSION AGENTS

D.R. Elmaleh, H. Kizuka, G. Boudreaux and \*R.N. Hanson  
Physics Research Laboratory, Massachusetts General Hospital  
and \*Department of Medicinal Chemistry, Northeastern  
University, Boston, MA 02114

The preparation and evaluation of radioiodinated N-isopropyl-4 ( $^{123}\text{I}$ )iodoamphetamine (IMP) (1-3), and N,N,N'-trimethyl-N' (2-hydroxy-3-methyl-5- $^{123}\text{I}$ )-iodobenzyl 1,3-propanediamine (HIPDM) (4-5) as brain perfusion imaging agents for single photon tomography was reported in the last several years.

Since some of the tritium substituted phentermine analog studies suggested that the p-halo phentermines had a greater concentration in the brain and prolonged retention time, we prepared and evaluated the biological behavior of N- $^{11}\text{C}$  methyl analogs of p-chloro (I) and p-fluoro (II) phentermine and  $^{123},^{131}\text{I}$  p-iodophentermine (III).

The N-methylphentermines (I) and (II) were prepared by methylation of their primary amines using  $^{11}\text{CH}_3\text{I}$  (Scheme 1). Biodistribution studies in rats showed brain uptake in the range of 1% dose/gr at 5 and 15 min for both agents. The activity in blood and eyes was low.

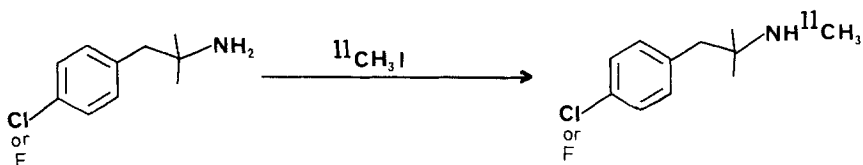
p-Iodophentermine (III) was prepared by diazotization of p-aminophentermine followed by decomposition of the diazonium salt with KI. The radioiodinated analog was prepared either by the solid-phase isotopic exchange reaction of Mangner et al or by decomposition of the piperidinotriazine derivative with a radiochemical yield of 40-60% (Scheme 2). Brain uptake of (III) was 1.7% dose/per gram at 5 and 30 min.

The imaging results in dogs showed high brain extraction and slow activity washout. The synthesis, biodistribution and imaging will be discussed.

This work is supported by 5PONS10828-9

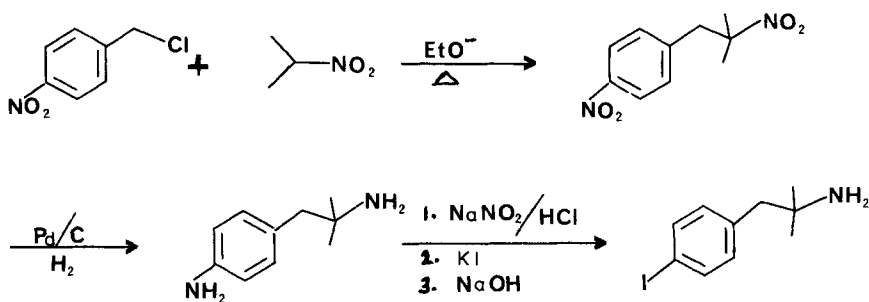
- (1) LaFrance N.D., et al, J. Nucl. Med., 22:1081 (1981).
- (2) Kuhl D.E., et al., J. Nucl. Med., 23:196 (1982).
- (3) Hill T.C., et al., J. Nucl. Med., 23:191 (1982).
- (4) Kung H.F., et al., J. Nucl. Med., 24:66 (1983).
- (5) Trampusch K.M., et al., J. Med. Chem., 26:121 (1983)

## SCHEME 1

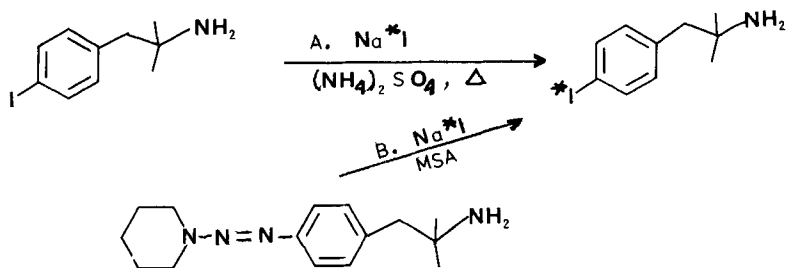


Synthesis of 4-halo-N-methyl-[C-11]-phentermines.

## SCHEME 2



Synthesis of 4-iodophentermine



Radioiodination of phentermine

6-HALO-9-BENZYL PURINES AS CARRIERS OF VARIOUS RADIOHALOGEN IONS INTO BRAIN

K. Fukushi, T. Irie, O. Inoue, T. Yamasaki and T. Nozaki  
Division of Clinical Research, National Institute of Radiological Sciences, Chiba, Japan.

As previously reported (1) the title compound (6-XBP) labeled with F-18 is localized in the brain of mice. Subsequently (2) it was found that the purine derivative is able to be metabolized in the brain. As a result of metabolism, F-18 fluorides were liberated in brain and trapped. Calf intestine adenosine deaminase was shown to defluorinate it in vitro. Since this enzyme is known present in brain, it is most probable that this enzyme participates in the metabolism of 6-FBP in mice.

In view of these data, one can expect that 6-halopurine with a lipophilic group at 9 position would work as a carrier of various radiohalogen ions into brain. The present study shows examples for this, using the title compounds labeled with F-18, Br-77 and I-125.

F-18 6-FBP was prepared as previously reported (1). 6-Bromopurine was obtained by a known method (3) from mercaptopurine and Br<sub>2</sub>, and 6-iodopurine from chloropurine and HI (4). Both were benzylated in DMSO at 30-50° and 9-benzyl isomers were obtained free of 7 isomers. The labeling was done by isotope exchange using DMF as solvent for several hrs at 140°. Products were purified and purities were determined by TLC on silicagel using benzene-ethyl acetate mixture (3:2, vols). The radiochemical yields, though not optimized, were reasonably high, 40% for Br-77 and 80% for I-125.

The labeled compounds were emulsified, made isotonic and i.v. injected to mice. Carriers in the injection solution were 0.01, 0.8 and 0.1  $\mu$  moles for F-18, Br-77 and I-125 labeled compound, respectively. Uptakes in brain and several organs were determined at 1, 5, 15, 30 and 60 min. Initial uptakes in brain were almost the same among three compounds, in the range of 6-8% dose/g brain at 1 min. At 1 and 5 min after injection, radioactivities as halogen ions were determined for brain and blood. As shown in Table, for both tissues at 5 min, all the activity was present as halogen ions.

From above data of uptakes in brain and blood and of radiochemical analyses, we can calculate the amount of radioactivity of halide-form present in brain. As shown in Figure, it decreases following a single exponential curve. Half times of clearances are 6.2, 40 and 76 min for iodide, bromide and fluoride, respectively. Qualitatively these values of halide efflux rates out of mice brains can be explained by iodide pumps, known present in brain for active transport of iodide and some other monovalent anions from brain to blood.

Thus, 6-halopurines such as 6-XBP act as carriers of various halides into brain in a rapid, non-invasive way. These compounds with a proper label would be useful for nuclear medical brain studies by measuring halide efflux from brain to blood.

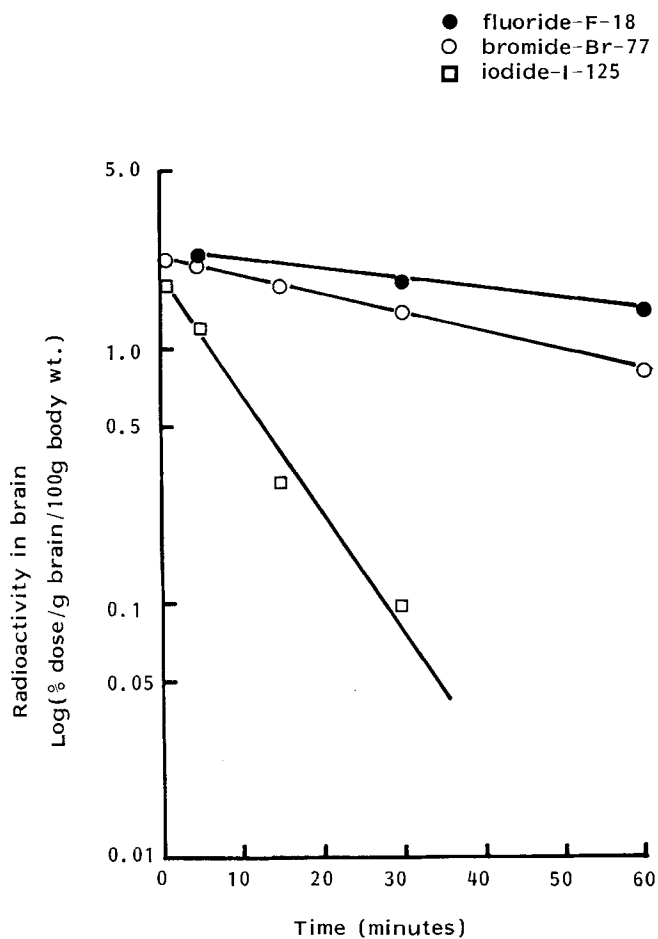
- (1) Irie T., Fukushi K., Inoue O., Yamasaki T., Ido T. and Nozaki T., *J. Appl. Radiat. Isotop.*, **33**, 633 (1982)
- (2) Fukushi K., Irie T., Inoue O. and Yamasaki T., *J. Nucl. Med.*, **23**, P 23 (1982)
- (3) Beaman A. G., Geroter J. F., and Robins R. K., *J. Org. Chem.*, **27**, 986 (1962)
- (4) Elion G. B. and Hitchings G. H., *J. Amer. Chem. Soc.*, **78**, 3508 (1956)



Table. The Rate of Dehalogenation of F-18, Br-77 and I-125 Labeled 6-Halo-9-Benzylpurines in Brain and Blood Following I.V. Administration to C3H Mice

Tissues	percent halide activity in tissues					
	F-18		Br-77		I-125	
	1 min	5 min	1 min	5 min	1 min	5 min
Brain	79	94	85	100	77	96
Blood	73	99	83	99	74	97

Figure. Comparison of Clearances of Various Halides from Brain Following I.V. Administration of F-18, Br-77 and I-125 Labeled 6-Halo-9-Benzylpurines to C3H Mice



## RADIOIODINATED 1-SUBSTITUTED-4-PHENYL PIPERAZINES AS POTENTIAL BRAIN IMAGING AGENTS

R.N. Hanson, T. El-Shourbagy, and M. Hassan.

Department of Medicinal Chemistry, College of Pharmacy, Northeastern University, Boston, MA 02115.

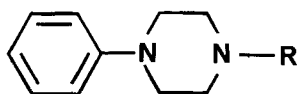
In recent years new radioiodinated compounds have been developed for imaging the brain. The two most extensively evaluated are N-isopropyl-p-iodoamphetamine IMP (1,2) and HIPDM (3,4). Although both agents show significant uptake and prolonged retention in the brain, with good brain to blood ratios ( $\approx 20:1$ ), they have several drawbacks including low specific activity, some problems with labeling, and high lung uptake. To overcome these problems we chose to evaluate the 1-substituted-4-phenylpiperazines as potential brain imaging agents. As a class of compounds they can be easily synthesized; they have been evaluated as CNS-active drugs and they can be readily radioiodinated.

We have synthesized and characterized two series of 1-substituted-4-phenylpiperazines (Figure 1). Electrophilic radioiodination followed by purification with HPLC gave the products, free of starting material or side products, in 50-90% radiochemical yields at the no-carrier-added level. The radiochemicals were then evaluated for their tissue distribution in rats at 0.25, 1 and 4 hours after administration.

The levels of radioactivity in the brain and brain to blood ratios were determined at 0.25, 1 and 4 hrs for the radioiodinated compounds (Table 1). In the first series, the best uptake and retention are found with the 1-n-butyl derivative 1c, although high brain to blood ratios are found with compounds 1c-1e. For the 1-aminoamides in the second series, high uptake, retention and selectivity are observed only with the dialkylaminoacetyl derivatives 2a-2c. The compound 2d did not show retention but instead redistributed rapidly. The radioiodine in all of the compounds was relatively stable to metabolism with thyroid uptake constituting less than 0.25% ID at 4 hours. Because of their distributional characteristics, compounds 1c and 2c were chosen for evaluation in dogs. The high uptake, retention and brain to blood ratios were comparable to IMP and HIPDM while their uptake in the lung at no-carrier-added levels was much lower, i.e., less than 5% ID. Their ability to be readily labeled and purified also contributes to their further consideration as potential brain imaging agents.

- (1) Winchell H.S., Baldwin R.M., Lin T.H., *J. Nucl. Med.*, 21, 940 (1980).
- (2) Winchell H.S., Horst W.D., Braun L., et al., *J. Nucl. Med.*, 21, 947 (1980).
- (3) Kung H.F., Tramposch K.M., Blau M., *J. Nucl. Med.*, 24, 66 (1983).
- (4) Tramposch K.M., Kung H.F., Blau M., *J. Med. Chem.*, 26, 121 (1983).

Figure 1




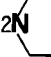
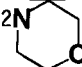
	<u>R</u>		<u>R</u>
1a	CH <sub>3</sub>	2a	COCH <sub>2</sub> NEt <sub>2</sub>
1b	C <sub>2</sub> H <sub>5</sub>	2b	COCH <sub>2</sub> N 
1c	n-C <sub>4</sub> H <sub>9</sub>	2c	COCH <sub>2</sub> N 
1d	i-C <sub>4</sub> H <sub>9</sub>	2d	COCH <sub>2</sub> N 
1e	c-C <sub>6</sub> H <sub>11</sub>		

Table 1

Compound	Time					
	0.25		1		4	
	% ID Brain	Brain/ Blood	% ID Brain	Brain/ Blood	% ID Brain	Brain/ Blood
1a	1.3	3.4	0.24	1.8	0.14	1.1
1b	1.5	5.7	1.0	2.4	0.25	0.6
1c	2.1	31	2.0	34	2.1	34
1d	2.1	38	2.1	40	1.4	15
1e	1.8	22	1.6	27	0.8	35
2a	1.2	25	1.3	29	1.1	39
2b	1.7	21	1.6	31	1.3	31
2c	1.2	33	1.1	26	0.9	39
2d	1.0	3.8	0.5	1.0	0.15	0.4

## SYNTHESIS OF IODOALIPHATIC AMINES FOR LUNG IMAGING

S. Selvaraj, D.N. Abrams, A.A. Noujaim and S.F.P. Man

Faculty of Pharmacy, U of A, Edmonton, Alberta, Canada.

Metabolism of endogenous and exogenous circulating amines by the monoamine oxidase enzyme (MAO) system of the pulmonary endothelial cells has been documented (1). Changes in the lung morphology and physiology which occur during injury may affect the uptake and subsequent metabolism of radiolabelled amines. Straight chain aliphatic amines are efficiently extracted and metabolized by the lung (2) and C-11 labelled n-alkylamines have been proposed as radiotracers for the study of lung MAO function.

We have synthesized a number of  $\omega$ -iodo-labelled straight and branched chain aliphatic amines as potential radiotracers for evaluating pulmonary metabolic status in disease states. The synthesis of  $\beta$ -substituted amines was also considered because substitution at this position has been found to alter the lung uptake and residence time of C-11-labelled substrates (3).

6-Amino-1-hexanol 1 was readily converted (Scheme 1) to 6-iodo-1-hexylamine 2 in aqueous hydroiodic acid at reflux temperature under a nitrogen atmosphere for 45-60 min. The presence of  $I_2$  in the reaction mixture complicated the reaction, presumably due to oxidation of the amino functionality. This resulted in a complex mixture from which it was difficult to separate preparatively, the desired product 2 by either extraction or chromatographic methods. Reaction of 1 with trimethylsilylchloride and sodium iodide in acetonitrile also resulted in liberation of iodine and a mixture of reaction products similar to that obtained with HI (as determined by tlc analysis). Removal of the free iodine from the reaction medium during the reaction allowed the synthesis to proceed smoothly to completion.

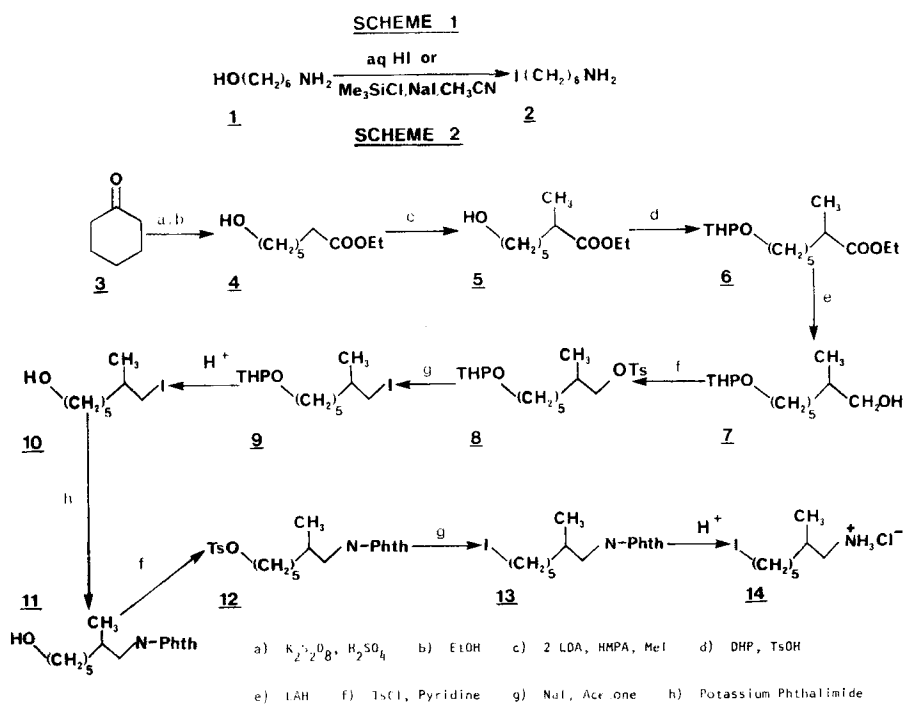
2-Methyl-6-iodo-1-hexylamine 14, the first in a series of  $\beta$ -alkyl substituted- $\omega$ -iodohexylamines was prepared as outlined in Scheme 2. The ester 4 prepared by Bayer-Villager oxidation (40 %) of cyclohexanone 3, was treated with LDA and methyl iodide to afford 5 (67 %) which contains the  $\beta$ -methyl functionality required of the final product. The THP ether 6 (82 %) prepared by treatment of 5 with DHP and TsOH was reduced with LAH to the alcohol 7 (92 %) which was tosylated to afford 8. Treatment of 8 with NaI in acetone afforded 9 which was hydrolysed to provide 10 (72 %). Compound 10 was converted to 11 (65 %) with potassium phthalimide and tosylated to give 12. Iodination of 12 with NaI in acetone afforded 13 in 61 % yield. Acid hydrolysis of the phthalimide derivative 13 with aqueous HI or  $HClO_4$  in acetic acid afforded intractable reaction mixtures. Hydrolysis with aqueous HCl afforded 14 in low yield due to concomitant formation of the chloro derivative.

Radiochemical synthesis of 2 and 14 via the reaction of the appropriate alcohol with trimethylsilylchloride, NaI and acetonitrile, direct iodide exchange and nucleophilic displacement of the tosylate have been investigated.

(1) Gillis C.N. and Pitt B.R., *Ann. Rev. Physiol.* **44**, 269 (1982).

(2) Abrams D.N., Man S.F.P., Noujaim A.A. and Washburn L.C., presented at the "Third International Symposium on Radiopharmacology" in Freiburg, West Germany, Sept 21–25, 1983.

(3) Washburn L.C., personal communication.



DESIGN, SYNTHESIS AND EVALUATION OF  $\omega$ -IODOVINYL AND  $\omega$ -IODOALKYL-SUBSTITUTED METHYL-BRANCHED LONG-CHAIN FATTY ACIDS

M. M. Goodman, E. B. Cunningham and F. F. Knapp, Jr., Nuclear Medicine Group, Oak Ridge National Laboratory, Oak Ridge, TN 37830, U.S.A.

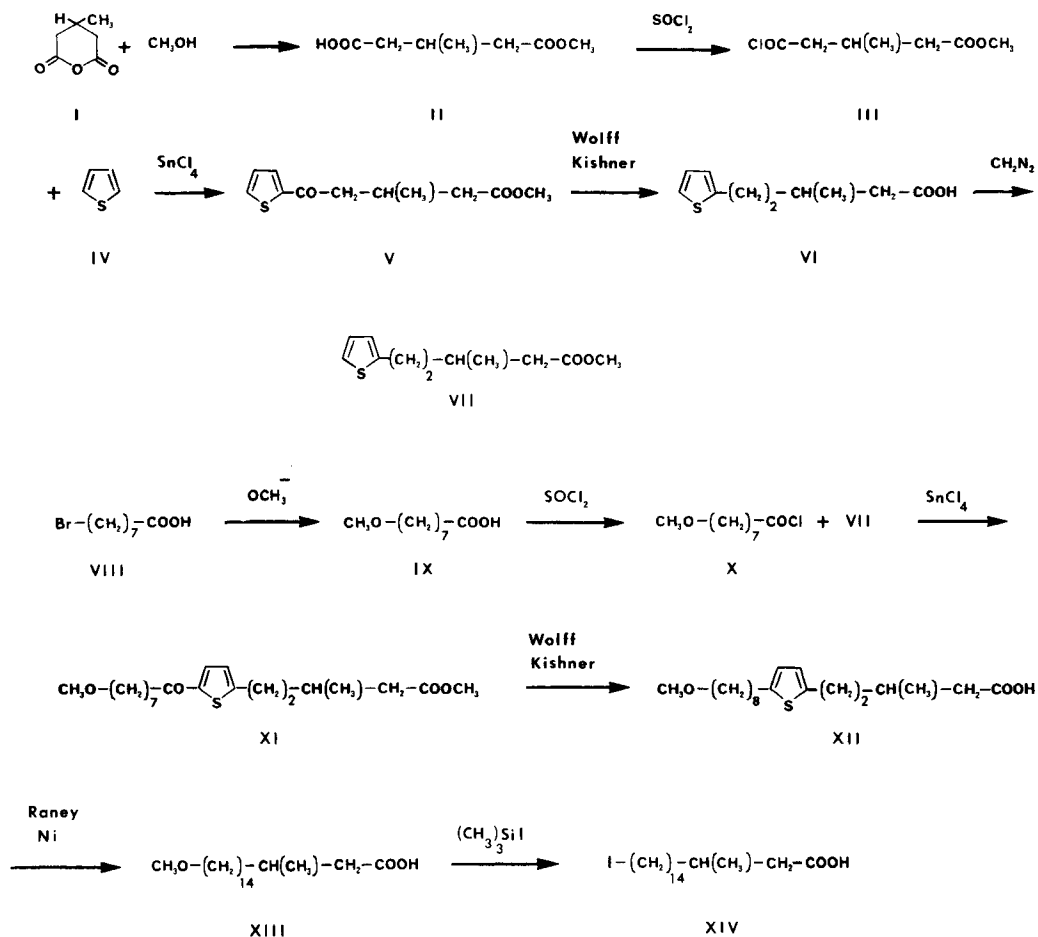
Recent high resolution autoradiographic analyses of myocardial slices from normotensive and severe hypertensive rats have demonstrated a heterogeneous distribution of a model carbon-14 labeled methyl-branched fatty acid in regions of hypertensive tissue that exhibited normal perfusion as determined with  $^{201}\text{Tl}$ (1). These results indicate that severe hypertension is associated with changes in fatty acid utilization. Because of the potential clinical importance of using structurally modified fatty acids labeled with  $\gamma$ -emitting radionuclides to further explore this phenomenon, we have now developed a general synthetic method for the preparation of terminal radioiodinated methyl-branched fatty acids with the radiolabel stabilized as a vinyl iodide. In this study we report the syntheses (Schemes 2 and 3) and tissue distribution in rats (Table 2) of (E)-19-[ $^{125}\text{I}$ ]iodo-3-(RS)-methyl-18-nonadecenoic acid (XVIII) and the unbranched analogue, (E)-19-[ $^{125}\text{I}$ ]iodo-18-nonadecenoic acid (XXIII).

The route chosen for the construction of the methyl-branched long chain fatty acid skeleton involved the thiophene chain elongation synthesis. Using this synthetic approach, the substituents introduced into the 2- and 5-positions of the thiophene ring can be selected and would provide a variety of 3-methyl-branched fatty acids of various chain lengths for structure activity studies. The key substrate, 17-iodo-3-(RS)-methylheptadecanoic acid (XIV), was prepared as described in Scheme 1, which involved Raney Nickel desulfurization of the 2,5-disubstituted thiophene (XII). Compound XII was prepared by treatment of the methyl-branched 2-substituted thiophene (VII) with  $\text{CH}_3\text{O}(\text{CH}_2)_7\text{COCl}$  (X) followed by Wolff-Kishner reduction. The methoxy derivative (XIII) was treated with  $(\text{CH}_3)_3\text{SiI}$  to afford 17-iodo-3-(RS)-methylheptadecanoic acid (XIV). The availability of this key 17-iodo intermediate provided an opportunity to gain further insight into the mechanism of in vivo deiodination in terminal radioiodinated long chain fatty acids. Since loss of halide from an iodinated coenzyme A product would not be expected, the evaluation of  $^{125}\text{I}$  labeled XIV would focus on the direct cleavage of the carbon-iodide bond. Tissue distribution studies of  $^{125}\text{I}$ -labeled XIV (Table 1) demonstrated rapid dehalogenation indicating significant carbon-iodide cleavage in the apparent absence of  $\beta$ -oxidation. These results confirm our earlier studies using  $\text{I}(\text{CH}_2)_7\text{Te}(\text{CH}_2)_7\text{COOH}$  (2). More recently, Otto et al (3) have obtained similar results with a 13 carbon analogue of (XIV).

The pivotal step in the synthesis of the (E)-iodovinyl acid (XVIII) (Scheme 2) involved hydrostannylation of the terminal ethynyl substrate (XVI) with  $(n\text{-Bu})_3\text{SnH}$  to give the key intermediate, (E)- $(n\text{-Bu})_3\text{SnHC}=\text{CH}(\text{CH}_2)_{14}\text{CH}(\text{CH}_3)\text{CH}_2\text{COOCH}_3$  (XVII). Compound XVI was prepared by treatment of the 17-iodo methyl-branched acid (XIV) with lithium acetylide-ethylenediamine (LAEDA). Iodostannylation of (XVII) by treatment with NCS and  $\text{I}^-$  followed by basic hydrolysis gave (XVIII). The unbranched analogue (XXIII) was prepared in the same manner (Scheme 3).

Tissue distribution studies of  $^{125}\text{I}$ -labeled (XVIII) and (XXIII) were performed in rats (Table 2). Over the first 30 minute period, both compounds showed significant heart uptake. The branched fatty acid showed greater myocardial retention than the straight chain analogue. The availability of iodine-123 labeled substrates of this type may now allow the further evaluation of the hypertensive model (1) by single photon emission computerized tomographic techniques (SPECT).

Research sponsored by the Office of Health and Environmental Research, U.S. Department of Energy under contract W-7405-eng-26 with the Union Carbide Corporation.

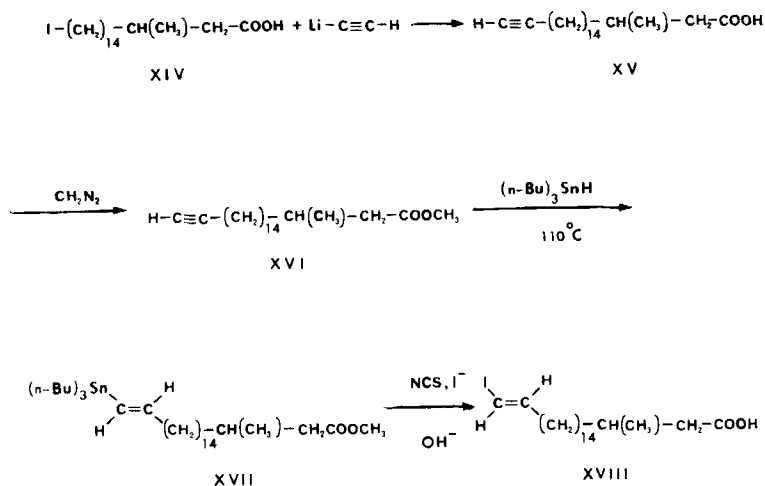


Scheme 1

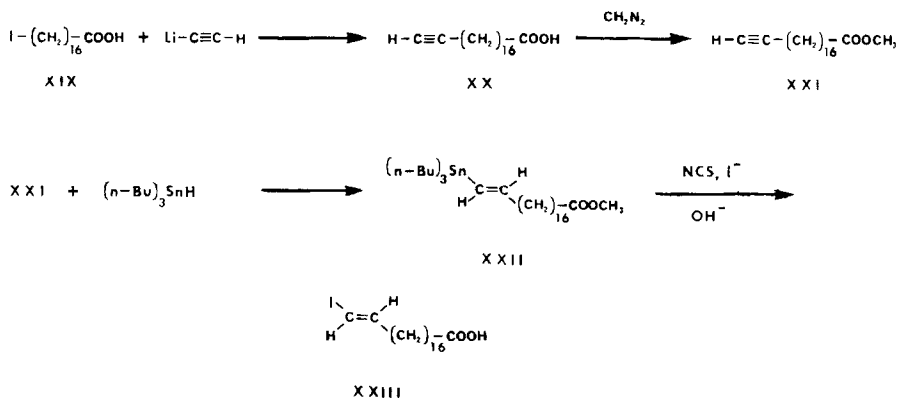
 Table 1. Tissue distribution of 17- $^{125}\text{I}$ iodo-3-(R,S)-methylheptadecanoic acid (XIV) in tissues of Fischer female rats.

Time After Injection	Mean percent injected dose/gm (range) for 5 rats						
	Blood	Liver	Kidney	Heart	Lung	Thyroid	Heart/Blood
2 min	2.47 (1.97-2.84)	3.93 (3.09-4.60)	1.35 (1.22-1.61)	2.68 (2.11-3.42)	1.75 (1.41-2.07)	22.50 (19.56-24.76)	1.08 (0.99-1.27)
5 min	1.43 (0.93-1.65)	2.50 (1.89-2.80)	1.06 (0.78-1.23)	1.93 (1.16-2.78)	1.03 (0.60-1.31)	30.19 (14.96-40.15)	1.40 (0.70-1.91)
10 min	1.31 (1.19-1.39)	2.54 (2.34-2.69)	0.96 (0.85-1.01)	1.77 (1.29-2.21)	1.16 (0.98-1.38)	43.25 (39.57-46.56)	1.36 (0.97-1.71)
1 h	0.72 (0.58-0.78)	0.95 (0.90-0.98)	0.59 (0.52-0.66)	0.95 (0.49-1.25)	0.68 (0.61-0.80)	217 (170-283)	1.29 (0.85-1.73)

- (1) Yonekura, Y., Bizais, Y., Som, P. et al. *J. Nucl. Med.*, **24**, P 125 (1983).
- (2) Goodman, M. M., Knapp, F. F., Jr. et al. *J. Med. Chem.*, **25**, 613 (1982).
- (3) Otto, C. A., Brown, L. E., and Scott, A. M., *J. Nucl. Med.*, **25**, 75 (1984).



Scheme 2



Scheme 3

Table 2. Tissue distribution of  $^{125}\text{I}$ -labeled (E)-19-Iodo-18-nonadecenoic acids in tissues of Fischer female rats.

Fatty Acid, Minutes After Injection	$^{125}\text{I}$ -labeled (iodo vinyl)	Range % dose/gm values for 5 rats				Mean Percent Relative Heart Retention
		Heart	Blood	Liver	Thyroid	
Methyl- Branched (XVIII)	2	3.30-4.43	0.84-1.15	7.75-8.89	5.64-8.50	95
	5	3.48-4.07	0.54-0.81	7.30-8.21	8.95-10.04	
	15	3.48-3.94	0.37-0.45	7.86-9.04	14.81-19.28	
	30	3.86-4.48	0.54-0.62	5.62-6.36	21.81-41.87	100
Straight Chain (XXIII)	2	3.79-5.30	0.37-0.50	6.44-7.61	7.22-9.49	84
	5	3.37-3.04	0.24-0.45	5.86-7.07	7.42-9.88	
	15	2.27-3.81	0.24-0.45	4.53-6.84	10.24-19.55	
	30	2.62-4.80	0.43-0.67	5.30-6.28	17.90-25.77	85



RADIOHALOGENATED  $\omega$ -HALOFATTY ACIDS FOR STUDYING THE INTEGRITY OF CELL MEMBRANES USING THE ISOLATED PERFUSED HEART TECHNIQUE.

G. Kloster, G. Stöcklin, E.F. Smith III, and K. Schrör  
Institut für Chemie 1 (Nuklearchemie), KFA Jülich GmbH,  
D-5170 Jülich, FRG

Long-chain  $\omega$ -halofatty acids, especially  $\omega$ - $^{123}\text{I}$ -iodoheptadecanoic acid (IHA), are used clinically as radiopharmaceuticals for functional heart imaging. The metabolic interpretation of the various elimination rates observed, however, remained open to discussion.

Isolated perfused organs are test systems that are ideally suited to clarify the metabolic interpretation of elimination rates for a particular organ, since all influences from other organs are excluded. Furthermore, perfusion rate and composition of the perfusion fluid can be controlled to yield interpretable results.

Previously, we have shown (1) that, in isolated perfused Guinea pig hearts, diffusion of metabolically formed halide ion from the mitochondrion to the blood is the rate-determining step of IHA-pharmacokinetic in normal myocardium. This was shown by hpl-chromatographic identification of the radioactive species eliminated from the heart in the perfusion fluid.

We have now extended these in-vitro experiments to normal and globally ischemic isolated perfused rabbit hearts. Again, in normal hearts a single phase iodide elimination half-time ( $14.3 \pm 2.1$  min) was observed. In hearts made globally ischemic for 90 min (by reducing the perfusion rate to 6% of normal), the iodide elimination was biphasic with a first fast ( $T_{1/2} = 3.8 \pm 0.49$  min) and a late slow phase ( $T_{1/2} = 60.5 \pm 14.0$  min). The first fast phase is attributed to iodide ion released by residual  $\beta$ -oxidation (more rapid than in normal hearts due to damaged membranes in ischemia) while the late slow phase is explained by  $\beta$ -oxidation of IHA slowly released by hydrolysis of intracellular lipid stores.

Furthermore, intracellular lipids are lost to the perfusion fluid in both normal and ischemic hearts. In normal hearts, this washout is very rapid ( $T_{1/2} = 0.65 \pm 0.31$  min), while in the globally ischemic heart it is prolonged and dominant ( $T_{1/2} = 4.0 \pm 0.67$  min). The washout is attributed to diffusion across the outer cellular membrane. Treatment of the hearts during ischemia by infusion of the prosta-cyclin mimetic ZK 36,374 (a substance acting on the outer cellular membrane) reverts the washout of intracellular lipids to almost normal values ( $1.2 \pm 0.2$  min) while the iodide elimination half-times remain unchanged as expected for an agent acting on the outer membranes.

In conclusion, IHA was shown to be an agent for studying the integrity of cellular membranes in-vitro. The isolated perfused heart technique in conjunction with radiohalogen labelled fatty acids seems to be a good probe for membrane integrity and the approach should be applicable to pharmacological intervention studies and to therapy control.

(1) Kloster G., Stöcklin G., Radioakt. Isotope Klin. Forsch. 15, 235-241 (1982)

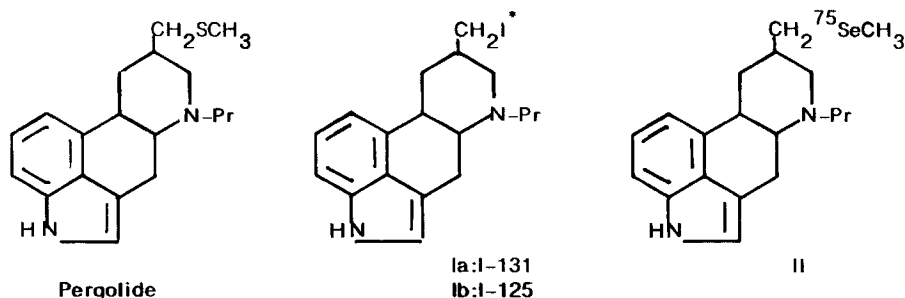
[<sup>131,125</sup>I]IODO- and [<sup>75</sup>Se]SELENO-ERGOLINE DERIVATIVES AS POTENTIAL RADIOPHARMACEUTICALS.

S.A. Sadek and G.P. Basmadjian, Nuclear Pharmacy Programs, College of Pharmacy, Oklahoma University, Oklahoma City, OK 73190, USA.

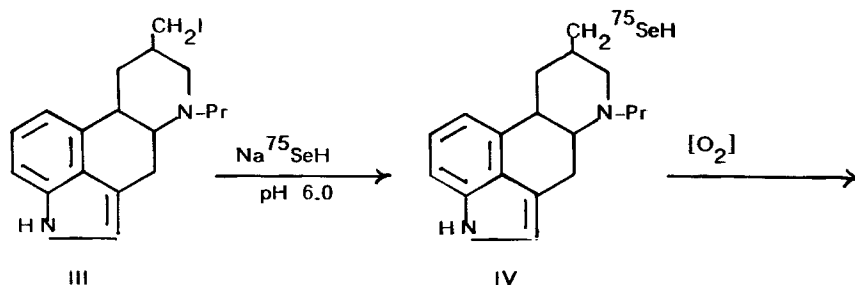
Ligands with high affinity for dopaminergic receptors and labeled with gamma- or positron-emitting radionuclides are ideal agents for mapping dopamine receptor sites. To develop such ligands, several investigators have labeled and studied different dopamine antagonists e.g. [Br-82]bromperidol (1), [Br-77]bromospiroperidol (2), [F-18]haloperidol (3) and [C-11]spiroperidol (4).

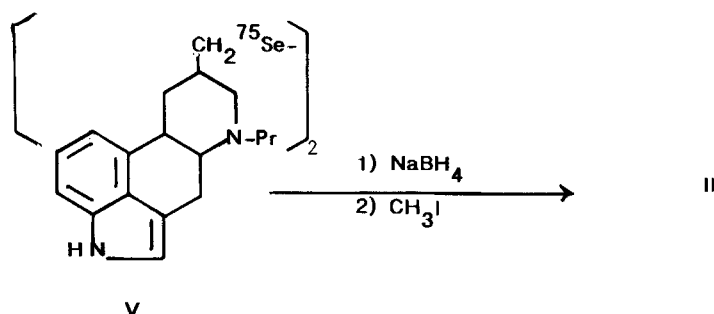
Pergolide, a new synthetic ergoline, has been shown to be a very potent dopamine agonist in animals (5) and in man (6). It has been reported that [H-3]pergolide binds specifically to dopamine receptor sites in the brain homogenate of rats and calves (7).

Two pergolide analogs labeled with I-125/I-131 and Se-75 were prepared. The radioactive iodoergoline derivative (Ia/Ib) was synthesized by refluxing the mesyl derivative with NaI[<sup>131</sup>I/<sup>125</sup>I] in acetone.



The [<sup>75</sup>Se]Selenopergolide derivative (II) was prepared starting with [<sup>75</sup>Se]selenious acid (S.A. 400 mCi/mg Se). NaHSe-75 was prepared by reducing [<sup>75</sup>Se]selenious acid with NaBH<sub>4</sub> in phosphate buffer (pH 6.0) (8). The generated NaHSe-75 was used as a nucleophile to displace the iodo group of compound III to form the corresponding selenol IV which upon exposure to air formed the diselenide V in excellent yield. Reduction of the diselenide V with NaBH<sub>4</sub> and subsequent addition of methyl iodide provided the desired [<sup>75</sup>Se]selenopergolide (II) in 74% overall yield.





The radioactive compounds were matched with authenticated nonradioactive samples on silica gel plates using benzene/methanol (9.5:0.5) as solvent:  $R_f$  values for diselenide V, selenopergolide (II) and iodoergoline (Ia/Ib) are: 0.13, 0.32 and 0.4, respectively.

Biodistribution studies of Ia & II in mature male rats showed relatively high uptake by the adrenals and brain. The data obtained are summarized below.

Time	Compound	%Dose/gm $\pm$ SEM*		
		Adrenal	Brain	Blood
5 min	Ia	3.61 $\pm$ 0.43	1.14 $\pm$ 0.06	0.19 $\pm$ 0.01
	II	3.67 $\pm$ 0.59	1.31 $\pm$ 0.24	0.12 $\pm$ 0.01
15 min	Ia	3.57 $\pm$ 0.37	1.10 $\pm$ 0.10	0.15 $\pm$ 0.01
	II	4.20 $\pm$ 0.45	0.90 $\pm$ 0.01	0.06 $\pm$ 0.00
30 min	Ia	1.90 $\pm$ 0.23	0.74 $\pm$ 0.06	0.13 $\pm$ 0.01
	II	3.93 $\pm$ 0.62	0.70 $\pm$ 0.04	0.05 $\pm$ 0.00

\* The values represent the mean and standard error of the mean of three evaluations.

Sequential images of dogs with Ib and II showed fast brain uptake with good retention for at least 20 min. Studies are in progress to evaluate the mechanism of uptake of Ib & II in rat and dog brains.

- (1) Vincent S.H., Shambhu M.B. and Digenis G.A., *J. Med. Chem.* **23**, 75 (1980).
- (2) Kulmala H.K., Huang C.C., Dinerstein R.J. and Friedman A.M., *Life Sci.* **28**, 1911 (1981).
- (3) Zanzonico P.B., Bigler R.E. and Schmall B., *J. Nucl. Med.* **24**, 408 (1983).
- (4) Fowler J.S., Arnett C.D., Wolf A.P., MacGregor R.R., Norton E.F. and Findley A.M., *J. Nucl. Med.* **23**, 437 (1982).
- (5) Fuller R.W., Clemens J.A., Kornfeld E.C., Snoddy H.D., Smalsting E.B. and Bach N.J., *Life Sci.* **24**, 375 (1979).
- (6) Lemberger L. and Crabtree R.E., *Science* **205**, 1151 (1979).
- (7) Wong D.T., Bymaster F.P., Lane P.T., Kau D., Bach N.J. and Kornfeld E.C., *Res. Commun. Chem. Pathol. Pharmacol.* **30**, 195 (1980).
- (8) Sadek S.A., Basmadjian G.P. and Ice R.D., *Nucl. Med. Commun.* **3**, 247 (1982).

$\alpha$ -AMINO-(3-[ $^{131}\text{I}$ ]-4-HYDROXYBENZYLIDENE)-DIPHOSPHONATE A NEW  
RADIOPHARMACEUTICAL FOR THE PALLIATIVE TREATMENT OF BONE METASTASES

---

M. Eisenhut<sup>1</sup>, B. Kimmig<sup>1</sup>, B. Bubeck<sup>1</sup>, D.M. Taylor<sup>2</sup>, K. zum Winkel<sup>1</sup>

1) Klinikum der Univ. Heidelberg, Zentrum Radiologie, Abt. klin. Nuklearmedizin, and 2) Theoretikum der Univ. Heidelberg, Inst. für Strahlentoxikologie

The efforts to introduce  $^{32}\text{P}$ -labeled diphosphonates as a substitute of the long lived  $^{89}\text{Sr}$  for palliative therapy of intractable pain often associated with bone metastases were of limited success. Despite the palliative effectiveness the lack in wide acceptance of i.e. [ $^{32}\text{P}$ ]-1-hydroxyethylidene-1,1-diphosphonate ( $^{32}\text{P}$ -HEDP) was mainly due to the drop in peripheral white count and platelets during therapy and due to the difficulties in preparing the  $^{32}\text{P}$ -labeled diphosphonates (1). Because of these disadvantages we decided to apply  $^{131}\text{I}$  bound to an osteotropic diphosphonate as a  $\beta^-$  source with much shorter ranging electrons. The 90-percentile distance of  $^{131}\text{I}$  in water is 0.882 mm compared to 3.03 mm for  $^{89}\text{Sr}$  and 3.51 mm for  $^{32}\text{P}$  (2). This characteristic would reduce the radiation burden to the bone marrow. The shorter  $\beta^-$  range, the convenient radioactive waste disposal in nuclear medical therapy wards and the ease of the radiolabeling procedure were therefore the major reasons for the choice of  $^{131}\text{I}$ .

$\alpha$ -amino-(4-hydroxybenzylidene)-diphosphonate (pHOBDPNH<sub>2</sub>) was synthesized according to a route recently described in the literature (3) (see reaction scheme 1). Labeling of pHOBDPNH<sub>2</sub> with radioiodine was performed by electrophilic aromatic substitution with  $^{131}\text{I}^-$  and  $\text{IO}_3^-$  in 1 N HCl (reaction scheme 2). After a reaction time of 5 minutes at ambient temperature the mixture was neutralized with 1 N NaOH and treated with  $\text{Na}_2\text{S}_2\text{O}_5$  to reduce unreacted  $\text{IO}_3^-$ . Unreacted  $^{131}\text{I}^-$  was then removed by filtration over AgCl. About 95% radiochemical yield was generally achieved after sterile filtration. The specific activity of the product was 15.6 Ci/mmol diphosphonate. If necessary  $^{131}\text{I}$ -pHOBDPNH<sub>2</sub> can be isolated in a non-carrier added concentration by chromatography over Biogel P2 (Bio Rad). The preparation time lasted less than one hour.

The organ distribution of  $^{131}\text{I}$ -pHOBDPNH<sub>2</sub> was measured in male SD rats. The tissue activities as summarized in the Table show by comparison to the other organs only high uptake in the bone tissue. The total bone uptake of  $^{131}\text{I}$ -pHOBDPNH<sub>2</sub> in rats was measured by the total-body retention of the activity. The 24 hr retention value was 47%. The biological half life of  $^{131}\text{I}$ -pHOBDPNH<sub>2</sub> was calculated from the physiological decay of the total-body activity in the rats to 46.3 days.

The total-body retention of  $^{131}\text{I}$ -pHOBDPNH<sub>2</sub> after 24 hr was in accordance with the urinary excreted activity. 49.2 % was collected with the 22 hr urine while at that

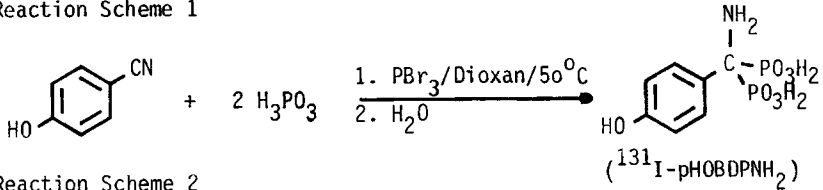
time only 0.3 % appeared in the feces. The chromatographical analysis revealed unchanged  $^{131}\text{I}$ -pHOBDPNH<sub>2</sub>.

$^{131}\text{I}$ -pHOBDPNH<sub>2</sub> disappeared very rapidly from the blood pool. The distribution into the two compartments bone and urine occurred somewhat faster than  $^{99\text{m}}\text{Tc}$ -diphosphate complexes (4). The return of activity into the blood via the contribution of  $^{131}\text{I}$ -pHOBDPNH<sub>2</sub> in erythropoiesis could not be observed. This behaviour stood in contrast to the observed blood cell depression after application of  $^{32}\text{P}$ -phosphate and  $^{32}\text{P}$ -HEDP. The latter which is structurally related to benzylidenediphosphonates thus represents also a potential  $^{32}\text{P}$ -phosphate source, since liberation of  $^{32}\text{P}$ -phosphate may occur by oxidative in vivo cleavage of the P-C bonds. The same cleavage reaction in  $^{131}\text{I}$ -pHOBDPNH<sub>2</sub> would, however, lead to metabolites containing the  $^{131}\text{I}$ -pHO-benzylidene group which do not participate in blood cell formation.

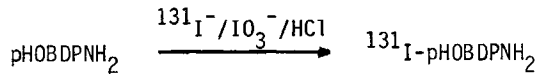
The high affinity of  $^{131}\text{I}$ -pHOBDPNH<sub>2</sub> to bone metastases was proved by scintigraphy. The activity-time kinetics over a lesion compared to normal bone are shown in the Figure. The high target/non target ratio of 6.3 after 24 hr and 10.1 after 450 hr were far above the ratios ever obtained with  $^{99\text{m}}\text{Tc}$ -diphosphonate complexes. The effective half life in the metastases appeared to be enhanced compared to the effective half life in normal bone. They were 186.7 hr (metastatic vertebra) and 145.8 hr (reference vertebra). The biological half lives must be at least in the order of magnitude of that observed with the total-body retention measurements in rats. First palliative therapies with  $^{131}\text{I}$ -pHOBDPNH<sub>2</sub> were promising: 1 to 3 days after application of 6 - 12 mCi  $^{131}\text{I}$ -pHOBDPNH<sub>2</sub> we observed pain relief in four out of five treated patients.

- (1) O'Mara R.E., "Therapy in Nuclear Medicine", Grune & Stratton, New York, San Francisco, London, 1978, p. 257
- (2) Berger M.J., NM/MIRD Pamphlet No. 7, J. Nucl. Med. Suppl. No. 5
- (3) Worms K.H. and Blum H., Z. anorg. allg. Chemie 457, 209 (1979)
- (4) Eisenhut M., Kristen P., Garnier-Moiroux A. and zum Winkel K., Nucl.-Med. 23, (1984) in press

Reaction Scheme 1



Reaction Scheme 2

Table TISSUE DISTRIBUTION OF  $^{131}\text{I}$ -pHOBDPNH<sub>2</sub> IN SD RATS

Time (hr)	F. Diaph.	Femur	Blood	Heart	Lung	Spleen	Liver	Kidney
4	273 <sup>1</sup> (107-293)	256 (200-306)	4 (3-12)	2 (2-4)	10 (7-19)	3 (3-6)	6 (5-9)	40 (36-45)
24	196 (107-305)	264 (202-269)	0	0	2 (1-3)	2 (2-2)	4 (3-5)	21 (20-22)
96	278 (133-321)	281 (172-316)	0	0	1 (0-2)	4 (2-4)	8 (5-9)	14 (10-16)
192	291 (102-310)	278 (132-249)	0	0	1 (0-2)	6 (3-8)	12 (3-17)	10 (8-12)
384	215 (119-304)	212 (148-242)	0	0	1 (0-1)	7 (4-8)	9 (4-12)	5 (5-6)

<sup>1</sup>) in % g dose/g as median of three rats with range

Figure

